SH
11
.A2
F53
FISH

U.S. Department
of Commerce

Volume 122
Number 1–2
January–April 2024

Fishery Bulletin

U.S. Department of Commerce

Gina M. Raimondo
Secretary

National Oceanic and Atmospheric Administration

Richard W. Spinrad
Administrator

National Marine Fisheries Service

Janet Coit
Assistant Administrator
for Fisheries

Fishery Bulletin

Scientific Editor
José I. Castro
National Marine Fisheries Service, NOAA
263 13th Avenue South
Saint Petersburg, Florida 33701

Managing Editor
Kathryn Dennis
Scientific Publications Office
National Marine Fisheries Service, NOAA
1845 Wasp Boulevard, Building 176
Honolulu, Hawaii 96818

Associate Editor
Cara Mayo
Scientific Publications Office
National Marine Fisheries Service, NOAA
7600 Sand Point Way NE
Seattle, Washington 98115-0070

Editorial Board

Henry L. Bart Jr.	Tulane University, New Orleans, Louisiana
Katherine E. Bemis	National Systematics Laboratory, Washington, DC
Matthew D. Campbell	National Marine Fisheries Service, Pascagoula, Mississippi
William B. Driggers III	National Marine Fisheries Service, Pascagoula, Mississippi
Gretchen L. Grammer	South Australian Research and Development Institute, Adelaide, Australia
Eric R. Hoffmayer	National Marine Fisheries Service, Pascagoula Mississippi
Richard Langton	National Marine Fisheries Service, Walpole, Maine (retired)
J. Fernando Márquez-Farías	Universidad Autónoma de Sinaloa, Mazatlán, México
Richard S. McBride	National Marine Fisheries Service, Woods Hole, Massachusetts
Richard L. Merrick	National Marine Fisheries Service, Falmouth, Massachusetts (retired)
Richard D. Methot	National Marine Fisheries Service, Seattle, Washington
Lisa J. Natanson	National Marine Fisheries Service, Narragansett, Rhode Island (retired)
Mark S. Peterson	University of Southern Mississippi, Ocean Springs, Mississippi
André E. Punt	University of Washington, Seattle, Washington
Joseph M. Quattro	University of South Carolina, Columbia, South Carolina
John F. Walter III	National Marine Fisheries Service, Miami, Florida

***Fishery Bulletin* website: https://spo.nmfs.noaa.gov/fb.htm**

Fishery Bulletin carries original research reports on investigations in fishery science, engineering, and economics. It began as the Bulletin of the United States Fish Commission in 1881; it became the Bulletin of the Bureau of Fisheries in 1904 and the *Fishery Bulletin* of the U.S. Fish and Wildlife Service in 1941. Separates were issued as documents through volume 46; the last document was no. 1103. Beginning with volume 47 in 1931 and continuing through volume 62 in 1963, each separate appeared as a numbered bulletin. A new system began in 1963, with volume 63, in which papers are bound together in a single issue. Beginning with volume 70, number 1, January 1972, *Fishery Bulletin* became a periodical, issued quarterly. In this form, it is available by subscription from the Superintendent of Documents, U.S. Government Publishing Office, Washington, DC 20401. It is also available free in limited numbers to libraries, research institutions, and state and federal agencies and in exchange for other scientific publications.

Fishery Bulletin (ISSN 0090-0656) is published quarterly by the Scientific Publications Office, National Marine Fisheries Service, NOAA, 7600 Sand Point Way NE, Seattle, WA 98115-0070.

Although the contents of this publication have not been copyrighted and may be reprinted entirely, reference to source is appreciated.

The Secretary of Commerce has determined that the publication of this periodical is necessary according to law for the transaction of public business of this Department. Use of funds for printing of this periodical has been approved by the Director of the Office of Management and Budget.

For Sale by the Superintendent of Documents, U.S. Government Publishing Office, Washington, DC 20401. Subscription price per year: $32.00 domestic and $44.80 foreign. Cost per single issue: $19.00 domestic and $26.60 foreign. **See back for order form.**

U.S. Department of Commerce
Seattle, Washington

Volume 122
Number 1–2
January–April 2024

Fishery Bulletin

Contents

Articles

1–12 Jeff Kneebone, Connor F. White, Caroline Collatos, and Nicholas M. Whitney

High survivorship of sandbar sharks (*Carcharhinus plumbeus*) following catch and release in a growing land-based fishery in Massachusetts

13–25 Valéria M. Lemos, Ana C. G. Mai, Ana C. Martins, José V. Martins, Sandra Andrade, Henrique Cabral, and João P. Vieira

Variation in otolith microchemistry for Lebranche mullet (*Mugil liza*) in southern Brazil and its potential use in identifying their nursery grounds

26–43 Matthew D. Damiano, Mandy Karnauskas, Wessley Merten, and Jie Cao

Spatiotemporal dynamics of dolphinfish (*Coryphaena hippurus*) in the western Atlantic Ocean

44–57 Benjamin R. LaFreniere, Briony Donahue, Jillian E. Price, Alicia Cruz-Uribe, Nate Miller, Benjamin T. Manard, Richard McBride, and John A. Mohan

Chemical clocks: using otolith geochemistry to enhance estimation of age and growth of white hake (*Urophycis tenuis*)

59–62 Guidelines for authors

The National Marine Fisheries Service (NMFS) does not approve, recommend, or endorse any proprietary product or proprietary material mentioned in this publication. No reference shall be made to NMFS, or to this publication furnished by NMFS, in any advertising or sales promotion that would indicate or imply that NMFS approves, recommends, or endorses any proprietary product or proprietary material mentioned herein or that has as its purpose an intent to cause directly or indirectly the advertised product to be used or purchased because of this NMFS publication.

The NMFS Scientific Publications Office is not responsible for the contents of the articles.

SMITHSONIAN
JUL 24 2024
LIBRARIES

National Marine
Fisheries Service
NOAA

Fishery Bulletin
established in 1881

Spencer F. Baird
First U.S. Commissioner
of Fisheries and founder
of *Fishery Bulletin*

High survivorship of sandbar sharks (*Carcharhinus plumbeus*) following catch and release in a growing land-based fishery in Massachusetts

Jeff Kneebone (contact author)[1]
Connor F. White[2]
Caroline Collatos[1,3]
Nicholas M. Whitney[1]

Email address for contact author: jkneebone@neaq.org

[1] Anderson Cabot Center for Ocean Life
New England Aquarium
1 Central Wharf
Boston, Massachusetts 02110

[2] Department of Organismic and Evolutionary Biology
Harvard University
26 Oxford Street
Cambridge, Massachusetts 02138

[3] School for the Environment
University of Massachusetts Boston
100 Morrissey Boulevard
Boston, Massachusetts 02125

Abstract—Directed land-based recreational catch-and-release fishing for sandbar sharks (*Carcharhinus plumbeus*) is growing in popularity in Massachusetts. Working with 21 volunteer fishermen of varying experience levels, we observed and documented the fishing gear, tackle, and techniques used to catch and release 67 sandbar sharks. The postrelease fate of each shark was monitored by using an acceleration data logger (ADL) tag embedded in a custom float package that was secured to the first dorsal fin with a galvanic timed release. All 67 packages were recovered after detachment following monitoring periods of 0.15–9.98 d. Examination of the depth, tailbeat period (TBP), pitch, and roll time series from 65 ADLs that recorded data revealed high survivorship for tagged sharks, with all of them alive at the time of tag detachment. Behavioral recovery was estimated to have occurred at an average of 6.36 h after release on the basis of trends in TBP for 54 sandbar sharks with at least 10 h of postrelease acceleration data. These results indicate that sandbar sharks are remarkably resilient to catch and release in the land-based shark fishery in Massachusetts.

Manuscript submitted 28 July 2023.
Manuscript accepted 14 February 2024.
Fish. Bull. 122:1–12 (2024).
Online publication date: 5 March 2024
doi: 10.7755/FB.122.1-2.1

The views and opinions expressed or implied in this article are those of the author (or authors) and do not necessarily reflect the position of the National Marine Fisheries Service, NOAA.

Recreational shark fishing is a popular activity with significant socioeconomic value to coastal communities along the East Coast of the United States and in the Gulf of Mexico region (Hutt and Silva, 2019; Guay et al., 2021). Traditionally, a large portion of the recreational shark fishing effort has occurred at sea aboard federally permitted charter boats and private fishing vessels. However, a recent rise in the popularity of shore- or land-based shark angling has resulted in increased effort within state waters (senior author, personal observ.; Guay et al., 2021). Because of how recreational catch and effort data are collected by the National Marine Fisheries Service Marine Recreational Intercept Program and Large Pelagics Survey, as well as the lack of a federal permit requirement for land-based shark fishing, data on the magnitude of catch or effort across this fishery are very limited (Weber et al., 2020; Guay et al., 2021). Nonetheless, it is well-documented that several shark species targeted or incidentally captured by land-based anglers are experiencing population declines and are prohibited from retention under state and federal laws (Kilfoil et al., 2017; Gibson et al., 2019). One such species is the overfished sandbar shark (*Carcharhinus plumbeus*) (SEDAR, 2017).

Directed land-based recreational fishing for sandbar sharks has occurred in Massachusetts for decades (Skomal, 2007). However, evidence indicates that land-based fishing effort for sandbar sharks and shark catch rates have increased dramatically in Massachusetts over the last decade (Skomal[1]). For example, conversations with recreational land-based anglers have revealed that catches of 5–10 sandbar sharks in a single trip are now common (senior author, personal observ.), and individual land-based anglers have conventionally tagged over 100 sandbar sharks in a single season (Zewinski[2]). Under current Massachusetts state law, circle hooks must be used when targeting sharks with natural baits, and all sandbar sharks must be released (Regulation . . . 2023). However, anglers in Massachusetts are not required to possess an additional permit to engage in land-based shark angling nor undergo training on catch-and-release best practices prior to engaging in the fishery; in contrast, both a permit and training are required in Florida (Sharks . . . 2019).

---

[1] Skomal, G. 2023. Personal commun. Mass. Div. Mar. Fish., 836 S Rodney French Blvd., New Bedford, MA 02744.

In few studies have the effects of land-based capture and handling on shark mortality rates been examined. Weber et al. (2020) reported a postrelease mortality (PRM) rate of 17% for blacktip sharks (*C. limbatus*) caught in South Carolina, with mortality occurring because of physical trauma incurred during capture and foul hooking. Similarly, Kilfoil et al. (2017) reported low (6%) PRM of sand tigers (*Carcharias taurus*) caught in Delaware, with all mortality attributed to internal hooking. Most recently, Binstock et al. (2023) reported variable, species-specific PRM rates for bull (*Carcharhinus Leucas*) (7%), blacktip (50%), and tiger (*Galeocerdo cuvier*) (0%) sharks caught in Texas, with evidence that increasing water temperatures resulted in higher mortality rates for blacktip sharks. Mortality has also been suspected to have occurred in land-based fishing operations because of the removal of sharks from the water (i.e., air exposure) for extended periods during handling (Shiffman et al., 2017). However, to date, no direct relationship between time out of water and mortality has been reported. Because PRM rates for sharks are highly specific to species (e.g., Whitney et al., 2021) and geographic location (e.g., Mohan et al., 2020), there is a continued need to estimate these rates across all species, fisheries, fishing areas, and environmental conditions. Accordingly, the goals of this study were to assess the PRM rate of sandbar sharks caught in the land-based shark fishery in Massachusetts and to identify factors that adversely affect animal condition, postrelease behavior, and survival. We also briefly assessed the effect of animal behavior on tag retention.

Materials and methods

Activities of this project were conducted under the New England Aquarium Animal Care and Use Committee protocol 2019-06.

Study area and design

All project activities were conducted in cooperation with volunteer recreational land-based shark fishermen on Cape Cod and Nantucket in Massachusetts. Scientific researchers accompanied and observed fishermen during all trips, but anglers were free to choose the location of angling and received no input from scientific staff regarding the gear (e.g., rod and reel type or size), tackle (e.g., hook type or size), or techniques used to capture and handle sandbar sharks. Each participant's experience with land-based shark fishing was determined at the time of each trip on the basis of the following criteria:

Novice: less than 1 year of experience with land-based shark fishing or a total of <5 sharks captured and handled from land in their angling career;

Intermediate: more than 1 year of experience with land-based shark fishing or a total of 5–10 sharks captured and handled from land in their angling career; and

Expert: more than 2 years of experience with land-based shark fishing or a total of >10 sharks captured and handled from land in their angling career.

When a volunteer angler captured a sandbar shark, the following data were collected: rod and reel type (e.g., conventional versus spinning) and size (e.g., model or pound class); line type and strength; leader type, length, and strength; hook type (circle or J) and size; and bait type. Fight time (i.e., the time from when the shark was hooked to the time it was landed) was recorded to the nearest second. Handling location, or position of the shark during landing, unhooking, and tagging, was recorded as 1 of 3 locations: shark left in water (i.e., the majority of the body, including the head and gills, remained in the water), shark brought to the water line (i.e., only a portion of the animal remained in the water; this location includes instances when wave action briefly exposed the head and gills to air), or shark removed from water (i.e., the entire shark was out of the water for the entirety of the handling event). Air and water temperature at the time of capture were also noted.

Biological assessment and tagging activities were conducted where the shark was landed, and efforts were made to note the sex, measure the fork length (FL) to the nearest centimeter, and apply a tag package that included an acceleration data logger (ADL) (methods described in the next section) while fishermen were removing or attempting to remove the hook, so as not to artificially extend handling time. Hooking location was noted (jaw, inside mouth [esophagus or pharynx], gills, gut [hook not visible or accessible], or body [foul hooked]) along with the disposition of the hook (removed or retained). The presence, location, and severity of bleeding (none, light, moderate, or heavy), overt signs of physical trauma (e.g., abrasions and lacerations), and the extent to which fishermen physically restrained the shark (e.g., holding the body of the shark in place during unhooking) were also noted. Handling time (i.e., the time from landing to release, including time needed for tagging) was recorded to the nearest second, and total capture and handling duration was noted as the sum of fight and handling times. Following tagging, fishermen were responsible for releasing the shark and left to determine if revival was necessary. Revival time was noted to the nearest second, if applicable. Finally, each shark was assigned a release condition based in part on the ordinal scale reported in Weber et al. (2020) (Table 1).

---

[2] Zewinski, K. 2021. Personal commun. Popul. Ecosyst. Monit. Anal. Div., Northeast Fish. Sci Cent., Natl. Mar. Fish. Serv., NOAA, 28 Tarzwell Dr., Narragansett, RI 02882.

Table 1

Release condition categories assigned to sandbar sharks (*Carcharhinus plumbeus*) captured off Cape Cod and Nantucket in Massachusetts from June through September in 2019–2021. Conditions are based in part on those used by Weber et al. (2020).

Category	Physical condition and release behavior
Excellent	No physical trauma other than hook wound, no bleeding, swam away rapidly
Good	No physical trauma other than hook wound, no bleeding, swam away slowly or appeared disoriented
Fair	Overt signs of physical trauma (abrasions and minor cuts), minor bleeding, swam away slowly or appeared disoriented
Poor	Overt signs of physical trauma (abrasions, minor cuts, and lacerations), moderate or severe bleeding, swam away slowly or appeared disoriented

Postrelease monitoring

To monitor the postrelease behavior and fate of sandbar sharks, custom tag packages that included an ADL and a float were created following the design outlined in Whitmore et al. (2016) and Whitney et al. (2021). Each package consisted of an ADL (Axy 4[3]; TechnoSmArt, Rome, Italy) that recorded triaxial acceleration at 25 Hz and depth and temperature every second, a SPOT-6 satellite transmitter (Wildlife Computers Inc., Redmond, WA), and a VHF transmitter (Advanced Telemetry Systems Inc., Isanti, MN). Each of these components was embedded in a custom tag float (107 × 68 × 50 mm in size and 151 g in weight in air). The package was designed to be <2% of the body weight of a tagged sandbar shark, meeting the recommended threshold intended to minimize the likelihood of tag-induced impairment to movement (Use of Fishes in Research Committee, 2014).

During tagging of each shark, 2 holes were drilled in the first dorsal fin, and a float package was secured on the left side of the fin (relative to the cranial–caudal axis) with cable ties, vinyl Peterson discs (Floy Tag & Mfg. Inc., Seattle, WA), and a galvanic timed release (GTR) (International Fishing Devices Inc., Northland, New Zealand). The GTRs dissolved in seawater and were sized in a manner to keep the ADL packages secured to sharks for a predetermined duration of approximately 1–4 d, and once that time was reached, the tags would release from the shark and float to the surface (Whitmore et al., 2016). The satellite transmitter would report its location through the Argos satellite network once it had reached the surface, and land- or sea-based excursions were made to recover the tag by using a multichannel VHF receiver (Advanced Telemetry Systems) following the methods described by Lear and Whitney (2016).

Data analysis

All analyses were performed by using the statistical software R (vers. 4.1.2; R Core Team, 2021), and statistical significance was accepted at $P<0.05$.

Capture and handling characteristics A series of qualitative and quantitative assessments were used to examine basic relationships between physical and biological aspects of the capture and handling events that may relate to release condition and PRM of sandbar sharks. Because of the opportunistic nature of sampling in this study, sample sizes were heavily unbalanced among many capture- and handling-related variables (e.g., line class, hooking location, and handling location) and autocorrelation structures violated model assumptions about sample independence (e.g., some anglers used only a single type or size of hook or line strength). Accordingly, box plots were created to qualitatively demonstrate general trends in the relationship between categorical variables related to capture and handling, with individual categories containing ≤5 observations.

Individual generalized linear models (GLMs) were constructed to quantitatively examine the effect of continuous and categorical variables with a sufficient number of observations on fight time and handling time. In fight time GLMs, data from a single anomalous capture event with an artificially inflated fight time were excluded from analysis (for a description of this event, see the "Results" section). Handling time GLMs were constructed with FL and *restraint* (binomial) as fixed effects. Data from 2 handling events were excluded from analysis because difficulties in the application of the ADL package artificially extended handling time beyond what was necessary for fishermen to prepare the shark for release. All GLMs were fit with data that had a Gaussian distribution in the R package lme4 (vers. 1.1-30; Bates et al., 2015). Model fit was assessed by visually examining residual plots.

Postrelease fate and mortality and survival rates After recovery of the ADL package, acceleration, depth, and temperature data were downloaded from the ADL, and the time of detachment of the package was noted as the time when the tag achieved an upright position and floated to the surface. To correct for variation in tag placement on the fin and attachment angle, acceleration data were rotated to be in the same orientation across all deployments. Rotation angles were determined by ensuring that the average acceleration of the *x*- and *y*-axis was close to 0; the *x*-axis correlated with the vertical velocity (i.e., ascending or descending in the water column), and the *y*-axis contained the largest dynamic acceleration. This approach ensured that the *x*-axis corresponded to the cranial–caudal axis of the animal (this axis pitches up and down as the animal ascends and descends), the *y*-axis corresponded to the lateral axis of the animal (which experiences dynamic acceleration during tailbeats), and the *z*-axis corresponded to the dorsal–ventral axis of the animal (Jorgensen et al., 2015).

---

[3] Mention of trade names or commercial companies is for identification purposes only and does not imply endorsement by the National Marine Fisheries Service, NOAA.

Static acceleration (accel) was calculated by using a 3-s (75-point) running mean of the raw data, and dynamic acceleration was calculated as the remainder when subtracting the dynamic acceleration from the raw acceleration (Shepard et al., 2008). Body pitch and roll were calculated from the static acceleration, and the overall dynamic body acceleration (ODBA) (Wilson et al., 2006) was calculated from the dynamic acceleration:

$$Roll = \tan^{-1}(Y_{\mathrm{accel}}, Z_{\mathrm{accel}}); \tag{1}$$

$$Pitch = \tan^{-1}(-X_{\mathrm{accel}}, Y_{\mathrm{accel}} \sin Roll + Z_{\mathrm{accel}} \cos Roll); \text{ and} \tag{2}$$

$$ODBA = \mathrm{abs}(X_{\mathrm{accel}}) + \mathrm{abs}(Y_{\mathrm{accel}}) + \mathrm{abs}(Z_{\mathrm{accel}}). \tag{3}$$

A continuous wavelet transformation of the *y*-axis acceleration data was used to calculate the power of periodicities over a period of 0.2–4.0 s by using the R package biwavelet, vers. 0.20.21 (Gouhier et al., 2021). The periodicity with the greatest power each second was ascribed as the individual's tailbeat period (TBP).

Postrelease fate was determined through visual examination of fine-scale vertical movement and acceleration profiles recorded by the ADL (Whitney et al., 2016, 2017, 2021). The sandbar shark is an obligate ram-ventilating species, and the fate of each shark at the time of tag detachment was assessed by using the following criteria:

Alive: consistent tailbeat patterns and changes in depth (i.e., vertical movements) and body position (i.e., pitch and roll) indicative of active swimming;
Dead: prolonged cessation of tailbeats in concert with a constant depth (indicative of rest on the seafloor); and
Predation: shift in the pitch and roll, an alteration of TBP and dive patterns, and potentially a lack of vertical thermal variation, which can indicate presence of the tag in a predator's stomach.

Total PRM was calculated as the proportion of all mortality events observed across monitored individuals. We calculated 95% confidence intervals (CIs) by using the Wilson method (Brown et al., 2001) in the R package binom, vers. 1.1-1 (Dorai-Raj, 2014).

Postrelease recovery period Behavioral recovery periods were evaluated for surviving sandbar sharks to address the sublethal effect of capture and handling on swimming or predator avoidance capabilities. Results from previous studies indicate that TBP is a suitable metric for assessing postrelease behavioral changes (e.g., Whitney et al., 2017, 2021; Grainger et al., 2022). Therefore, average TBP was calculated every 10 min from the time of release to 48 h after release for all sharks. With this approach, it has been found that behavioral recovery often occurs less than 10 h after release in multiple species (e.g., Whitney et al., 2017, 2021). Therefore, recovery time was not calculated for any sharks for which less than 10 h of postrelease acceleration data were available. Patterns in TBP were modeled by using nonlinear mixed effects models as an asymptotic relationship executed in the lme4 package (Bates et al., 2015):

$$TBP = A_{\mathrm{sym}} + \left(R_0 - A_{\mathrm{sym}}\right)\left(1 - e^{-e^{lrc}T}\right), \tag{4}$$

where A_{sym} = the fully recovered TBP;
R_0 = the TBP immediately after release;
lrc = the log rate constant that describes the rate at which recovery occurs; and
T = the time after release.

To account for the repeated measures of TBP for each individual over 48 h, we included random effects so that all 3 model parameters (A_{sym}, R_0, and lrc) varied by individual. Recovery period was defined as the time after release when TBP reached 80% of the difference between R_0 and A_{sym} (Whitney et al., 2016, 2017, 2021). By incorporating *individual* as a random effect, time to recovery could be calculated for each shark.

Fixed-effect GLMs were fit to time-to-recovery data to assess the influence of FL, fight time, handling time, and total time by using the lme4 package (Bates et al., 2015). Because of low and unequal samples sizes evident in some conditions nested in categorical variables (e.g., recovery time was only estimated for 2 sharks in poor condition and for 3 sharks that were left in the water), the following variables were excluded from models: hook disposition, handling location, and fish condition. Instead, box plots were created to qualitatively describe relationships between these variables and recovery period.

Tag detachment The results of the preliminary analysis of pitch, roll, and ODBA data revealed that numerous tagged sandbar sharks exhibited rolling behavior in which the body of the shark temporarily rolled >75° to the left (along the axis of forward motion, to the side with the ADL package) or to the right while the animal was actively swimming. In addition to these observations, multiple recovered float packages had scratches and abrasions, indicating that the rolling behavior might have resulted in contact of the tag with the seafloor. To investigate the extent to which rolling was linked to premature tag detachment, the depth, pitch, and roll of each individual were visually inspected for the 50 s surrounding the time of tag detachment. Tag detachment was identified as a positive pitch, indicating that the tag nose was pointed to the seafloor, while the depth was decreasing (i.e., the tag was floating to the surface). Rolling behavior was identified if individuals rolled to either the left or right side (>75°) while pitch values indicate that they were horizontal (<25° and >–25°) (Suppl. Figure) (online only). Additionally, this rolling behavior had to occur when the shark was presumed to be at the seafloor (i.e., within 1 m of the maximum depth the shark experienced in the 5 min before and after the roll) and <2 s prior to the estimated time of tag detachment. Each individual's tag detachment was categorized as associated with a left roll (<−75°) or a right roll (>75°) or was not associated with a roll.

To determine if rolls influenced tag retention, we analyzed the estimated error in tag retention across the 3 tag detachment categories. Release error was calculated as the duration the tag remained on the animal divided by the expected duration based on GTR size. Releases were classified as premature if the tag detached more than 25% (i.e., <−25%) earlier than expected. Release error was then compared across the 3 detachment categories to determine if rolling behavior immediately before a tag detachment influenced tag retention. Pairwise comparisons were performed by using Tukey's honestly significant difference (HSD) test. Data from tags that were retained on sharks for greater than 100% longer than the estimated GTR release time were excluded from analysis and were considered outliers.

Results

A total of 67 sandbar sharks (47 females and 20 males), measuring 113–187 cm FL (mean: 140 cm FL [standard deviation (SD) 17]), were captured by 21 volunteer recreational fishermen (9 novice, 7 intermediate, and 5 expert anglers) and were tagged with ADL packages from June through September in 2019 (sample size [n]=14), 2020 (n=8), and 2021 (n=45) (Suppl. Table) (online only). Females and males ranged from 113 to 187 cm FL (mean: 144 cm FL [SD 18]) and from 113 to 152 cm FL (mean: 132 cm FL [SD 12]), respectively. Individual anglers were observed capturing 1–20 sharks (mean: 3 sharks [SD 4]), with expert anglers accounting for the largest number of sharks captured (n=39). Novice and intermediate anglers captured 17 and 11 sharks, respectively.

To capture sandbar sharks, fishermen used a range of bait and tackle, including 13–36 kg (30–80 lb) class conventional (n=1) and spinning (n=66) rod and reel setups spooled with 13–36 kg braided main fishing line and steel single-strand wire (n=33) or multistrand cable (n=34) leaders with lengths of 0.6–1.2 m (~2–4 ft) and rated at weight test of 36–181 kg (80–400 lb). Sharks were primarily captured with 8/0–18/0 circle hooks (n=58, 86.6% of capture events), but 9 sharks (13.4% of events) were captured on 8/0–10/0 J-hooks (Table 2). To capture sharks, volunteers used a variety of natural baits, including cut sections of Atlantic menhaden (*Brevoortia tyrannus*), bluefish (*Pomatomus saltatrix*), and little tunny (*Euthynnus alletteratus*) and whole live or dead American eels (*Anguilla rostrata*).

Sandbar sharks were primarily hooked in the jaw (n=59, 88.1%) but were also hooked inside the mouth (n=2), in the gills (n=4), and on the body (pectoral fin, n=2). All hooking locations were observed with both circle and J-hooks; however, a larger percentage of sharks caught on J-hooks were hooked inside the mouth, in the gills, or on the body (Fig. 1). Anglers removed hooks from 92.5% of captured sharks (n=62); the leader was cut and the hook retained in 5 sharks caught on circle hooks, 3 sharks hooked in the jaw and 2 sharks hooked in the gills. The majority of sharks had no bleeding or had minor bleeding localized around the hook wound. Two sharks hooked in the gills experienced heavy bleeding. In one of these animals, the J-hook was removed by using a dehooking device, and in the other, the leader was cut, leaving the circle hook embedded in the gills. Fight times ranged from 2.57 to 32.40 min (mean: 6.90 min [SD 4.75]), and 98.5% of fight times were less than 20 min. The longest fight time (32.40 min) was observed when a fisherman, fishing alone, hooked 2 sandbar sharks at the same time and did not begin retrieving the second animal until the first was released. Excluding this anomalous capture event, there was a significant positive relationship between shark FL and fight time (coefficient of multiple determination [R^2]=0.306, P<0.001) (Fig. 2A).

Table 2

Breakdown of data collected for the 67 sandbar sharks (*Carcharhinus plumbeus*) for which land-based capture and handling events were observed during June–September in 2019, 2020, and 2021 in Massachusetts.

	Observations	
Variable	Number	Percentage
Sex		
Females	47	70.1
Males	20	29.9
Hook type		
Circle	58	86.6
J	9	13.4
Hooking location		
Jaw	59	88.1
Mouth	2	3.0
Gills	4	6.0
Body	2	3.0
Hook disposition		
Removed	62	92.5
Retained	5	7.5
Handling location		
Brought out of water	23	34.3
Brought to water line	39	58.2
Left in water	5	7.5
Shark restrained		
Yes	47	70.1
No	20	29.9
Fish condition at release		
Excellent	16	23.9
Good	44	65.7
Fair	5	7.5
Poor	2	3.0
Bleeding		
None	62	92.5
Light	2	3.0
Moderate	1	1.5
Heavy	2	3.0

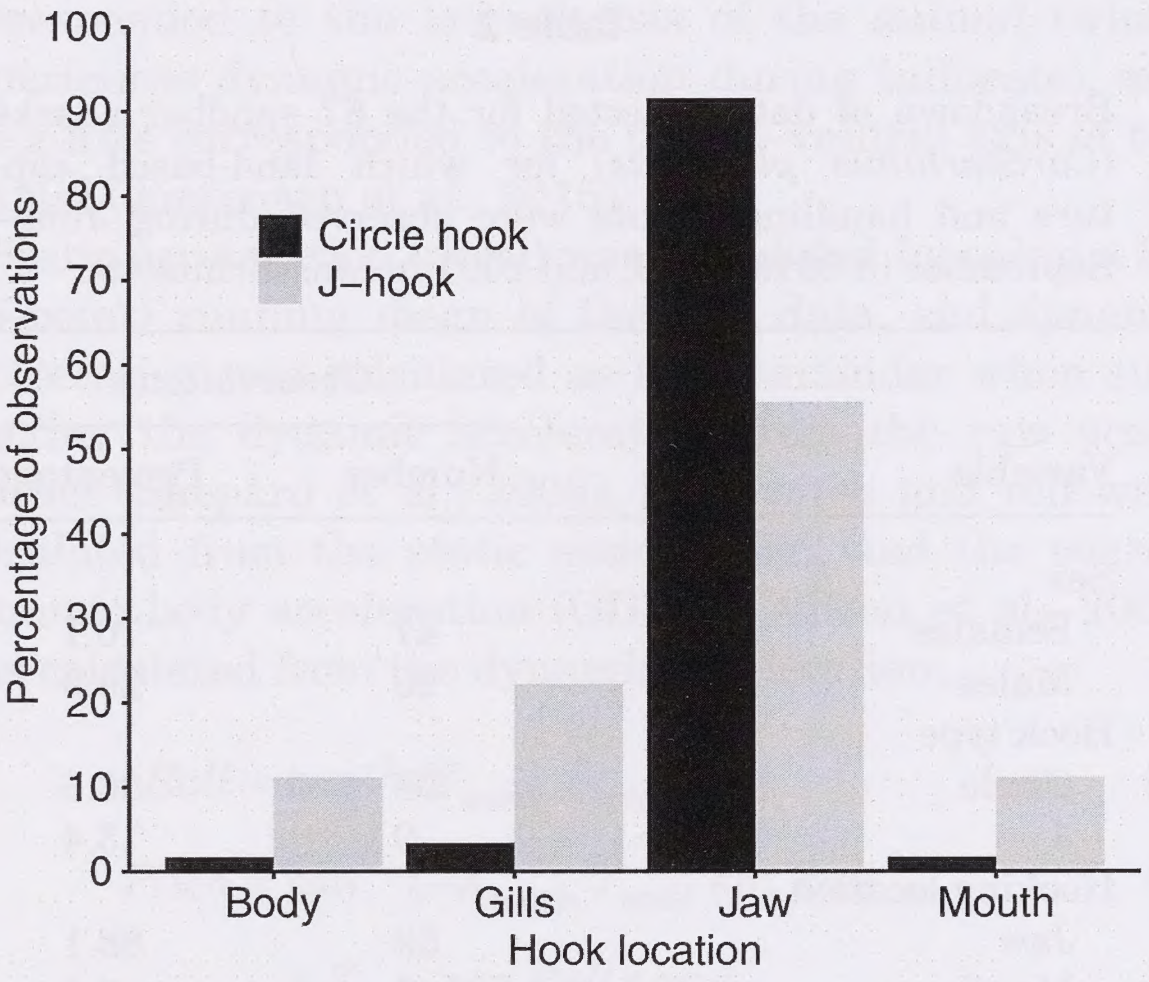

Figure 1

Relative percentage of hook locations observed by hook type for 67 sandbar sharks (*Carcharhinus plumbeus*) captured off Cape Cod and Nantucket in Massachusetts from June through September in 2019–2021. Fifty-eight sharks were caught on circle hooks, and 9 sharks were caught on J-hooks. Use of circle hooks yielded a higher percentage of capture events in which sharks were hooked in the jaw, and use of J-hooks had a higher probability of hooking sharks on the body, in the gills, or inside the mouth.

Once brought into the surf zone, sharks in the majority of cases were dragged to the water line (*n*=39, 58.2%) or completely out of the water (*n*=23, 34.3%) by fishermen holding them by the tail. Anglers left the shark in the water in 5 instances (7.5% of observed capture events). Forty-seven sharks (70.1%) were restrained during handling. Handling times ranged from 1.50 to 9.25 min (mean: 3.82 min [SD 1.27]), yielding total capture and handling event times of 5.25–34.33 min (mean: 10.72 min [SD 4.96]). There was a significant, positive relationship between FL and handling time (R^2=0.131, *P*<0.001) (Fig. 2B), but handling time was not significantly affected by the restraint of sharks (*P*=0.152). Qualitatively, sharks that were handled in the water or that were hooked in the gills generally experienced longer handling times (Fig. 3). At the time of release, all sharks were alive and assigned the following release conditions: excellent (*n*=16), good (*n*=44), fair (*n*=5), and poor (*n*=2). During handling, sharks experienced air temperatures ranging from 15.9°C to 28.9°C (mean: 23.4°C [SD 2.9]) and were captured in water temperatures ranging from 21.2°C to 27.7°C (mean: 24.1°C [SD 1.7]).

Tag recovery and performance

All 67 ADL packages deployed on sandbar sharks detached and were recovered. Forty-one tags were recovered at sea, and 26 tags were recovered after washing ashore on Cape Cod or Nantucket. The ADLs remained attached to sandbar sharks for periods of 0.15–9.98 d (mean: 2.67 d [SD 2.08]) or 3.6–239.5 h (mean: 64.0 h [SD 49.9]). Two ADLs malfunctioned and did not record any data during the deployment period, and 3 ADLs stopped recording prior to detaching. Altogether, data sufficient for determining postrelease fate were available from 65 ADLs. A total of 27 tags (40.3%) released prematurely, earlier than their expected time based on the size of the GTR used.

Postrelease survival and recovery

Results from the examination of the depth, TBP, pitch, and roll time series from the 65 ADLs reveal high survivorship for tagged sharks. All sharks were alive at the time of tag detachment, yielding a PRM rate of 0% (95% CI: 0.0–5.6%) or survival rate of 100% (95% CI: 94.4–100%).

Time to recovery was estimated for 54 of 56 sandbar sharks with at least 10 h of postrelease acceleration data. Recovery time was not estimated for 2 sharks whose TBP failed to reach their recovery value (i.e., 80% of the fully recovered TBP) and whose change in TBP was in the lowest 25th percentile during the time from release to 48 h after release. Of note, both of these sharks consistently had a TBP that was similar to the “recovered” values of the 54 sharks for which recovery time was estimated. Behavioral recovery in TBP for the 54 sharks was evident from 1.33 to 17.18 h after release (mean: 6.36 h [SD 3.52]) (Fig. 4). Results from the GLMs reveal no significant relationships between recovery time and fight time, handling time, total time, or FL (*P*>0.11). However, findings from qualitative analyses with box plots provide some evidence that sharks hooked in the gills and classified in fair or poor condition took longer to recover (Fig. 5).

Tag detachment

Tag detachment in association with rolling behavior was examined for 60 individuals whose ADLs recorded data at the time of release. In 32 instances (53.3%), tags appeared to detach without any clear indication of rolling behavior. These tags detached close (mean: −9.2% [SD 36.1]) to the expected GTR duration, and only 25.0% (*n*=8) of these tags released prematurely (Fig. 6). Rolling was observed in 28 instances (46.7%) of tag detachment, including 11 instances (39.3%) when sharks rolled to the right (non-tag side) and 17 cases (60.7%) when sharks rolled to the left side (tag side). Only 4 tag detachments associated with rolls to the right (36.4%) occurred prematurely, a number that is not significantly different than the number of premature detachments not associated with rolling behavior (*n*=6) (Tukey’s HSD test: *P*=0.99). However, 88.2% (*n*=15) of tag detachments associated with rolls to the left side occurred prematurely, significantly earlier than detachments associated with rolls to the right (Tukey’s HSD test: *P*<0.001) and with detachments that were not associated with rolling behavior (Tukey’s HSD test: *P*<0.001). In total, 55.6% (*n*=15) of all premature releases (*n*=27) occurred when sharks rolled to their left side.

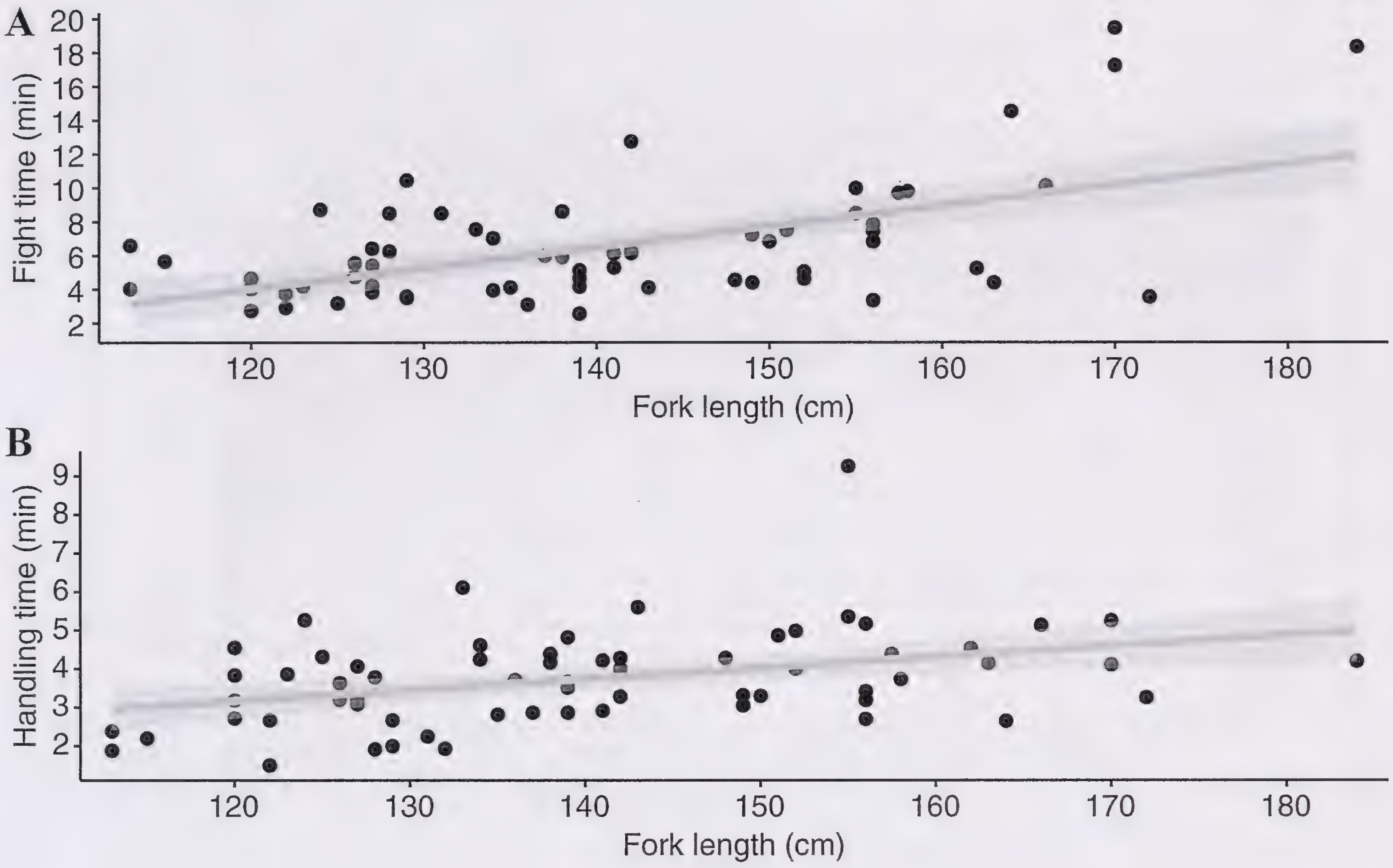

Figure 2

Relationship of (**A**) fight time (sample size [*n*]=66) and (**B**) handling time (*n*=65) with fork length (FL) for sandbar sharks (*Carcharhinus plumbeus*) captured in Massachusetts during 2019–2021. The gray line represents the linear relationship, and the gray shaded area indicates the standard error around the predicted relationship. In panel A, data for a single 32-min event of the capture of a 132-cm-FL female shark was excluded (and not plotted) because the volunteer angler hooked 2 sharks simultaneously and did not begin reeling this shark in until the first one was released. In panel B, data for 2 handling events were excluded because of difficulties in applying the acceleration data logger package that artificially extended handling time.

Discussion

The lack of mortality (100% survival) observed in sandbar sharks following land-based catch-and-release activities adds to the growing body of evidence that this species is resilient and capable of surviving both the physical and physiological effects of capture and handling (e.g., Marshall et al., 2015; Whitney et al., 2021). Postrelease mortality of sharks caught on recreational hook-and-line fishing gear has been linked to physical trauma from internal hooking in the gut or gills (Kneebone et al., 2013; French et al., 2015; Kilfoil et al., 2017), foul hooking on the body (Sepulveda et al., 2015; Weber et al., 2020), extended fight times due to foul hooking (Heberer et al., 2010), and prolonged handling times (Mohan et al., 2020; Knotek et al., 2022). However, in our study, no mortality was identified in 2 sandbar sharks that were hooked in the gills and were bleeding severely at the time of release, with one foul-hooked individual having been fought for 32.40 min (i.e., nearly 5 times longer than the mean fight time observed across all sharks). In addition, no mortality was observed in 23 individuals that were completely removed from the water for 2.20–6.67 min during handling. These observations and the finding that the majority (90%) of sharks monitored in our study were released in excellent or good condition indicate that sandbar sharks are likely to survive land-based catch-and-release fishing in Massachusetts, as long as best practices are used consistently throughout the fishery.

Despite the resilience of this species, it should be understood that the true PRM rate of sandbar sharks caught and released by using land-based techniques in Massachusetts is most certainly greater than zero. Indeed, our research team necropsied 2 sandbar sharks that washed ashore 24–36 h after they were caught and released by land-based fishermen, as confirmed by the presence of an M-tag of the National Marine Fisheries Service Cooperative Shark Tagging Program in each carcass and information reported (by the capturing anglers) to this program (Zewinski[2]). Although the capture-and-handling event was not directly observed for either shark, anglers mentioned in their testimonials that 1 shark was hooked "deep" and was bleeding heavily during hook removal and that the other shark seemed physically exhausted and would not swim away despite being revived for several minutes. The specific cause of these mortalities cannot be determined, but their occurrence confirms that mortality can, and does, occur in the land-based shark fishery. For this reason, we recommend that a PRM rate of 5.6% (the upper limit of the 95% CI) be used when estimating mortality for stock assessment purposes.

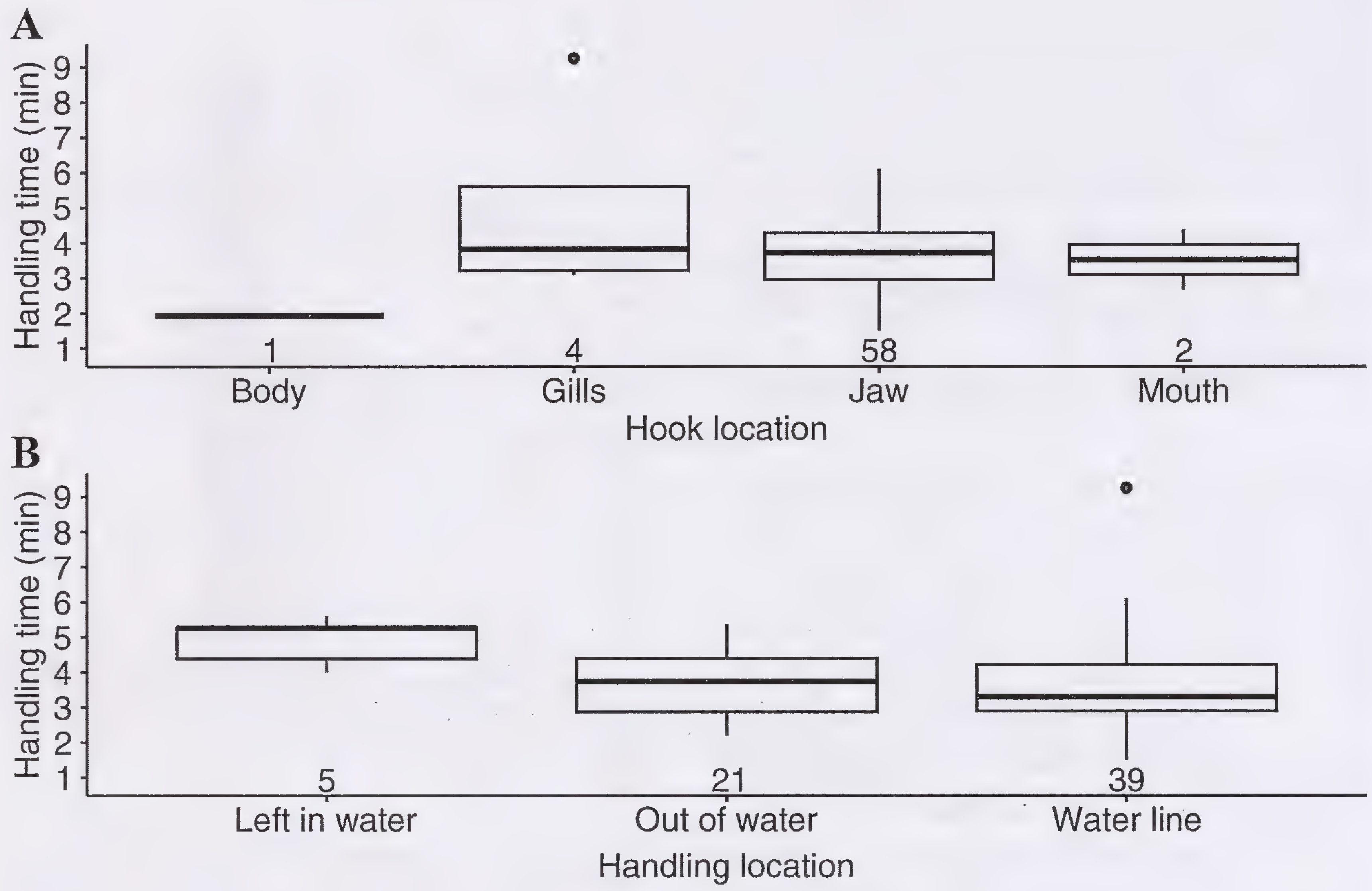

Figure 3

Box plots of the relationship of (**A**) hook location and (**B**) handling location with handling time for sandbar sharks (*Carcharhinus plumbeus*) captured in Massachusetts in 2019–2021. The numerals below the plots are the sample sizes for the types of hook and handling locations. The thick line within each box indicates the median, the upper and lower parts of each box represent the first and third quartiles (the 25th and 75th percentiles), the whiskers extending above and below each box correspond to 1.5 times the interquartile range, and the dots represent values outside this range.

Behavioral recovery from land-based catch and release occurred relatively rapidly in sandbar sharks (1.33–17.18 h), with 63% of individuals in our study recovering within 6.36 h after release (i.e., the mean recovery observed over all individuals). This mean recovery time is comparable to, but also faster than, what has been estimated for blacknose (*C. acronotus*) (11.7 h, Knotek et al., 2022), blacktip (10.5 h, Whitney et al., 2017; 29.6 h, Binstock et al., 2023), and bull (8.0 h, Binstock et al., 2023) sharks following catch and release in recreational fishing events and for sandbar sharks following capture in bottom longline fishing (11.7 h, Whitney et al., 2021). Although low and unequal sample sizes precluded statistical analysis in our study, sharks that incurred physical injury from being hooked in the gills or that were foul hooked and in poorer condition at release had longer recovery times than uninjured sharks (Fig. 5). A similar relationship has also been found for tiger sharks following bottom longline capture (Whitney et al., 2021). The ability of sandbar sharks to rapidly recover from land-based catch and release is likely a major factor contributing to the high survivorship observed in this fishery.

Postrelease monitoring periods achieved in our study were relatively short (mean: 2.5 d, 60 h) but were sufficient for monitoring the period during which the majority of PRM typically occurs in sharks (Ellis et al., 2017). For example, Whitney et al. (2021) documented that all (n=61) PRM events for several carcharhinid sharks, including sandbar sharks, occurred within 12 h, and Weber et al. (2020) reported that all PRM events for blacktip sharks caught in a land-based shark fishery occurred within 6 h of release, despite their monitoring of animals for weeks after release. These trends, combined with the direct observation of the mortalities of 2 sandbar sharks within 24–36 h of release (see the previous mention of necropsies in this “Discussion” section), provide strong evidence that the durations of ADL package deployments achieved in this study were sufficient for the detection of the majority of mortality events. This notion is also supported by reports from several other studies on recreationally caught sharks documenting that most or all PRM events occur within 24 h (e.g., Heberer et al., 2010; French et al., 2015; Whitney et al., 2017; Mohan et al., 2020). Nonetheless, it is possible that mortality occurred after monitoring ceased, particularly for the few sharks that were hooked in the gills or experienced physical trauma (e.g., Kneebone et al., 2013). Regardless, undocumented, delayed mortalities of sharks in poor condition were unlikely to have yielded total PRM rates exceeding the upper value of the 95% CI (i.e., 5.6%).

The experience level and attitudes of volunteer anglers may have contributed to the high survivorship of sandbar sharks monitored during this study. Efforts were made to observe anglers of all experience levels, but there was no

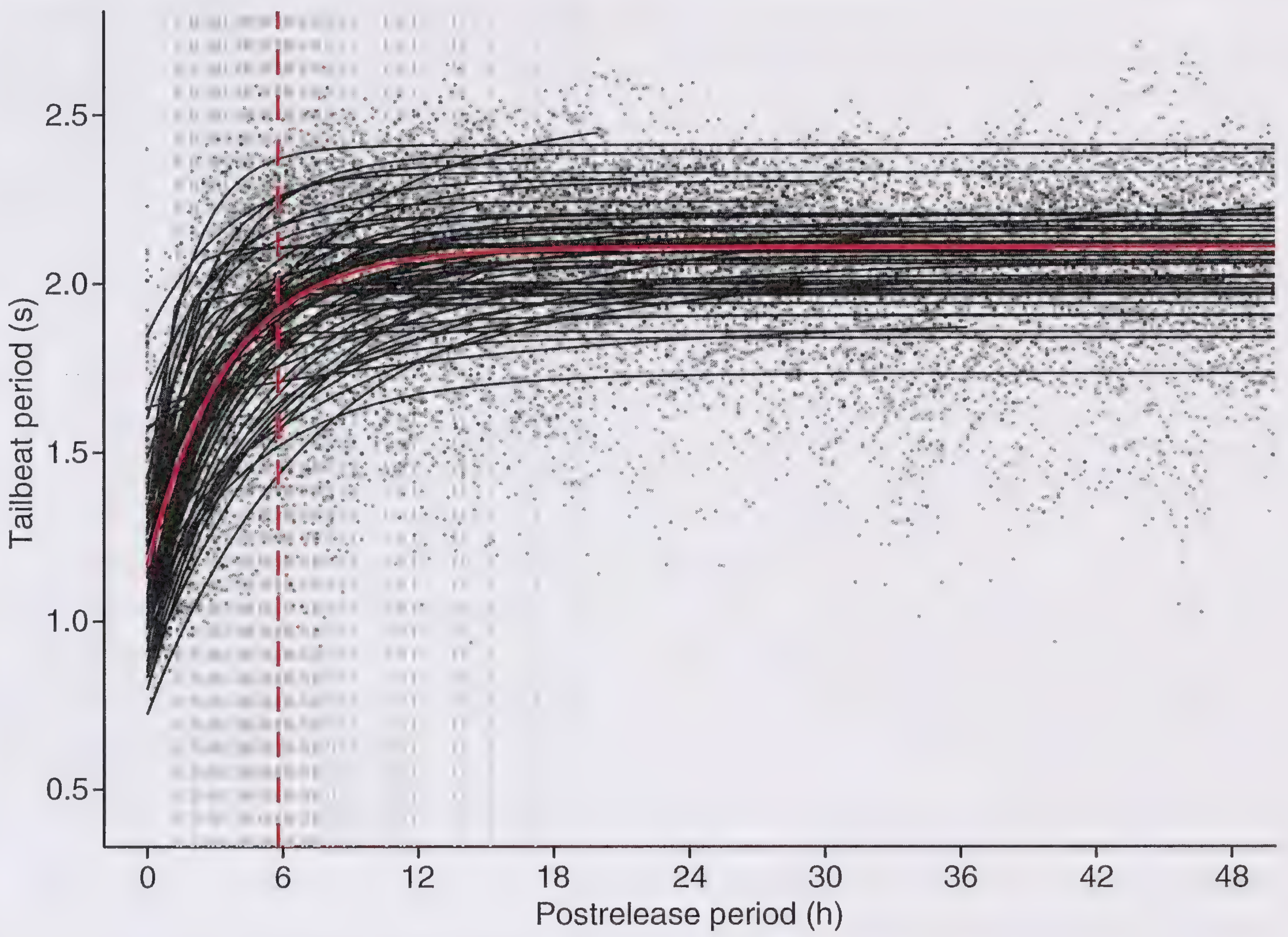

Figure 4

Estimated periods for postrelease behavioral recovery of 54 sandbar sharks (*Carcharhinus plumbeus*) for which at least 10 h of acceleration data were available. Sharks were captured in Massachusetts from June through September in 2019–2021. Recovery was modeled as a function of the tailbeat period (TBP) in seconds. The solid dark gray lines represent nonlinear mixed model estimates of TBP, and the vertical dashed gray lines indicate when behavioral recovery occurred (i.e., when TBP reached 80% of its asymptote). The solid red line depicts the nonlinear mixed model estimate for all sharks combined, and the vertical dashed red line represents the predicted recovery time over all sharks. The gray dots represent the average 10-min TBP calculated for each shark; darker shades of gray indicate overlapping values.

discernable effect of angler experience on fight time, handling time, or animal release condition. Furthermore, volunteer fishermen of all experience levels used similar techniques and fishing gear to capture and handle sandbar sharks, and many anglers expressed their intent to minimize fight and handling times however possible. Similar acknowledgement of the need to reduce negative effects of land-based recreational shark fishing has been observed in surveys of land-based shark fishermen in Florida (Guay et al., 2021) and Texas (Gibson Banks et al., 2023). Nevertheless, multiple anglers used J-hooks to capture sandbar sharks, a violation of current Massachusetts state law. Candid conversations with these anglers revealed that some of them were unaware of the regulation requiring circle hooks and that others assumed the hooks they purchased were circle hooks or never transitioned to circle hooks because of their familiarity with the use of J-hooks but not circle hooks. Given that J-hooks were more likely to hook sandbar sharks in places other than the jaw, improved outreach is needed to better inform land-based shark fishermen of fishing regulations and the benefits of using circle hooks to reduce physical injury.

Premature detachment of an ADL package was frequently encountered during this study (40.3% of packages were released more than 25% prematurely). The cause of premature release could not be determined in every instance; however, the correlation between shark rolling behavior and tag detachment provides evidence that some of the packages released because the sharks rubbed against the bottom. Identifying positional changes of animals from acceleration-only data during highly dynamic movements can be difficult (Noda et al., 2014), and it was particularly challenging to identify the exact instant when a tag detached from an animal (i.e., when acceleration data transitioned from indicating shark movements to indicating the release of a tag). Together, these factors introduced the potential for incorrect categorization of rolling behavior during tag release. However, the observation that premature releases were more common when sharks rolled to the left side supports our hypothesis of behaviorally driven detachment because rolling to the left would bring the tag package toward the seafloor. In the context of postrelease survival, the observance of rolling behavior in 19 of 27 instances (70.4%) of premature tag

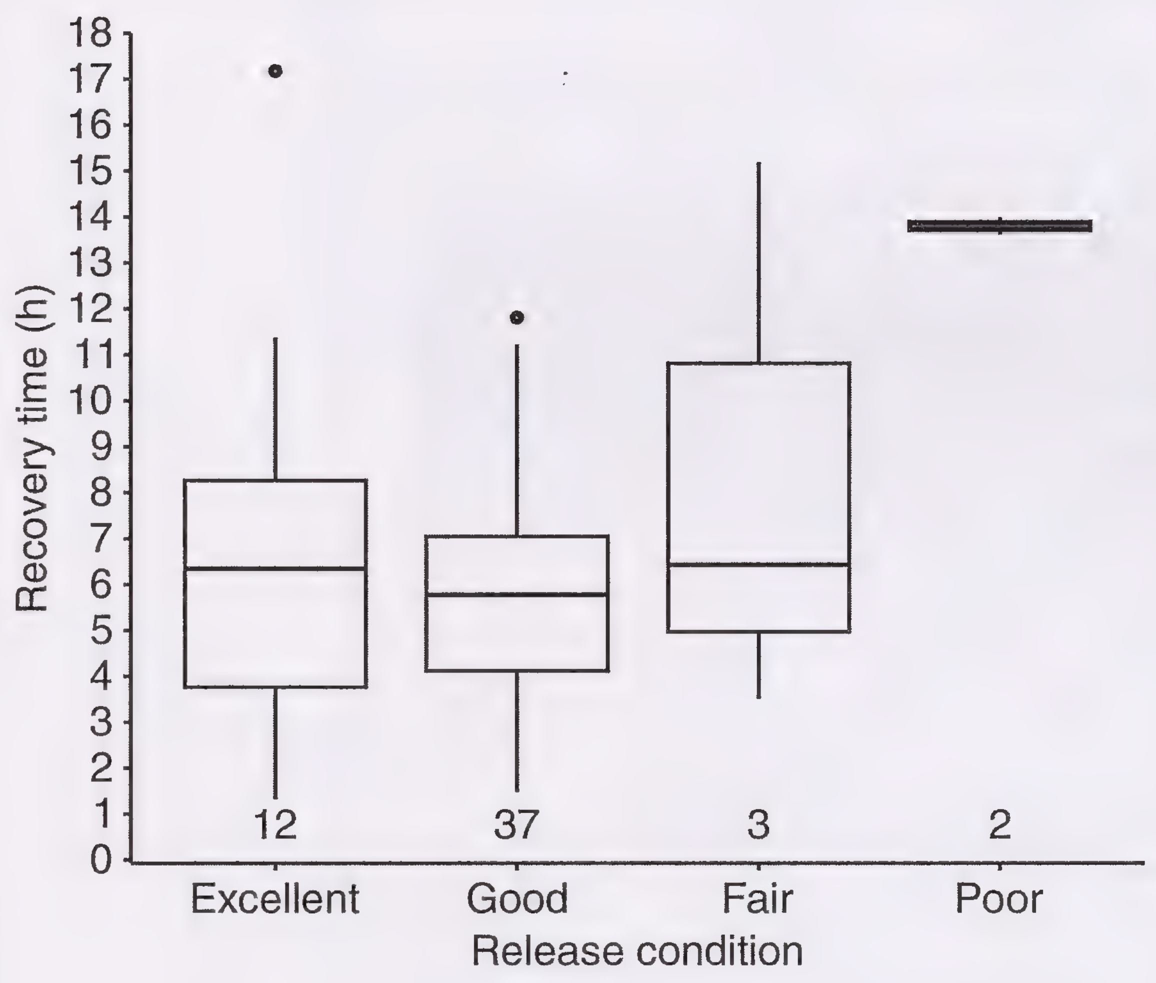

Figure 5

Box plots of the relationship between release condition and behavioral recovery period for sandbar sharks (*Carcharhinus plumbeus*) captured in Massachusetts during 2019–2021. The numerals below the plots are the sample sizes for the release conditions. The thick line within each box indicates the median, the upper and lower parts of each box represent the first and third quartiles (the 25th and 75th percentiles), the whiskers extending above and below each box correspond to 1.5 times the interquartile range, and the dots represent values outside this range.

release is evidence of animal vigor and indicates that the individuals in these instances were likely to survive following premature detachment of the ADL package.

Conclusions

The results of this study provide strong evidence that land-based catch-and-release fishing for sandbar sharks in Massachusetts is a sustainable practice when state regulations and best-practice guidelines are followed. Although total catch of sandbar sharks of the land-based shark fishery in Massachusetts, as well as across all U.S. states, is not well quantified, our estimated PRM rate of 5.6% indicates that incidental mortality in this fishery is very low and should minimally affect the ongoing recovery of the sandbar shark population in the Atlantic Ocean and Gulf of Mexico. Regardless, outreach efforts, particularly those targeting new entrants into the land-based fishery, should promote the awareness and use of best practices and compliance with existing state shark fishing regulations (e.g., requirements to use circle hooks and to leave animals in the water). Future research should be conducted to estimate PRM of sandbar sharks in land-based fisheries occurring in other states or regions where environmental conditions (e.g., warmer air and water temperatures) and handling practices may be different.

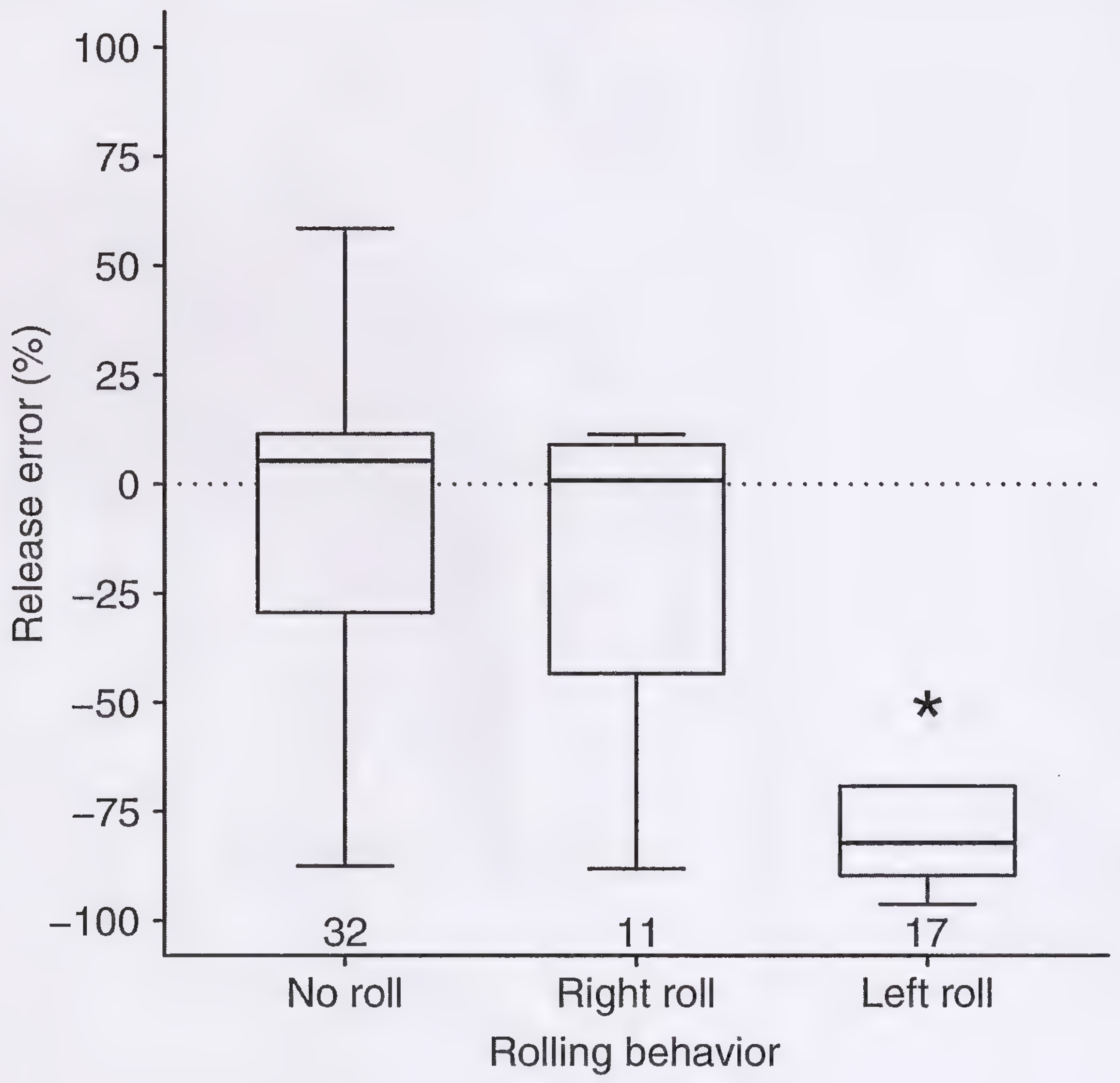

Figure 6

Box plots of the timing of the release of tag packages in relation to observations of rolling behavior at the time of tag release for sandbar sharks (*Carcharhinus plumbeus*) captured in Massachusetts during 2019–2021. Release error represents the deviation from the expected time of release (based on the size of the galvanic timed release used), with positive values indicating delayed release and negative values indicating premature release. The asterisk (*) denotes a significant difference in the occurrence of premature release following rolls to the left side (tag side). The numerals below the plots are the sample sizes for the rolling behaviors. The thick line within each box indicates the median, the upper and lower parts of each box represent the first and third quartiles (the 25th and 75th percentiles), and the whiskers extending above and below each box correspond to 1.5 times the interquartile range.

Resumen

La captura y liberación de tiburones aleta de cartón (*Carcharhinus plumbeus*) en la pesca recreativa de orilla es cada vez más popular en Massachusetts. En colaboración con 21 pescadores voluntarios con distintos niveles de experiencia, observamos y documentamos los artes de pesca, los cebos y las técnicas empleadas para capturar y liberar 67 tiburones aleta de cartón. El destino de cada tiburón liberado se monitoreó utilizando una marca de registro de datos de aceleración (ADL) incrustada en un paquete flotador personalizado que se fijó a la primera aleta dorsal con una liberación galvánica temporal. Los 67 paquetes se recuperaron tras su desprendimiento después de periodos de seguimiento de 0.15-9.98 d. El examen de las series temporales de profundidad, periodo de latido de la cola (TBP), cabeceo y balanceo de 65 ADL que registraron datos reveló una elevada supervivencia de los tiburones marcados, todos ellos vivos al momento del desprendimiento de la marca. Se estimó que la recuperación del comportamiento se había producido de 6.36 h en promedio, después de la liberación, con base en las tendencias del TBP de 54 tiburones aleta de cartón con al menos 10 h de datos de aceleración tras la liberación. Estos resultados indican que los tiburones aleta de cartón son notablemente resistentes a la captura y liberación en la pesquería de orilla de tiburones de Massachusetts.

Acknowledgments

This research would not have been possible without the cooperation of volunteer recreational fishermen who allowed their catch to be sampled. We especially thank J. Malloy, S. Coffey, R. Franklin, B. Sherman, D. McElroy, and M. Winton for their generosity in and dedication to helping this project achieve its goals. This work was supported by award NA18NMF4720289 from the NOAA Bycatch Reduction and Engineering Program.

Literature cited

Bates, D., M. Mächler, B. Bolker, and S. Walker.
2015. Fitting linear mixed-effects models using lme4. J. Stat. Soft. 67:1–48.

Binstock, A. L., T. M. Richards, R. D. Wells, J. M. Drymon, K. Gibson-Banks, M. K. Streich, G. W. Stunz, C. F. White, N. M. Whitney, and J. A. Mohan.
2023. Variable post-release mortality in common shark species captured in Texas shore-based recreational fisheries. PLoS ONE 18(2):e0281441.

Brown, L. D., T. T. Cai, and A. DasGupta.
2001. Interval estimation for a binomial proportion. Stat. Sci.16:101–133.

Dorai-Raj, S.
2014. binom: binomial confidence intervals for several parameterizations. R package, vers. 1.1-1. [Available at website, accessed April 2023.]

Ellis, J. R., S. R. McCully Phillips, and F. Poisson.
2017. A review of capture and post-release mortality of elasmobranchs. J. Fish Biol. 90:653–722.

French, R. P., J. Lyle, S. Tracey, S. Currie, and J. M. Semmens.
2015. High survivorship after catch-and-release fishing suggests physiological resilience in the endothermic shortfin mako shark (*Isurus oxyrinchus*). Conserv. Physiol. 3:cov044.

Gibson, K. J., M. K. Streich, T. S. Topping, and G. W. Stunz.
2019. Utility of citizen science data: a case study in land-based shark fishing. PLoS ONE 14(12):e0226782.

Gibson Banks, K., M. K. Streich, J. M. Drymon, S. B. Scyphers, J. A. Mohan, R. J. D. Wells, A. L. Binstock, T. M. Richards, C. F. White, N. M. Whitney, et al.
2023. Talk is cheap: direct evidence of conservation-based changes in angler behavior. Conserv. Sci. Pract. 5(9):e13001.

Gouhier, T. C., A. Grinsted, and V. Simko.
2021. biwavelet: conduct univariate and bivariate wavelet analyses. R package, vers. 0.20.21. [Available at website, accessed September 2022.]

Grainger, R., D. Raubenheimer, V. M. Peddemors, P. A. Butcher, and G. E. Machovsky-Capuska.
2022. Integrating biologging and behavioral state modeling to identify cryptic behaviors and post-capture recovery processes: new insights from a threatened marine apex predator. Front. Mar. Sci. 8:791185.

Guay, J. D., J. L. Brooks, J. M. Chapman, H. Medd, S. J. Cooke, and V. M. Nguyen.
2021. Survey-derived angler characteristics and perspectives in the shore-based shark fishery in Florida. Mar. Coast. Fish. 13:693–711.

Heberer, C., S. A. Aalbers, D. Bernal, S. Kohin, B. DiFiore, and C. A. Sepulveda.
2010. Insights into catch-and-release survivorship and stress-induced blood biochemistry of common thresher sharks (*Alopias vulpinus*) captured in the southern California recreational fishery. Fish. Res. 106:495–500.

Hutt, C. P., and G. Silva.
2019. The economic contributions of Atlantic highly migratory anglers and tournaments, 2016. NOAA Tech. Memo. NMFS-OSF-8, 44 p.

Jorgensen, S. J., A. C. Gleiss, P. E. Kanive, T. K. Chapple, S. D. Anderson, J. M. Ezcurra, W. T. Brandt, and B. A. Block.
2015. In the belly of the beast: resolving stomach tag data to link temperature, acceleration and feeding in white sharks (*Carcharodon carcharias*). Anim. Biotelem. 3:52.

Kilfoil, J. P., B. M. Wetherbee, J. K. Carlson, and D. A. Fox.
2017. Targeted catch-and-release of prohibited sharks: sand tigers in coastal Delaware waters. Fisheries 42:281–287.

Kneebone, J., J. Chisholm, D. Bernal, and G. Skomal.
2013. The physiological effects of capture stress, recovery, and post-release survivorship of juvenile sand tigers (*Carcharias taurus*) caught on rod and reel. Fish. Res. 147:103–114.

Knotek, R. J., B. S. Frazier, T. S. Daly-Engel, C. F. White, S. N. Barry, E. J. Cave, and N. M. Whitney.
2022. Post-release mortality, recovery, and stress physiology of blacknose sharks, *Carcharhinus acronotus*, in the Southeast U.S. recreational shark fishery. Fish. Res. 254:106406.

Lear, K. O., and N. M. Whitney.
2016. Bringing data to the surface: recovering data loggers for large sample sizes from marine vertebrates. Anim. Biotelem. 4:12.

Marshall, H., G. Skomal, P. G. Ross, and D. Bernal.
2015. At-vessel and post-release mortality of the dusky (*Carcharhinus obscurus*) and sandbar (*C. plumbeus*) sharks after longline capture. Fish. Res. 172:373–384.

Mohan, J. A., E. R. Jones, J. M. Hendon, B. Falterman, K. M. Boswell, E. R. Hoffmayer, and R. J. D. Wells.
2020. Capture stress and post-release mortality of blacktip sharks in recreational charter fisheries of the Gulf of Mexico. Conserv. Physiol. 8:coaa041.

Noda, T., Y. Kawabata, N. Arai, H. Mitamura, and S. Watanabe.
2014. Animal-mounted gyroscope/accelerometer/magnetometer: in situ measurement of the movement performance of fast-start behaviour in fish. J. Exp. Mar. Biol. Ecol. 451:55–68.

R Core Team.
2021. A language and environment for statistical computing. R Foundation for Statistical Computing, Vienna, Austria. [Available from website, accessed January 2022.]

Regulation of catches, Division of Marine Fisheries regulations, 322 Code Mass. Regul. 6.00 (Mass. Regist. 2023). [Available from website.]

SEDAR (Southeast Data, Assessment, and Review).
2017. SEDAR 54 stock assessment report: HMS sandbar shark, 179 p. SEDAR, North Charleston, SC. [Available at website.]

Sepulveda, C. A., C. Heberer, S. A. Aalbers, N. Spear, M. Kinney, D. Bernal, and S. Kohin.
2015. Post-release survivorship studies on common thresher sharks (*Alopias vulpinus*) captured in the southern California recreational fishery. Fish. Res. 161:102–108.

Sharks and rays, Fla. Admin. Code Regist. Chapter 68B-44 (2019). [Available from website.]

Shepard, E. L. C., R. P. Wilson, L. G. Halsey, F. Quintana, A. Gómez Laich, A. C. Gleiss, N. Liebsch, A. E. Myers, and B. Norman.
2008. Derivation of body motion via appropriate smoothing of acceleration data. Aquat. Biol. 4:235–241.

Shiffman, D. S., C. Macdonald, H. Y. Ganz, and N. Hammerschlag.
2017. Fishing practices and representations of shark conservation issues among users of a land-based shark angling online forum. Fish. Res. 196:13–26.

Skomal, G. B.
2007. Shark nursery areas in the coastal waters of Massachusetts. Am. Fish. Soc. Symp. 50:17–33.

Use of Fishes in Research Committee (joint committee of the American Fisheries Society, the American Institute of Fishery Research Biologists, and the American Society of Ichthyologists and Herpetologists).
2014. Guidelines for use of fishes in research, 83 p. Am. Fish. Soc., Bethesda, MD. [Available from website.]

Weber, D. N., B. S. Frazier, N. M. Whitney, J. Gelsleichter, and G. Sancho.
2020. Stress response and postrelease mortality of blacktip sharks (*Carcharhinus limbatus*) captured in shore-based and charter-boat-based recreational fisheries. Fish. Bull. 118:297–314.

Whitmore, B. M., C. F. White, A. C. Gleiss, and N. M. Whitney.
2016. A float-release package for recovering data-loggers from wild sharks. J. Exp. Mar. Biol. Ecol. 475:49–53.

Whitney, N. M., C. F. White, A. C. Gleiss, G. D. Schwieterman, P. Anderson, R. E. Hueter, and G. B. Skomal.
2016. A novel method for determining post-release mortality, behavior, and recovery period using acceleration data loggers. Fish. Res. 183:210–221.

Whitney, N. M., C. F. White, P. A. Anderson, R. E. Hueter, and G. B. Skomal.
2017. The physiological stress response, postrelease behavior, and mortality of blacktip sharks (*Carcharhinus limbatus*) caught on circle and J-hooks in the Florida recreational fishery. Fish. Bull. 155:532–543.

Whitney, N. M., K. O. Lear, J. J. Morris, R. E. Hueter, J. K. Carlson, and H. M. Marshall.
2021. Connecting post-release mortality to the physiological stress response of large coastal sharks in a commercial longline fishery. PLoS ONE 16(9):e0255673.

Wilson, R. P., C. R. White, F. Quintana, L. G. Halsey, N. Liebsch, G. R. Martin, and P. J. Butler.
2006. Moving towards acceleration for estimates of activity-specific metabolic rate in free-living animals: the case of the cormorant. J. Anim. Ecol. 75:1081–1090.

National Marine
Fisheries Service
NOAA

Fishery Bulletin
established in 1881

Spencer F. Baird
First U.S. Commissioner
of Fisheries and founder
of *Fishery Bulletin*

Variation in otolith microchemistry for Lebranche mullet (*Mugil liza*) in southern Brazil and its potential use in identifying their nursery grounds

Valéria M. Lemos (contact author)[1]
Ana C. G. Mai[1]
Ana C. Martins[2]
José V. Martins[3]
Sandra Andrade[3]
Henrique Cabral[4]
João P. Vieira[1]

Email address for contact author: vavadeleom@yahoo.com.br

[1] Laboratório de Ictiologia
Instituto de Oceanografia
Universidade Federal do Rio Grande
Avenida Italia km 8, S/N
Campus Carreiros
Rio Grande, Rio Grande do Sul 96203-900, Brasil

[2] Laboratório de Estatística Ambiental
Universidade Federal do Rio Grande
Avenida Italia km 8, S/N
Campus Carreiros
Rio Grande, Rio Grande do Sul 96203-900, Brasil

[3] Laboratório de Química e ICP
Instituto de Geociências
Universidade de São Paulo
Rua do Lago, 562
Cidade Universitária
São Paulo, São Paulo 05508-080, Brasil

[4] Centre Nouvelle-Aquitaine Bordeaux
INRAE
UR EABX
50 Avenue de Verdun
33612 Gazinet-Cestas, France

Abstract—The Lebranche mullet (*Mugil liza*) is an economically important estuarine species found along the coast of Brazil. The southern population of this species ranges from the coast of the state of São Paulo (23°S) to the coast of Argentina (36°S). It migrates annually among estuaries in Argentina, Uruguay, and southern Brazil to reproduce in their marine spawning grounds (~26°S). We evaluated whether variations in the otolith chemical composition for fish acquired at nursery grounds can be used to make distinctions among 4 nursery areas of the southern population. Analysis of otolith microchemistry included concentrations of 9 elements: lithium (Li), magnesium (Mg), copper, zinc, strontium (Sr), cadmium, barium, lanthanum, and lead. When using random forest classification algorithms, the maximum accuracy of 96% in assignment of nursery habitat for Lebranche mullet between 2 groups (fish caught at nurseries in Brazil and fish migrating from waters of Uruguay and Argentina) was achieved with the combination of Li, Mg, and Sr. Our results indicate that the elemental composition of otoliths can be an important tool for establishing connectivity between nursery areas used by Lebranche mullet. We discuss the implications of this result for the structure of the population and the management of the mullet fishery in southern Brazil relative to the limitations of the methods we employed.

The Lebranche mullet (*Mugil liza*) is one of the most economically important marine species in southern Brazil (Sant'Ana et al., 2017; dos Santos et al., 2018). This species ranges from the Gulf of Mexico to Argentina (Menezes et al., 2015), and the southern population, discriminated on the basis of population genetic analyses, is distributed from the coast of the state of São Paulo in Brazil (23°S) to Buenos Aires Province in Argentina (36°S) (Mai et al., 2014; Lemos et al., 2017). The states of Rio Grande do Sul and Santa Catarina alone account for approximately 90–95% of the total catch in Brazil (MPA and MMA, 2015). In this area in Brazil, the average annual catch of commercial fisheries was 7150 metric tons (t), with a maximum catch of 13,600 t in 2007 (MPA and MMA, 2015; Sant'Ana et al., 2017). To the south, in Uruguay, the average annual catch was 200 t for the period 2000–2007 (Lorenzo, 2010). In Argentina, the Lebranche mullet is a target of a small-scale fishery, mainly off the northern coast of the Buenos Aires Province, where it is a popular food resource and a favorite of sport fishermen (González Castro et al., 2009).

The Lebranche mullet is a marine migrant estuarine species (Mai et al., 2018, 2019). The southern population, to reproduce, migrates annually from estuaries and lagoons along the coasts of Argentina, Uruguay, and southern Brazil to offshore waters off the northern coast of Santa Catarina and the southern coast of the state of Paraná in Brazil (~26°S) (Vieira and Scalabrin, 1991; González Castro et al., 2009; Lemos et al., 2014, 2016). This migration has been reported to start gradually and to follow the temporal movement of the range of sea-surface temperatures of 19–21°C in a south–north direction from April to July (Lemos et al., 2014, 2016). According to Lemos et al. (2014), the broad geographical range of spawning locations along the coast of Santa

Manuscript submitted 20 January 2023.
Manuscript accepted 17 January 2024.
Fish. Bull. 122:13–25 (2024).
Online publication date: 20 March 2024
doi: 10.7755/FB.122.1-2.2

The views and opinions expressed or implied in this article are those of the author (or authors) and do not necessarily reflect the position of the National Marine Fisheries Service, NOAA.

Catarina indicates that spawning of Lebranche mullet is more closely related to oceanographic conditions than to specific locations. These oceanographic conditions are salinities of 32–35 and sea-surface temperatures of ~20 °C, found at depths of ~50 m in waters on the continental shelf (Lemos et al., 2014, 2016). The larvae and early juveniles of this species are neustonic and are carried, mainly through wind-driven currents, from spawning grounds toward the coast, where they concentrate in surf zones prior to recruitment to estuarine environments (Vieira, 1991; Lemos et al., 2021).

Many estuaries along the southern coast of Brazil and the coasts of Uruguay and Argentina are used by Lebranche mullet as nursery grounds (Ramos and Vieira, 2001; Loebmann and Vieira, 2005; González Castro et al., 2009; del Favero and Dias, 2015; Callicó Fortunato et al., 2017; Mai et al., 2018), and the Patos Lagoon estuary is considered the largest nursery area for the southern population of Lebranche mullet (Lemos et al., 2021). The Lebranche mullet has a flexible life history with a high degree of behavioral plasticity and wide salinity tolerance as juveniles. According to Mai et al. (2019), at least 3 patterns of coastal use and recruitment have been observed for juveniles. The majority (~90%) of juvenile Lebranche mullet migrate toward estuaries before completing their first year of life (64%) or after (25%) their first year of life (Mai et al., 2019). However, approximately 10% of the population does not always use estuaries as nurseries and can complete its entire life cycle in the marine environment (Callicó Fortunato et al., 2017; Mai et al., 2019). Furthermore, some adults return to an estuary after spawning in the ocean, but others never return to an estuary after spawning and remain in the marine environment (Mai et al., 2019).

Schroeder et al. (2023), combining otolith shape analyses and meristic and morphometric analyses of Lebranche mullet captured in waters of Brazil, discriminated 2 subpopulations. From the same study, results of analyses of the deposition of multiple elements in otolith cores from Lebranche mullet collected in Brazil and Argentina indicate the existence of more than one nursery area for this species (Schroeder et al., 2023). The identification of nursery origin of Lebranche mullet is extremely important and may help guide strategies to ensure the efficient management and sustainability of fisheries that target this species (Lotze et al., 2006).

The use of the chemical composition of otoliths has allowed stock identification (Thresher, 1999; Campana et al., 2000), descriptions of migration patterns and habitat utilization (Secor et al., 1995; Kennedy et al., 2002; Elsdon and Gillanders, 2003; Gillanders, 2005), descriptions of the life histories of different commercial fish species (Rooker et al., 2001; Artetxe-Arrate et al., 2019; Moll et al., 2019; Bae and Kim, 2020; Avigliano et al., 2021), and identification of nursery habitats (Gillanders and Kingsford, 2000; Vasconcelos et al., 2008; Reis-Santos et al., 2013; Tournois et al., 2017). Properties of otoliths allow them to form growth increments and retain chemical elements, associated with their metabolically inert capacity, and these signals of growth and chemistry provide a permanent record of the environmental conditions (such as the temperatures and chemical composition of the water) to which a fish was exposed (Campana and Neilson, 1985; Campana, 1999; Panfili et al., 2002). For this reason, researchers have long appreciated the importance of otoliths in studies on the biology of teleost fish (Campana and Neilson, 1985).

In this study, we tested the applicability of the elemental fingerprint in otoliths of Lebranche mullet to identification of nursery grounds utilized by the southern stock. For this purpose, the microchemistry of otoliths from Lebranche mullet was compared between 4 sampling sites, all nursery areas, off the southern coast of Brazil. The concentrations of the following chemical elements in otoliths were examined: lithium (Li), magnesium (Mg), copper (Cu), zinc (Zn), strontium (Sr), cadmium (Cd), barium (Ba), lanthanum (La), and lead (Pb).

Material and methods

Study area and fish collection

Adult Lebranche mullet (n=83) were collected directly from landings of the artisanal and commercial fisheries (gill-net fisheries) that operate in coastal waters and estuarine areas along the coasts of the southern states of Brazil (Fig. 1). Lebranche mullet use as nurseries several estuaries and lagoons that are part of the complex hydrographic system in and along the coastal plain in southern Brazil (Ramos and Vieira, 2001; Lemos et al., 2014). Therefore, we chose to collect specimens caught in 3 estuarine systems used as nursery grounds by juveniles on the southern coast of Brazil: Laguna (LAG, 28°S), Tramandaí (TRA, 29°S), and Patos Lagoon estuary (PLE, 32°S). We compared those specimens with individuals in prespawning migration that were coming from nurseries in Uruguay and Argentina; they were captured at the border between Brazil and Uruguay, near the city of Chuí (CHU, 33°S), by purse seine at the time of northern migration (Table 1). Individuals were collected between May and October 2011. All fish were transported on ice to the laboratory and preserved frozen until dissection. All specimens were measured for total length (TL) in millimeters and total weight (TW) in grams, and the sagittal otoliths were extracted, cleaned, dried, and stored for further analysis.

Otolith preparation and sample analysis

The method we used for obtaining otolith microchemical data follows that of Mai et al. (2018, 2019). Otoliths, one from each of the 83 collected specimens, were embedded in polyester resin, and transverse sections were cut by using an IsoMet Low Speed Saw[1] with a diamond blade (Buehler, Lake Bluff, IL). Prior to analysis through laser

---

[1] Mention of trade names or commercial companies is for identification purposes only and does not imply endorsement by the National Marine Fisheries Service, NOAA.

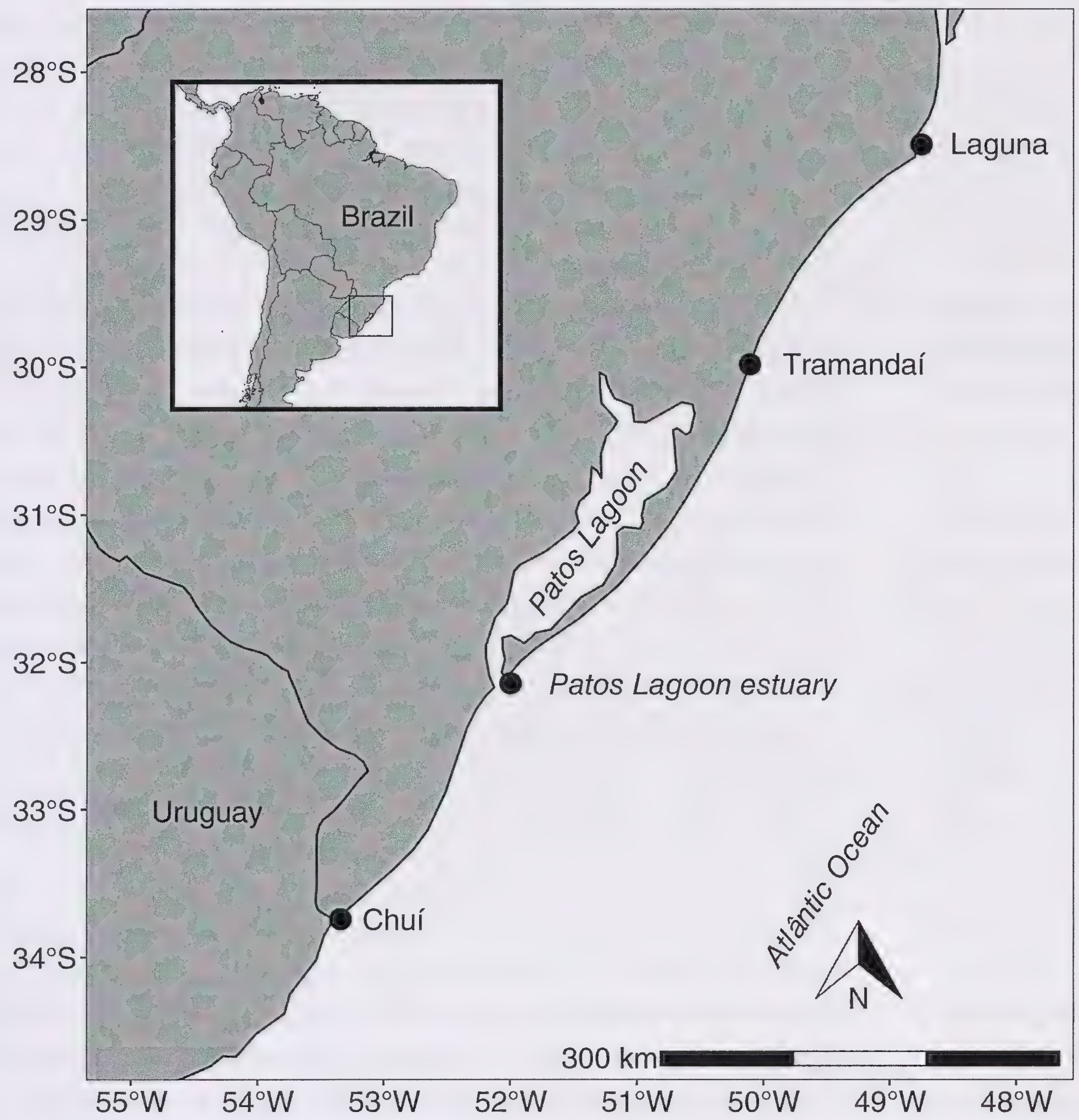

Figure 1

Map of southern Brazil showing the 4 sampling sites where Lebranche mullet (*Mugil liza*) were caught in May–October 2011. Laguna, Tramandaí, and Patos Lagoon estuaries are estuarine systems used by juvenile Lebranche mullet as nursery grounds, and the fourth site is near Chuí, a city at the border between Brazil and Uruguay.

ablation inductively coupled plasma mass spectrometry (LA-ICP-MS), the sections (0.5 mm) were mounted on glass slides (with cyanoacrylate glue), polished (with silicon-carbide sanding paper no. 8000), sonicated for 1 min, rinsed 3 times with ultrapure distilled water (Milli-Q, Merck-Millipore), and dried in a laminar flow cabinet (Mai et al., 2018, 2019).

The LA-ICP-MS analysis was done with a Thermo Scientific iCAP Q ICP-MS (Thermo Fisher Scientific Inc., Waltham, MA) coupled to a 213-nm New Wave neodymium-doped yttrium-aluminium-garnet laser (Electro Scientific Industries Inc., Beaverton, OR) at the Instituto de Geociências da Universidade de São Paulo. Using this analysis, we quantified the concentrations of the following isotopes in the otoliths of Lebranche mullet: ^{7}Li, ^{25}Mg, ^{65}Cu, ^{66}Zn, ^{86}Sr, ^{114}Cd, ^{137}Ba, ^{139}La, and ^{208}Pb. A crater with a width of approximately 30 µm was generated in otoliths with a pulse frequency of the laser of 10 Hz, a scan speed of 30 µm/s, and energy outputs of 10 and 12 J/cm^2 per pulse. The ablated material was placed through a Teflon-coated tube into the ICP-MS by using a combination of helium (^{4}He) and argon (^{40}Ar) as a carrier gas.

Before each otolith ablation, the background signal intensity was measured with the ICP-MS for 60 s. Counts per second for Sr and calcium (Ca) were subtracted from the background level, and the ratios of the concentrations of elements to those of Ca were then calculated for all otoliths analyzed. The maximum analyte intensities and minimum interferences in the performance of the ICP-MS were determined by using oxides and double charged ions. The equipment was calibrated and tuned with the certified reference material MACS-3 (U. S. Geological Survey): 5.7% ^{86}Sr and 3.2% ^{137}Ba. To correct for mass bias and machine drift, after every 10 otoliths, a certified glass reference standard, NIST 612 (National Institute of Standards and Technology), was run.

Otolith transects were ablated from the core to the edge to capture the entire life history of the collected fish. Knowing that Lebranche mullet spawn at sea (Lemos

Table 1

Number and size of Lebranche mullet (*Mugil liza*) caught at each sampling site on the coast of southern Brazil from May through October 2011. n=sample size; SD=standard deviation.

		Total length (mm)		Total weight (g)	
Site (latitude)	n	Range	Mean (SD)	Range	Mean (SD)
Laguna (28°S)	23	353–558	435 (59)	377–1538	749 (300)
Tramandaí (29°S)	22	319–540	403 (49)	271–1260	597 (212)
Patos Lagoon estuary (32°S)	25	360–430	402 (20)	506–919	698 (106)
Chuí (33°S)	13	490–590	545 (34)	1145–2322	1771 (413)

et al., 2014, 2017; Mai et al., 2019), the sampling zone around the otolith core was chosen manually to represent the otolith section formed while the fish was in a nursery area, with the ratios of concentrations of Sr and Ba to concentrations of Ca in otoliths assumed to be characteristic of the water chemistry of an estuarine zone (Mai et al., 2018, 2019). According to Mai et al. (2019), values of 0.02–0.13 µmol/mol for ratios of Ba concentration to Ca concentration after the core zone indicate that a species was living in a nursery area that was an estuarine zone. For characterization of the nursery origins of specimens, at least 20 chemistry readings (by laser ablation spot) in the nursery zone of each otolith were made.

Data reduction, including background corrections, conversion of mass count data to concentrations (in parts per million), and limits of detection, was done for each sample by using Glitter software (Australia Research Council National Key Centre for Geochemical Evolution and Metallogeny of Continents, Macquarie University, Sydney, Australia). In further analysis, we considered the concentrations of 9 elements (Li, Mg, Cu, Zn, Sr, Cd, Ba, La, and Pb) that were all well above the detection limits calculated by using Glitter (0.020, 0.080, 0.025, 0.057, 0.155, 0.004, 0.007, 0.014, and 0.015 ppm, respectively). Concentrations of trace elements (originally in parts per million) were transformed to ratios of concentrations of elements to concentrations of Ca, expressed as units of millimoles per mole or micromoles per mole (Thorrold et al., 1998; Forrester and Swearer, 2002; Swearer et al., 2003; Dorval et al., 2005; Brown, 2006).

Statistical analyses

We used a nonmetric multidimensional scaling plot to visualize the elemental composition of otoliths and potential chemical differences among sampling sites from a dissimilarity matrix of calculating the Euclidean distances. For each nursery area, we analyzed the element concentration distributions by using box plots. We visualized otolith chemical signatures for each nursery area by using radar plots, based on the mean proportion of each element concentration among the 83 otoliths analyzed. Concentrations of all elements were checked for normality and homoscedasticity prior to statistical analyses. Parametric assumptions were not met (according to results of Shapiro–Wilk and Bartlett tests), even after $\log_{10}$ transformation; therefore, we used nonparametric statistics. To detect whether otolith elemental fingerprints differed among nursery areas, we employed the Kruskal–Wallis test with Dunn's post hoc test. Spearman correlation analysis was used to examine the correlation between the ratios of element concentrations in the otoliths.

We used the elemental fingerprinting index (EFI) created by Moll et al. (2019) as a measure of the similarity among individuals when considering numerous chemical signatures in their otoliths. The EFI ranges from 0 to 1, with a value of 0 indicating that the elemental compositions in the otoliths of the 2 compared individuals are most different and a value of 1 indicating the highest similarity in the elemental compositions in the otoliths of the 2 compared individuals. We conducted comparisons of element concentrations in otoliths for all individuals within one sampling area and comparisons for all individuals among the different sampling areas. The EFI values were tested for significant differences within and between the 4 sampling areas by using the Welch test and Games–Howell post hoc test.

To identify the optimal combination of elements for habitat discrimination, we used a machine learning method based on the random forest algorithm developed by Breiman (2001). Machine learning methods, such as random forest, have been reported to have greater classification efficiency for nursery identification based on otolith microchemistry, especially when data sets include multiple specific otolith signatures or several chemical elements (Mercier et al., 2011). Following this method, 5000 classification trees were built, considering all possible combinations of the 9 elements measured. The analysis proceeded in 2 steps. First, a random forest classifier was built by using the chemical signatures in otoliths for 75% of individuals that were randomly selected from specimens of known nursery origin. Second, the otolith signatures from the remaining individuals (25%) were used in the random forest classifier to predict origin and to test the prediction accuracy by measuring the proportion of individuals correctly assigned to their known origin (CHU, LAG, TRA, or PLE). Additionally, the algorithm was also executed with the origin site defined as binary, classified as either the coasts of Uruguay and Argentina (CHU) or estuaries of Brazil (LAG, TRA, and PLE). Details of the method and application are provided in Mercier et al. (2011, 2012).

All statistical analyses were done in statistical software R (vers. 4.2.2; R Core Team, 2022) with the packages dplyr (vers. 1.0.10; Wickham et al., 2022), class (vers. 7.3-22; Venables and Ripley, 2002), FactoMineR (vers. 2.9; Lê et al., 2008), FSA (vers. 0.9.5; Ogle et al., 2023), ggplot2 (vers. 3.4.4; Wickham, 2016), gtools (vers. 3.9.3; Warnes et al., 2022), MASS (vers. 7.3-58.1; Venables and Ripley, 2002), mda (vers. 0.5-3; Hastie et al., 2022), randomForest (vers. 4.7-1.1; Liaw and Wiener, 2002), and stats (vers. 4.2.2; R Core Team, 2022).

Results

Otolith microchemistry

Mean concentrations of elements in examined otoliths varied greatly across the 4 sampling sites, CHU, PLE, TRA, and LAG (Table 2, Fig. 2). The ratios of concentrations of 5 elements, Li, Cu, La, Pb, and Sr, to concentrations of Ca in the otoliths from specimens differed significantly (Kruskal–Wallis pairwise test: $P<0.05$) between 2 or 3 sites. The ratios of the concentrations of Li to Ca in otoliths were significantly higher for fish caught at CHU than for those caught at the other 3 sampling sites. Concentration ratios of La to Ca were lower in otoliths from fish caught at CHU than in those from fish

Table 2

Mean ratios of the chemical concentrations of 9 elements to concentrations of calcium in the nursery zone in otoliths from Lebranche mullet (*Mugil liza*) caught at 4 sampling sites in southern Brazil, Chuí (CHU), Patos Lagoon estuary (PLE), Tramandaí (TRA), and Laguna (LAG), between May and October 2011. The elements are lithium (Li), magnesium (Mg), copper (Cu), zinc (Zn), strontium (Sr), cadmium (Cd), barium (Ba), lanthanum (La), and lead (Pb). Significant differences in chemical signatures in otoliths between sites were examined by using Kruskal–Wallis and Dunn's post hoc tests for each element with the significance level of 0.05. An asterisk (*) indicates that signatures were revealed in Kruskal–Wallis tests to be significantly different between sites. The results of Dunn's test for pairwise comparisons are provided. Standard deviations (SDs) of mean ratios are given in parentheses. NS=not significant.

	Mean ratio (SD)						
Element	CHU	PLE	TRA	LAG	χ^2	*P*	Dunn's test
Li	4.57 (1.62)	1.46 (1.16)	1.91 (1.06)	2.01 (1.11)	33.36	<0.01*	CHU>PLE, TRA, LAG
Mg	3.20 (0.87)	3.47 (1.56)	3.17 (1.20)	3.07 (1.29)	2.87	0.41	All NS
Cu	0.22 (0.20)	0.30 (0.44)	0.22 (0.14)	0.20 (0.24)	7.64	0.05*	PLE>LAG
Zn	0.43 (0.78)	0.60 (0.58)	0.67 (1.35)	0.59 (0.53)	5.24	0.16	All NS
Cd	2.03 (1.75)	2.25 (1.81)	2.57 (1.85)	2.22 (1.82)	1.79	0.62	All NS
Ba	0.07 (0.05)	0.08 (0.07)	0.06 (0.05)	0.07 (0.05)	0.71	0.87	All NS
La	1.22 (1.29)	1.81 (1.62)	1.73 (1.19)	1.44 (0.94)	13.34	<0.01*	CHU<PLE, TRA
Pb	0.21 (0.27)	0.30 (0.21)	0.47 (0.40)	0.34 (0.33)	16.04	<0.01*	TRA>CHU, PLE
Sr	0.43 (0.10)	0.45 (0.12)	0.46 (0.09)	0.48 (0.10)	8.35	0.04*	LAG>CHU, TRA

caught at PLE and TRA. The ratios of concentrations of Pb to Ca were higher in otoliths from specimens caught at TRA than in the otoliths of those caught at CHU and PLE. The concentration ratios of Cu to Ca were significantly higher for otoliths from fish caught at PLE than for otoliths from those caught at LAG. Ratios of the concentrations of Sr to Ca in otoliths was higher for specimens caught in LAG than for those from CHU and TRA, and ratios of the concentrations of Mg, Zn, Cd, and Ba to Ca in otoliths were similar between sites (Table 2).

Results from Spearman correlation analysis (Table 3) indicate that some of the correlations between ratios of element concentrations were significant ($P<0.05$). The correlations between the concentration ratios of Cu, Zn, Cd, La, and Pb to Ca indicate a significantly positive relationship. The only significant negative correlation was between the ratio of the concentration of Li to Ca and the ratio of the concentration of La to Ca.

Chemical signatures in the nursery zone of otoliths

Examination of the data set on the chemical composition of the nursery zone of otoliths included habitat-specific plots of elemental fingerprints with similarities and differences in proportions of element concentrations in otoliths (Fig. 3). The nonmetric multidimensional scaling plot indicates differences in chemical signatures in otoliths for each sampling site. Element concentrations in otoliths of specimens from CHU had lower variability among individuals than those in otoliths of fish from LAG, TRA and PLE, and they are clustered on the left side of the ordination plot. Elemental compositions in the nursery zone of otoliths from specimens caught at PLE, LAG, and TRA were similar and clustered on the right side of the plot, indicating more similarity in otolith compositions among these sites than between these sites and CHU (Fig. 4).

Results from the pairwise comparisons of multiple element concentrations for individuals within a single sampling site, made by using the EFI, indicate that the otolith compositions for individuals collected at CHU are significantly more similar to those of each other (higher EFI value) and are significantly different from those of specimens caught at the other 3 sites ($P<0.001$) (Table 4). Comparisons between sampling sites also identified similarities in element concentrations of otoliths from fish caught at PLE, TRA, and LAG (Table 4). The EFI values for comparisons of chemical signatures in otoliths of fish caught at CHU to those of fish caught at each of the other 3 sites, LAG, PLE, and TRA, indicate that similarities in element concentrations between otoliths within these groups of fish were significantly lower (lower EFI value) than the similarities between otoliths from fish collected at CHU ($P<0.001$). The EFI values from comparisons between 2 sites at a time for all 4 nurseries are smaller than the EFI values from within-site comparisons, indicating that element concentrations in otoliths of specimens are more similar within sites than between all 4 nurseries (Table 4).

Discrimination of nursery grounds

In using the random forest method to compare the 4 nursery grounds sampled, we built classification trees by considering multiple combinations of the 9 chemical elements tested. We observed that the addition of elements generally improved the accuracy of the random forest classifier, increasing the average levels of accuracy in discriminating fish nursery origin of Lebranche mullet (Fig. 5A). The maximum accuracy (55.1%) in assignment of nursery

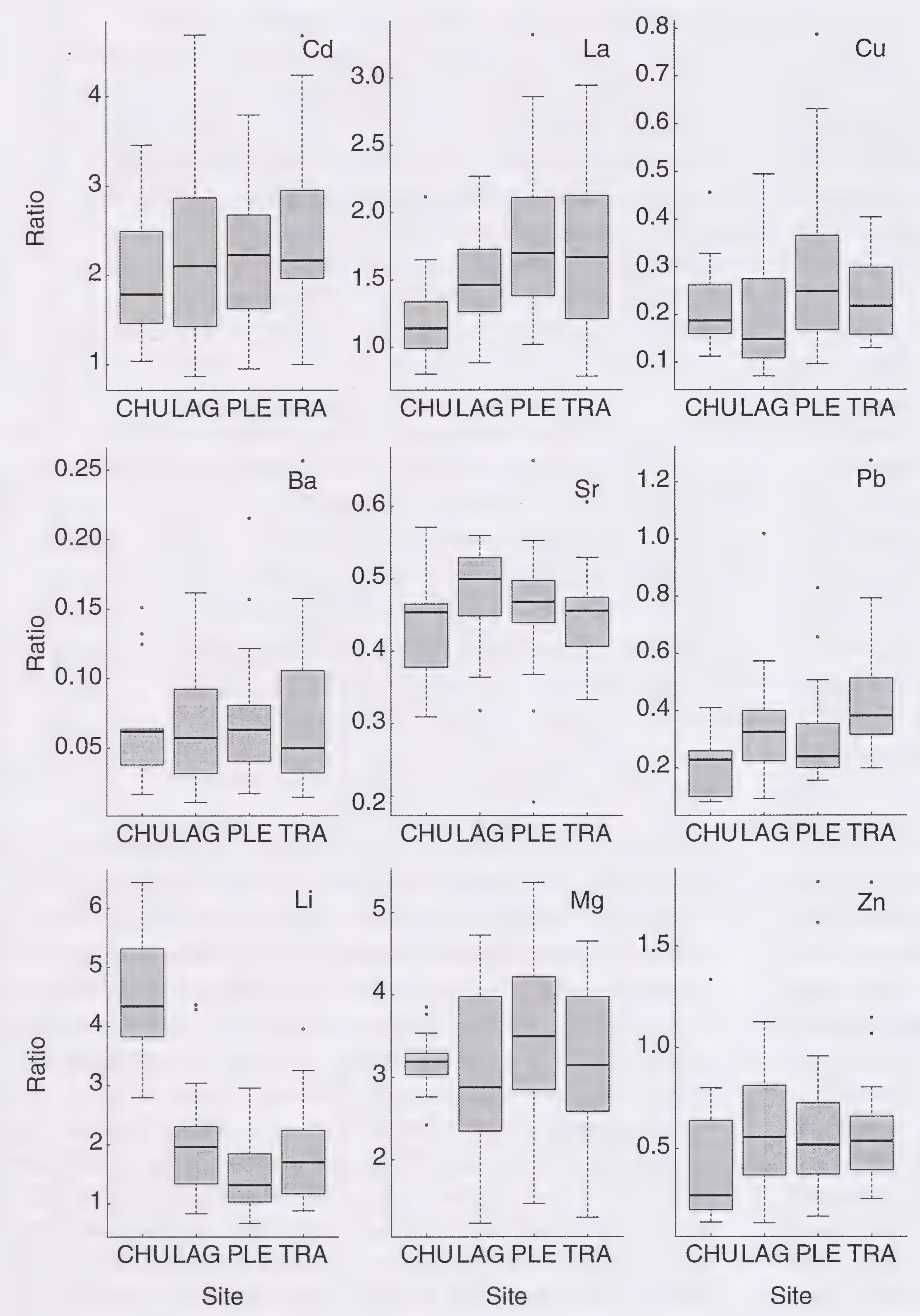

Figure 2

Mean ratios of the chemical concentrations of 9 elements to the concentrations of calcium in the nursery zone of otoliths of Lebranche mullet (*Mugil liza*) collected from May through October 2011 at 4 sampling sites in southern Brazil: Chuí (CHU), Patos Lagoon estuary (PLE), Tramandaí (TRA), and Laguna (LAG). The elements are cadmium (Cd), lanthanum (La), copper (Cu), barium (Ba), strontium (Sr), lead (Pb), lithium (Li), magnesium (Mg), and zinc (Zn). In each box plot, the thick black line is the median. The upper and lower parts of each box represent the first and third quartiles (the 25th and 75th percentiles). The whiskers extend above and below the box no more than 1.5 times the interquartile range. Data points that appear beyond the end of the whiskers are outliers.

origins to the 4 sampling sites was reached with the combination of the 4 elements Cu, Li, Pb, and Sr, specifically the ratios of their concentrations to concentrations of Ca.

On the basis of evidence that element concentrations in otoliths of specimens from CHU were significantly different from those in otoliths of fish from the remaining sites sampled and that the nursery habitats for specimens from PLE, TRA, and LAG could not be discriminated (Figs. 3 and 4, Table 4), we compared data for specimens from CHU to data for fish from the other 3 sampling sites combined (Fig. 5B). The maximum accuracy of 96% in assignment of nursery area was achieved with the combination of values for only 3 elements: the ratios of the concentrations of Li, Mg, and Sr to concentrations of Ca.

Discussion

Otolith chemical composition is not a direct representation of ambient water chemistry, and the relationship between environmental and physiological processes is still poorly understood (Thresher, 1999). Nonetheless, it is widely accepted that the mechanisms controlling the uptake and incorporation of elements into otoliths are mediated by both exogenous (e.g., salinity) and endogenous (e.g., growth) factors (Walther et al., 2010). Not all elements behave similarly in otoliths (Vrdoljak, 2020). Many studies have attempted to determine the causes of variations in otolith microchemistry (Elsdon and Gillanders, 2003; Sturrock et al., 2014, 2015), and knowledge of the factors that influence otolith microchemistry is far from complete. However, several scientists have claimed that it is not necessary to understand all these mechanisms to be able to use otolith microchemistry as a tool in fisheries management (Thorrold et al., 1998; Thresher, 1999; Elsdon et al., 2008).

As expected, results from the analysis in our study of element concentrations in the nursery zone of otoliths from Lebranche mullet indicate that the ratios of concentrations of Li, Sr, La, Pb, and Cu to concentrations of Ca were significantly different among the sampling sites. The concentrations of certain elements varied between nursery grounds in southern Brazil and the southernmost nursery areas in Uruguay and Argentina.

Signatures of Sr and Ba can be used to distinguish residences in waters of different salinities (Walther and Thorrold, 2006; Elsdon et al., 2008) and have been used to successfully reconstruct environmental histories and coast–estuary movement for Lebranche mullet in South America (Callicó Fortunato et al., 2017; Mai et al., 2018, 2019). We found no significant difference between sites in the ratio of concentrations of Ba to Ca in the nursery zone of otoliths from specimens of Lebranche mullet. This finding indicates that all

Table 3

Spearman correlation coefficients for the relationships between ratios of the concentrations of 9 elements, lithium (Li), magnesium (Mg), copper (Cu), zinc (Zn), strontium (Sr), cadmium (Cd), barium (Ba), lanthanum (La), and lead (Pb), to concentrations of calcium in the nursery zone of otoliths from Lebranche mullet (*Mugil liza*) collected from 4 sampling sites in southern Brazil from May through October 2011. An asterisk (*) indicates a significant correlation between concentrations of elements ($P<0.05$).

	Ratio of element to calcium								
Ratio	Li	Mg	Cu	Zn	Cd	Ba	La	Pb	Sr
Li									
Mg	0.17								
Cu	−0.01	0.15							
Zn	−0.13	0.12	0.52*						
Cd	0.02	0.04	0.59*	0.56*					
Ba	−0.23	−0.11	0.14	0.10	−0.04				
La	−0.26*	0.11	0.45*	0.56*	0.47*	0.09			
Pb	−0.08	−0.07	0.33*	0.67*	0.62*	0.07	0.55*		
Sr	−0.06	−0.07	0.02	0.24	0.13	−0.11	0.00	0.17	

sampled individuals developed in estuaries. However, we found significantly higher ratios of concentrations of Sr to Ca in otoliths of Lebranche mullet from LAG, a trend that may be associated with differences in ambient chemistry and physical factors. The other sampled nursery areas are affected by large drainage basins and, therefore, are heavily influenced by freshwater discharges; in comparison, LAG is a saline wedge estuary located at 28°S and is under the influence of higher temperatures than those at other sites (D'Aquino et al., 2011).

Fish absorb heavy metals (e.g., Pb and Cu) from their environments during their lives, and these elements are preserved within otolith structures (Reis-Santos et al., 2013; Sturrock et al., 2014). The accumulation of trace metals in fish otoliths depends on a number of factors, including the concentrations of elements in the water environment (Ranaldi and Gagnon, 2010). We found higher concentration ratios of Pb and Cu to Ca in otoliths from Lebranche mullet caught in the estuary at TRA and in the PLE, respectively. This result may be an indication of anthropogenic effects in estuarine environments. In fact, the average concentrations of metals in estuarine water in Patos Lagoon correspond to the natural base levels described for other estuarine systems, but sporadic increases in Cu and Pb concentrations have been related to the ingress of industrial effluents and activities in the limnic area of Patos Lagoon (Seeliger et al., 1997). Although findings from some other research indicate associations of the highest Pb concentrations in otoliths with port areas (Cuevas et al., 2019), the effects of the time during which fish are exposed to Pb and of physiological processes should be considered (Vrdoljak, 2020). The nurseries sampled at both TRA and PLE are in highly populated areas. Although concentrations of trace metals in the waters at these sites are low, they could be used to identify the contribution of polluted nurseries to the stock of Lebranche mullet in southern Brazil.

We found significantly higher ratios of the concentrations of Li to Ca in the nursery zone of the otoliths of Lebranche mullet sampled from the southern migratory contingent (at CHU) during the time of northern migration than in those of fish caught at other sampling sites, all estuaries in southern Brazil. In fact, Li was the most significant element in the use of otolith microchemistry to discriminate between sampling sites (Table 2, Fig. 2). According to Sturrock et al. (2012), among the various elements found in otoliths, Li has the most positive relationship with the environment and is one of the elements that are reliable geographic markers in marine species. Lithium is highly bioavailable; however, little attention has been given to determining the environmental and physiological factors that affect incorporation of Li into otoliths (Brown, 2006). Furthermore, information about Li in the aquatic environment is limited (Tkatcheva et al., 2015). This element seems to be associated with estuaries in the southern regions of South America, and results from other studies already indicate the power of Li in discriminating habitats for species collected in Brazil, Uruguay, and Argentina: the Brazilian codling (*Urophycis brasiliensis*) (Biolé et al., 2019) and the whitemouth croaker (*Micropogonias furnieri*) (Avigliano et al., 2021).

Through none of our analyses were we able to use the nursery zone of otoliths to differentiate between groups of fish caught in each of the estuaries in southern Brazil (PLE, TRA, and LAG). However, otoliths of fish caught from CHU were different from those of the combined group of fish caught in PLE, TRA, and LAG. The similarity between the chemical signatures in the nursery zone of otoliths of Lebranche mullet from the estuaries of Brazil can be explained by the similar physicochemical conditions of the waters in those estuaries; after all, water chemistry influences the chemical composition of otoliths (Kerr and Campana, 2014). According to Adelir-Alves

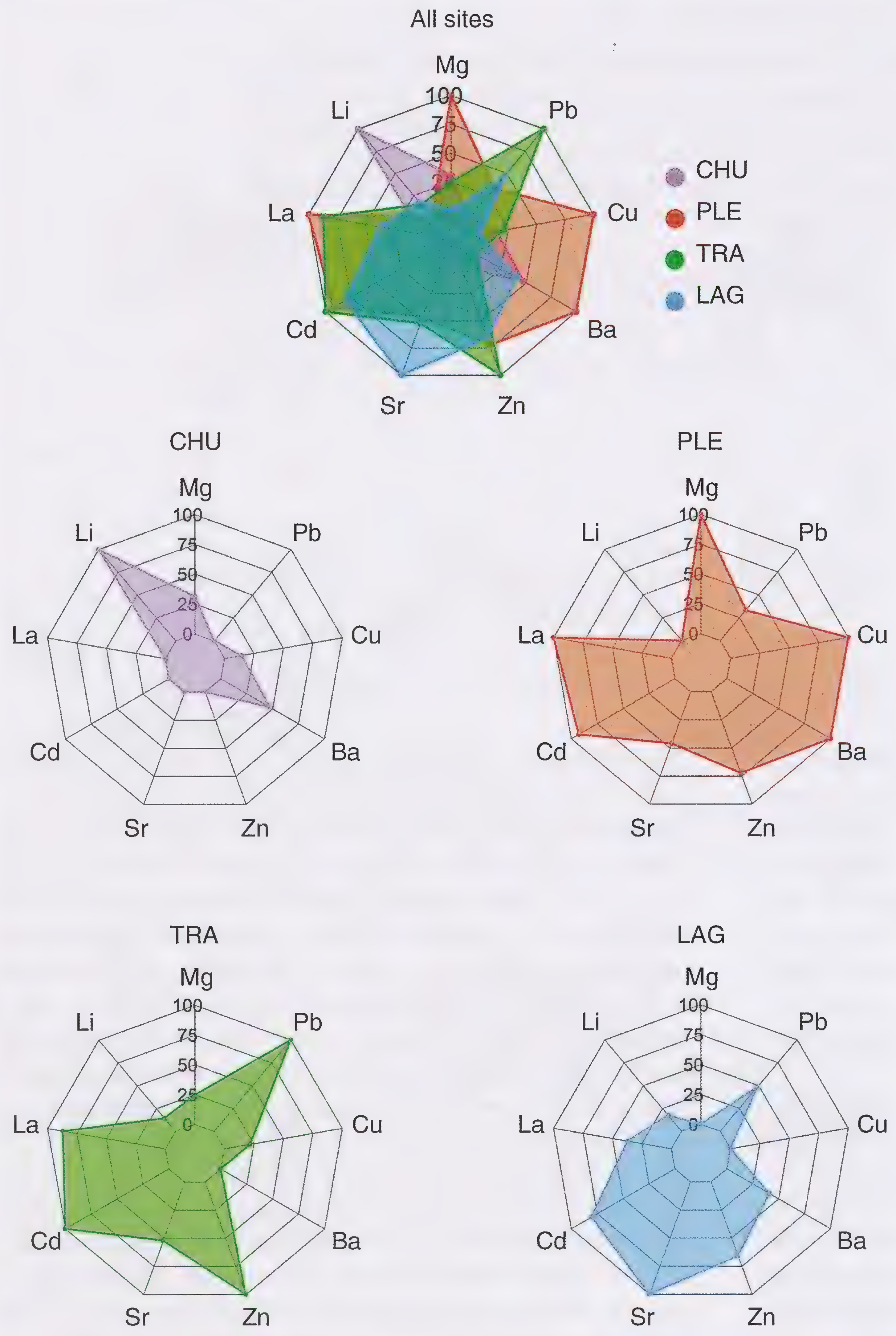

Figure 3

Radar plots of the proportions of element concentrations in the nursery zone of otoliths from Lebranche mullet (*Mugil liza*) collected at 4 sampling sites in southern Brazil in May–October 2011: Chuí (CHU, purple radii), Patos Lagoon estuary (PLE, red radii), Tramandaí (TRA, green radii), and Laguna (LAG, blue radii). The proportions (shown as percentages) are for concentrations of 9 elements, lithium (Li), magnesium (Mg), lead (Pb), copper (Cu), barium (Ba), zinc (Zn), strontium (Sr), cadmium (Cd), and lanthanum (La).

et al. (2019), otolith microchemistry analyses provide information for a given time and on a fine spatial scale, but the usefulness of element concentrations in otoliths as natural biogeochemical markers depends on the existence of measurable differences in otolith microchemistry on a geographic scale relevant to the life history of a species. In fact, the concentration of some elements in otoliths differed significantly between the sampling sites in the estuaries of southern Brazil, but the general signature in otoliths of fish from each habitat had a relatively low level of accuracy (55%) in the analysis done with the random forest method (Fig. 5A). According to Mercier et al. (2011), an acceptable degree of accuracy should be greater than 75%. Only after grouping the specimens from the estuaries in Brazil and comparing the element concentrations in their otoliths with those of specimens from CHU did the accuracy of nursery assignment increase to 96% (Fig. 5B).

Temporal variability in otolith microchemistry must be considered because otolith elemental fingerprints are unlikely to remain consistent over time (Gillanders, 2002; Hamer et al., 2003; Clarke et al., 2009; Walther and Thorrold, 2009). This temporal variability can confuse spatial differences, meaning differences in elemental composition of otoliths among fish from different nurseries. Therefore, it is important to consider interannual differences in otolith microchemistry (Gillanders, 2002; Cuveliers et al., 2010; Reis-Santos et al., 2012), and assignment of origin (to specific nurseries or sampling sites) should be done only for year-classes for which an otolith chemical signature has been identified for juveniles. For this reason, it would be ideal if sampling and monitoring programs systematically collect otoliths over a period of several years, compiling a library of reference elemental markers than can be later used to determine the nursery origin of coastal adult fish (Gillanders, 2002; Reis-Santos et al., 2013).

We assume that individuals collected at the southernmost sampling site, CHU, were from estuaries in Argentina and Uruguay, a notion that is reinforced by the distinction in otolith microchemistry for fish from this site and the low standard deviations of ratios of element concentrations. Several reports on previous scientific research have revealed that Lebranche mullet migrate from Argentina and Uruguay to waters in Brazil in order to reproduce (González Castro et al., 2009; Lemos et al., 2014; Mai et al., 2014; Lemos et al., 2016). This common finding reflects the local ecological knowledge of Brazilian fishermen regarding the existence of various morphotypes of Lebranche mullet with different geographical origins in the southwestern Atlantic Ocean (Herbst and Hanazaki, 2014). Distinct morphological characteristics are acquired in natural conditions of nurseries where

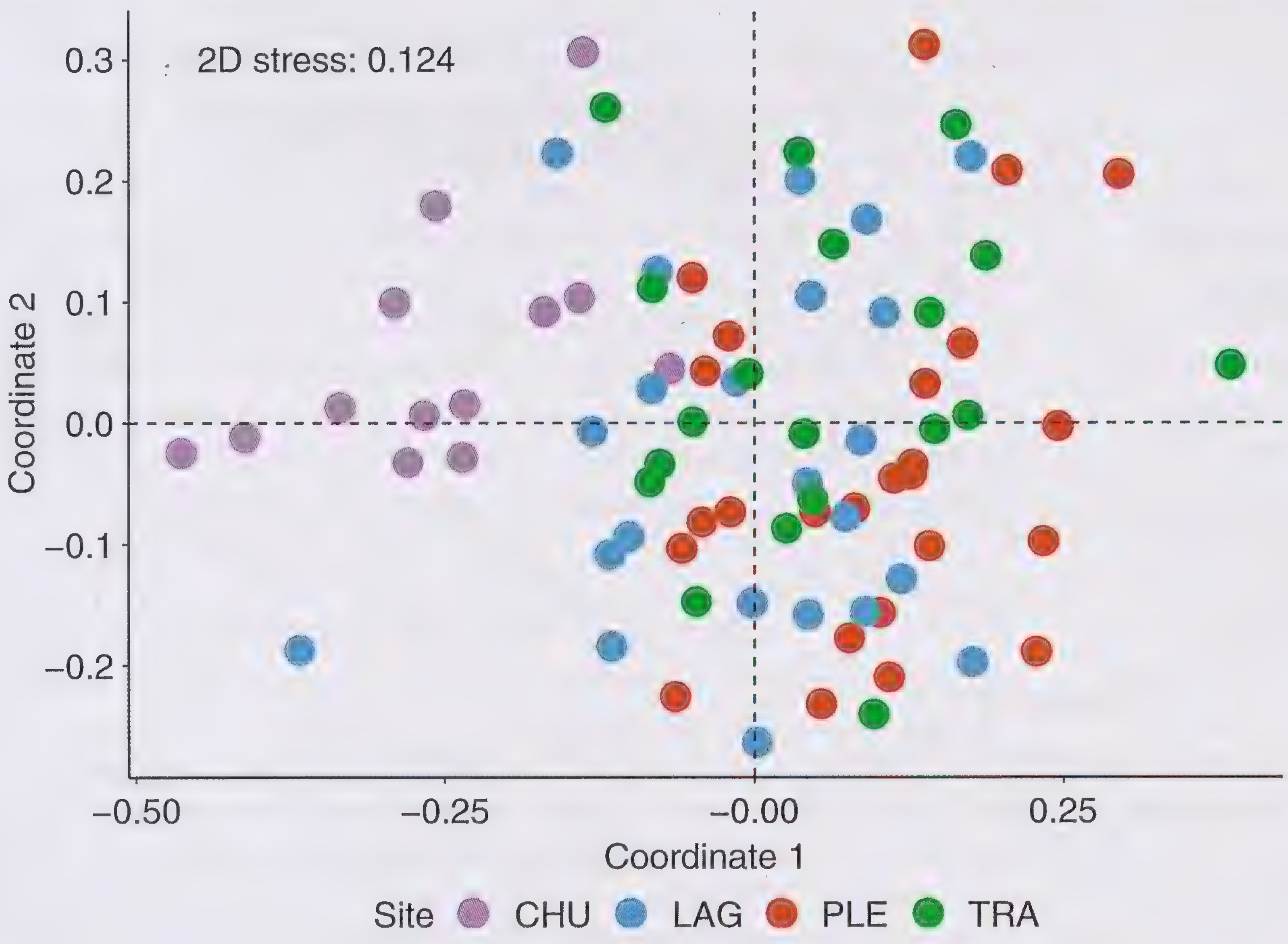

Figure 4

Nonmetric multidimensional scaling plot of element concentrations in the nursery zone of 83 otoliths from Lebranche mullet (*Mugil liza*) caught from May through October 2011 at 4 sampling sites in southern Brazil: Chuí (CHU), Laguna (LAG), Patos Lagoon estuary (PLE), and Tramandaí (TRA). The plot is based on a Euclidean distance matrix.

Lebranche mullet of these morphotypes grow for up to 4–5 years until they migrate to reproduce in coastal zones (~26°S) (Garbin et al., 2014; Lemos et al., 2014, 2016). Schroeder et al. (2023) recognized 2 subpopulations of Lebranche mullet: one subpopulation is associated with the central stock in Brazil, and another subpopulation is associated with the southern stock that comprises a mix of individuals from Brazil and Argentina. Locations or regions where Lebranche mullet are known to spawn are more associated to oceanographic conditions than to specific geographical locations (Lemos et al., 2014, 2016). The geographic breadth of the spawning region for this species varies annually, as does the annual contribution of individuals to the different subpopulations or contingents.

The mullet fishery in southeastern Brazil targets a stock that has been reported to be overfished in recent decades (de Miranda et al., 2011; MPA and MMA, 2015). This exploitation is further aggravated by the fact that Lebranche mullet are fished more intensively during the reproductive period of this species, especially when shoals are formed and gradually thickened as they migrate north from the nursery areas in Argentina, Uruguay, and southern Brazil (MPA and MMA, 2015; Lemos et al., 2016).

Proving that the 2 subpopulations described by Schroeder et al. (2023) mix with each other during the reproductive period and determining in which proportions this mixing occurs were the objectives of our study. Our work did not incorporate analysis of individuals from the same cohort that were born in different locations; therefore, it was not possible to estimate the actual contributions of specific nurseries to the adults of the southern population caught by commercial fisheries during the reproductive period of this species. However, we were able to conclude that the 2 subpopulations do mix during the reproductive period, and we have established that it is possible to estimate the relative contributions of different estuarine nurseries to the adult population of Lebranche mullet by using random forest classifiers generated with fingerprints of a combination of multiple elements in otoliths.

Table 4

Elemental fingerprinting indices (EFIs) for each sampling site (upper table) and between 2 sites (lower table), based on comparisons of chemical signatures in otoliths from Lebranche mullet (*Mugil liza*) collected in May–October 2011 in southern Brazil. The EFI ranges from 0 to 1, with a value of 0 indicating that the elemental compositions in the otoliths of 2 fish are most different and a value of 1 indicating that the elemental compositions in the otoliths of 2 specimens have the highest similarity (Moll et al., 2019). An asterisk (*) indicates a significant difference between EFI values ($P<0.05$). Standard deviations (SDs) of mean EFI values are provided in parentheses.

Comparisons within 1 site		
Site	No. of comparisons	Mean EFI (SD)
CHU	78	0.89 (0.04)*
PLE	276	0.86 (0.05)
TRA	231	0.86 (0.04)
LAG	210	0.85 (0.05)

Comparisons between 2 sites				
Site	Site	No. of comparisons	Mean EFI (SD)	*P*
CHU	PLE	234	0.81 (0.06)*	<0.001
CHU	TRA	208	0.82 (0.06)*	<0.001
CHU	LAG	195	0.83 (0.05)*	<0.001
PLE	TRA	297	0.86 (0.04)	0.960
PLE	LAG	294	0.84 (0.06)	0.203
TRA	LAG	252	0.87 (0.04)	0.074

Conclusions

The results of our study indicate that the elemental composition of otoliths from Lebranche mullet differed significantly between groups of nurseries and can potentially be used to estimate the relative contributions of nurseries to adults in the southern population. Using random forest classification algorithms with the chemical signatures of 3 elements (Li, Mg, and Sr) combined, we achieved the

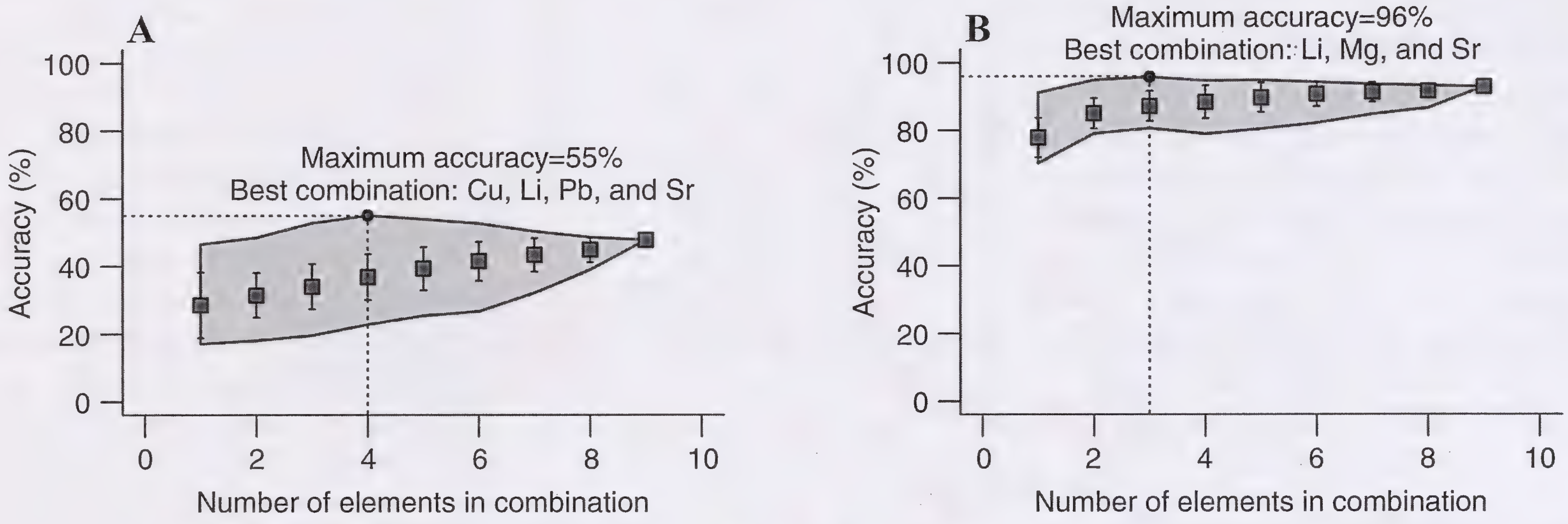

Figure 5

Accuracy in assigning nursery origins by using microchemistry in otoliths from Lebranche mullet (*Mugil liza*) caught between May and October 2011 at 4 sampling sites in southern Brazil, (**A**) when the origin was defined in a random forest algorithm as the site Chuí, Patos Lagoon estuary, Tramandaí, or Laguna and (**B**) when the origin was defined as either Chuí or the 3 nursery sites combined (Patos Lagoon estuary, Tramandaí, and Laguna). The classification trees of the algorithm were based on different combinations of up to 9 elements in otoliths. The polygon in each panel indicates the range of accuracy values. Error bars indicate standard deviations of mean accuracy levels. The dashed lines indicate maximum model accuracy. Cu=copper; Li=lithium; Mg=magnesium; Pb=lead; Sr=strontium.

maximum accuracy of 96% in identification of nursery origin for Lebranche mullet when assigning origin between CHU, where individuals of the southern migratory contingent were caught, and the nurseries in southern Brazil (PLE, TRA, and LAG combined). Given that analyses were done with individuals from the same population, our findings corroborate the existence of 2 subpopulations of Lebranche mullet off the coast of southern Brazil on the basis of their use of different nursery areas. Our results also confirm that signatures based on the concentrations of a combination of multiple elements in otoliths provide information valuable in establishing connectivity between nursery grounds and adult reproductive aggregation. Therefore, such analysis based on otolith microchemistry can be used to aid in the management of mullet fishing.

Resumen

El lisa Lebrancha (*Mugil liza*) es una especie estuarina de importancia económica que se encuentra a lo largo de la costa de Brasil. La población meridional de esta especie se extiende desde la costa del estado de São Paulo (23°S) hasta la costa de Argentina (36°S). Migra anualmente entre estuarios de Argentina, Uruguay y el sur de Brasil para reproducirse en sus zonas de desove marinas (~26°S). Evaluamos si las variaciones en la composición química de los otolitos de los peces colectados en las áreas de crianza pueden utilizarse para distinguir entre las 4 áreas de crianza de la población meridional. El análisis de la microquímica de los otolitos incluyó concentraciones de 9 elementos: litio (Li), magnesio (Mg), cobre, zinc, estroncio (Sr), cadmio, bario, lantano y plomo. Al utilizar algoritmos de clasificación de bosque aleatorio, se alcanzó una máxima precisión del 96% en la asignación del hábitat de críanza de la lisa Lebrancha entre 2 grupos (peces capturados en criaderos de Brasil y peces migrando desde aguas de Uruguay y Argentina) con la combinación de Li, Mg y Sr. Nuestros resultados indican que la composición de elementos de los otolitos puede ser una herramienta importante para establecer la conectividad entre las áreas de crianza utilizadas por la lisa Lebrancha. Discutimos las implicaciones de este resultado para la estructura de la población y el manejo de la pesquería de lisa en el sur de Brasil en relación con las limitaciones de los métodos que empleamos.

Acknowledgments

The authors thank the Conselho Nacional de Desenvolvimento Científico e Tecnológico (CNPq), the Coordenação de Aperfeiçoamento de Pessoal de Nível Superior (CAPES) (proces. no. 88887.461550/2019-00), the Programa de Pesquisas Ecológicas de Longa Duração (CNPq/CAPES/FAPs/BC-Fundo Newton 15/2016; CNPq process. no. 442206/2020-08), Instituto Brasileiro do Meio Ambiente e dos Recursos Naturais Renováveis, and the Instituto de Oceanografia, Universidade Federal do Rio Grande. The senior author is grateful for a postdoctoral grant from the Fundação de Amparo à Pesquisa do Estado do Rio Grande do Sul.

Literature cited

Adelir-Alves, J., F. A. L. M Daros, H. L. Spach, M. Soeth, and A. T. Correia.
2019. Otoliths as a tool to study reef fish population structure from coastal islands of South Brazil. Mar. Biol. Res. 14:973–988.

Artetxe-Arrate, I., I. Fraile, D. A. Crook, I. Zudaire, H. Arrizabalaga, A. Greig, and H. Murua.
2019. Otolith microchemistry: a useful tool for investigating stock structure of yellowfin tuna (*Thunnus albacares*) in the Indian Ocean. Mar. Freshw. Res. 70:1708–1721.

Avigliano, E., N. M. Alves, M. R. Rico, C. O. Ruarte, L. D'Atri, A. Méndez, J. Pisonero, A. V. Volpedo, and C. Borstelmann.
2021. Population structure and ontogenetic habitat use of *Micropogonias furnieri* in the Southwestern Atlantic Ocean inferred by otolith chemistry. Fish. Res. 240:105953.

Bae, S. E., and J.-K. Kim.
2020. Otolith microchemistry reveals the migration patterns of the flathead grey mullet *Mugil cephalus* (Pisces: Mugilidae) in Korean waters. J. Ecol. Environ. 44:21.

Biolé, F. G., G. A. Thompson, C. V. Vargas, M. Leisen, F. Barra, A. V. Volpedo, and E. Avigliano.
2019. Fish stocks of *Urophycis brasiliensis* revealed by otolith fingerprint and shape in the Southwestern Atlantic Ocean. Estuar. Coast. Shelf Sci. 229:106406.

Breiman. L.
2001. Random forests. Mach. Learn. 45:5–32.

Brown, J. A.
2006. Classification of juvenile flatfishes to estuarine and coastal habitats based on the elemental composition of otoliths. Estuar. Coast. Shelf Sci. 66:594–611.

Callicó Fortunato, R., M. González-Castro, A. Reguera Galán, I. García Alonso, C. Kunert, V. Benedito Durà, and A. Volpedo.
2017. Identification of potential fish stocks and lifetime movement patterns of *Mugil liza* Valenciennes 1836 in the Southwestern Atlantic Ocean. Fish. Res. 193:164–172.

Campana, S. E.
1999. Chemistry and composition of fish otoliths: pathways, mechanisms and applications. Mar. Ecol. Prog. Ser. 188:263–297.

Campana, S. E., and J. D. Neilson.
1985. Microstructure of fish otoliths. Can. J. Fish. Aquat. Sci. 42:1014–1032.

Campana, S. E., G. A. Chouinard, J. M. Hanson, A. Frechet, and J. Brattey.
2000. Otolith elemental fingerprints as biological tracers of fish stocks. Fish. Res. 46:343–357.

Clarke, L. M., B. D. Walther, S. B. Munch, S. R. Thorrold, and D. O. Conover.
2009. Chemical signatures in the otoliths of a coastal marine fish, *Menidia menidia*, from the northeastern United States: spatial and temporal differences. Mar. Ecol. Prog. Ser. 384:261–271.

Cuevas, M. J., K. Górski, L. R. Castro, A. Vivancos, and M. Reid.
2019. Otolith elemental composition reveals separate spawning areas of anchoveta, *Engraulis ringens*, off central Chile and northern Patagonia. Sci. Mar. 83:317–326.

Cuveliers, E. L., A. J. Geffen, J. Guelinckx, J. A. M. Raeymaekers, J. Skadal, F. A. M. Volckaert, and G. E. Maes.
2010. Microchemical variation in juvenile *Solea solea* otoliths as a powerful tool for studying connectivity in the North Sea. Mar. Ecol. Prog. Ser. 401:211–220.

D'Aquino, C. A., L. Franklin da Silva, M. A. A. Couceiro, M. D. Pereira, and C. A. F. Schettini.
2011. Transporte de Sal e Hidrodinâmica do Estuário do Rio Tubarão – SC, Brasil. Rev. Bras. Recur. Hidr. 16(3):113–125.

de Miranda, L. V., M. H. Carneiro, M. B. Peres, M. C. Cergole, and J. T. Mendonça.
2011. Contribuições ao processo de ordenamento da pesca da espécie *Mugil liza* (Teleostei: Mugilidae) nas regiões sudeste e sul do Brasil entre os anos de 2006 e 2010. Inst. Pesca, Sér. Relat. Téc. 49, 23 p. [Available from website.]

del Favero, J. M., and J. F. Dias.
2015. Juvenile fish use of the shallow zone of beaches of the Cananéia-Iguape coastal system, southeastern Brazil. Braz. J. Oceanogr. 63:103–114.

Dorval, E., C. M. Jones, R. Hannigan, and J. van Montfrans.
2005. Can otolith chemistry be used for identifying essential seagrass habitats for juvenile spotted seatrout, *Cynoscion nebulosus*, in Chesapeake Bay? Mar. Freshw. Res. 56:645–653.

dos Santos, M. L., V. M. Lemos, and J. P. Vieira.
2018. No mullet, no gain: cooperation between dolphins and cast net fishermen in southern Brazil. Zoologia 35:1–13.

Elsdon, T. S., and B. M. Gillanders.
2003. Reconstructing migratory patterns of fish based on environmental influences on otolith chemistry. Rev. Fish Biol. Fish. 13:217–235.

Elsdon, T. S., B. K. Wells, S. E. Campana, B. M. Gillanders, C. M. Jones, K. E. Limburg, D. H. Secor, S. R. Thorrold, and B. D. Walther.
2008. Otolith chemistry to describe movements and life-history parameters of fishes: hypotheses, assumptions, limitations and inferences. *In* Oceanography and marine biology: an annual review, vol. 46 (R. N. Gibson, R. J. A. Atkinson, and J. D. M. Gordon, eds.), p. 297–330. CRC Press, Boca Raton, FL.

Forrester, G. E., and S. E. Swearer.
2002. Trace elements in otoliths indicate the use of open-coast versus bay nursery habitats by juvenile California halibut. Mar. Ecol. Prog. Ser. 241:201–213.

Garbin, T., J. P. Castello, and P. G. Kinas.
2014. Age, growth, and mortality of the mullet *Mugil liza* in Brazil's southern and southeastern coastal regions. Fish. Res. 149:61–68.

Gillanders, B. M.
2002. Temporal and spatial variability in elemental composition of otoliths: implications for determining stock identity and connectivity of populations. Can. J. Fish. Aquat. Sci. 59:669–679.
2005. Using elemental chemistry of fish otoliths to determine connectivity between estuarine and coastal habitats. Estuar. Coast. Shelf Sci. 64:47–57.

Gillanders, B. M., and M. J. Kingsford.
2000. Elemental fingerprints of otoliths of fish may distinguish estuarine 'nursery' habitats. Mar. Ecol. Prog. Ser. 201:273–286.

González Castro, M., V. Abachián, and R. G. Perrotta.
2009. Age and growth of the striped mullet, *Mugil platanus* (Actinopterygii, Mugilidae), in a southwestern Atlantic coastal lagoon (37°32′S–57°19′W): a proposal for a life-history model. J. Appl. Ichthyol. 25:61–66.

Hamer, P. A., G. P. Jenkins, and B. M. Gillanders.
2003. Otolith chemistry of juvenile snapper *Pagrus auratus* in Victorian waters: natural chemical tags and their temporal variation. Mar. Ecol. Prog. Ser. 263:261–273.

Hastie, T., R. Tibshirani, F. Leisch, K. Hornik, B. D. Ripley, and B. Narasimhan.
2022. mda: mixture and flexible discriminant analysis. R package, vers. 0.5-3. [Available from website, accessed June 2022.]

Herbst, D. F., and N. Hanazaki.
2014. Local ecological knowledge of fishers about the life cycle and temporal patterns in the migration of mullet (*Mugil liza*) in southern Brazil. Neotrop. Ichthyol. 12:879–890.

Kennedy, B. P., A. Klaue, J. D. Blum, C. L. Folt, and K. H. Nislow.
2002. Reconstructing the lives of fish using Sr isotopes in otoliths. Can. J. Fish. Aquat. Sci. 59:925–929.

Kerr, L. A., and S. E. Campana.
2014. Chemical composition of fish hard parts as a natural marker of fish stocks. *In* Stock identification methods, 2nd ed. (S. X. Cadrin, L. A. Kerr, and S. Mariani, eds.), p. 205–234. Academic Press, Cambridge, MA.

Lê, S., J. Josse, and F. Husson.
2008. FactoMineR: a package for multivariate analysis. J. Stat. Softw. 25(1):1–18.

Lemos, V. M., A. S. Varela Jr., P. R. Schwingel, J. H. Muelbert, and J. P. Vieira.
2014. Migration and reproductive biology of *Mugil liza* (Teleostei: Mugilidae) in south Brazil. J. Fish Biol. 85:671–687.

Lemos, V. M., D. F. Ávila Troca, Castello, J. P. and J. P. Vieira.
2016. Tracking the southern Brazilian schools of *Mugil liza* during reproductive migration using VMS of purse seiners. Lat. Am. J. Aquat. Res. 44:238–246.

Lemos, V. M., C. Monteiro-Neto, H. Cabral, and J. P. Vieira.
2017. Stock identification of tainha (*Mugil liza*) by analyzing stable carbon and oxygen isotopes in otoliths. Fish. Bull. 115:201–206.

Lemos, V. M., H. Cabral, S. Pasquaud, and J. P. Vieira.
2021. Occurrence and abundance of young mullet *Mugil liza* (Teleostei: Mugilidae) in the surf zone along the southern coast of Brazil. Sci. Mar. 85:245–255.

Liaw, A., and M. Wiener.
2002. Classification and regression by randomForest. R News 2(3):18–22.

Loebmann, D., and J. P. Vieira.
2005. Distribuição espacial e abundância das assembléias de peixes no Parque Nacional da Lagoa do Peixe, Rio Grande do Sul, Brasil. Rev. Bras. Zool. 22:667–675.

Lorenzo, M. I.
2010. Otros recursos pesqueros del Uruguay. Frente Mariti. 21:143–146.

Lotze, H. K., H. S. Lenihan, B. J. Bourque, R. H. Bradbury, R. G. Cooke, M. C. Kay, S. M. Kidwell, M. X. Kirby, C. H. Peterson, and J. B. C. Jackson.
2006. Depletion, degradation, and recovery potential of estuaries and coastal seas. Science 312:1806–1809.

Mai, A. C. G., C. I. Miño, L. F. F. Marins, C. Monteiro-Neto, L. Miranda, P. R. Schwingel, V. M. Lemos, M. Gonzalez-Castro, J. P. Castello, and J. P. Vieira.
2014. Microsatellite variation and genetic structuring in *Mugil liza* (Teleostei: Mugilidae) populations from Argentina and Brazil. Estuar. Coast. Shelf Sci. 149:80–86.

Mai, A. C. G., M. L. dos Santos, V. M. Lemos, and J. P. Vieira.
2018. Discrimination of habitat use between two sympatric species of mullets, *Mugil curema* and *Mugil liza* (Mugiliformes: Mugilidae) in the rio Tramandaí Estuary, determined by otolith chemistry. Neotrop. Ichthyol. 16:e170045.

Mai, A. C. G., C. Q. Albuquerque, V. M. Lemos, P. R. Schwingel, G.-F. Ceni, T. D. Saint'Pierre, and J. P. Vieira.
2019. Coastal zone use and migratory behaviour of the southern population of *Mugil liza* in Brazil. J. Fish Biol. 95:1207–1214.

Menezes, N. A., M. Nirchio, C. de Oliveira, and R. Siccharamirez.
2015. Taxonomic review of the species of *Mugil* (Teleostei: Perciformes: Mugilidae) from the Atlantic South Caribbean and South America, with integration of morphological, cytogenetic and molecular data. Zootaxa 3918:1–38.

Mercier, L., A. M. Darnaude, O. Bruguier, R. P. Vasconcelos, H. N. Cabral, M. J. Costa, M. Lara, D. L. Jones, and D. Mouillot.
2011. Selecting statistical models and variable combinations for optimal classification using otolith microchemistry. Ecol. Appl. 21:1352–1364.

Mercier, L., D. Mouillot, O. Bruguier, L. Vigliola, and A. M. Darnaude.
2012. Multi-element otolith fingerprints unravel sea-lagoon lifetime migrations of gilthead sea bream *Sparus aurata*. Mar. Ecol. Prog. Ser. 444:175–194.

Moll, D., P. Kotterba, K. P. Jochum, L. von Nordheim, and P. Polte.
2019. Elemental inventory in fish otoliths reflects natal origin of Atlantic herring (*Clupea harengus*) from Baltic Sea juvenile areas. Front. Mar. Sci. 6:191.

MPA and MMA (Ministério da Pesca e Aquicultura and Ministério do Meio Ambiente).
2015. Plano de gestão para o uso sustentável da tainha, *Mugil liza* Valenciennes, 1836, no sudeste e sul do Brasil, 210 p. Minist. Pesca Aquic. and Minist. Meio Ambiente, Brasília, Brazil. [Available from website.]

Ogle, D. H., J. C. Doll, A. P. Wheeler, and A. Dinno.
2023. FSA: simple fisheries stock assessment methods. R package, vers. 0.9.5. [Available from website, accessed September 2023.]

Panfili, J., H. de Pontual, H. Troadec, and P. J. Wright (eds.).
2002. Manual of fish sclerochronology, 464 p. Ifremer-IRD, Brest, France. [Available from website.]

R Core Team.
2022. R: a language and environment for statistical computing. R Foundation for Statistical Computing, Vienna, Austria. [Available from website, accessed March 2023.]

Ramos, L. A., and J. P. Vieira.
2001. Composição específica e abundância de peixes de zonas rasas dos cinco estuários do Rio Grande do Sul, Brasil. Bol. Inst. Pesca 27:109–121.

Ranaldi, M. M., and M. M. Gagnon.
2010. Trace metal incorporation in otoliths of pink snapper (*Pagrus auratus*) as an environmental monitor. Comp. Biochem. Physiol., C 152:248–255.

Reis-Santos, P., B. M. Gillanders, S. E. Tanner, R. P. Vasconcelos, T. S. Elsdon, and H. N. Cabral.
2012. Temporal variability in estuarine fish otolith elemental fingerprints: implications for connectivity assessments. Estuar. Coast. Shelf Sci. 112:216–224.

Reis-Santos, P., S. E. Tanner, R. P. Vasconcelos, T. S. Elsdon, H. N. Cabral, and B. M. Gillanders.
2013. Connectivity between estuarine and coastal fish populations: contributions of estuaries are not consistent over time. Mar. Ecol. Prog. Ser. 491:177–186.

Rooker, J. R., D. H. Secor, V. S. Zdanowicz, and T. Itoh.
2001. Discrimination of northern bluefin tuna from nursery areas in the Pacific Ocean using otolith chemistry. Mar. Ecol. Prog. Ser. 218:275–282.

Sant'Ana, R., P. G. Kinas, L. V. de Miranda, P. R. Schwingel, J. P. Castello, and J. P. Vieira.
2017. Bayesian state-space models with multiple CPUE data: the case of a mullet fishery. Sci. Mar. 81:361–370.

Schroeder, R., E. Avigliano, A. V. Volpedo, R. Callicó Fortunato, P. Barrulas, F. A. Daros, P. R. Schwingel, M. C. Dias, and A. T. Correia.
2023. Lebranche mullet *Mugil liza* population structure and connectivity patterns in the southwest Altantic ocean [sic] using a multidisciplinary approach. Estuar. Coast. Shelf Sci. 288:108368.

Secor, D. H., A. Henderson-Arzapalo, and P. M. Piccoli.
1995. Can otolith microchemistry chart patterns of migration and habitat utilization in anadromous fishes? J. Exp. Mar. Biol. Ecol. 192:15–33.

Seeliger, U., C. Odebrecht, and J. P. Castello (eds.).
1997. Subtropical convergence environments: the coast and sea in the southwestern Atlantic, 308 p. Springer-Verlag, Berlin.

Sturrock, A. M., C. N. Trueman, A. M. Darnaude, and E. Hunter.
2012. Can otolith elemental chemistry retrospectively track migrations in fully marine fishes? J. Fish Biol. 81:766–795.

Sturrock, A. M., C. N. Trueman, J. A. Milton, C. P. Waring, M. J. Cooper, and E. Hunter.
2014. Physiological influences can outweigh environmental signals in otolith microchemistry research. Mar. Ecol. Prog. Ser. 500:245–264.

Sturrock, A. M., E., Hunter, J. A. Milton, EIMF, R. C. Johnson, C. P. Waring, and C. N. Trueman.
2015. Quantifying physiological influences on otolith microchemistry. Methods Ecol. Evol. 6:806–816.

Swearer, S. E., G. E. Forrester, M. A. Steele, A. J. Brooks, and D. W. Lea.
2003. Spatio-temporal and interspecific variation in otolith trace-elemental fingerprints in a temperate estuarine fish assemblage. Estuar. Coast. Shelf Sci. 56:1111–1123.

Thorrold, S. R., C. M. Jones, P. K. Swart, and T. E. Targett.
1998. Accurate classification of juvenile weakfish *Cynoscion regalis* to estuarine nursery areas based on chemical signatures in otoliths. Mar. Ecol. Prog. Ser. 173:253–265.

Thresher, R. E.
1999. Elemental composition of otoliths as a stock delineator in fishes. Fish. Res. 43:165–204.

Tkatcheva, V., D. Poirier, R. Chong-Kit, V. I. Furdui, C. Burr, R. Leger, J. Parmar, T. Switzer, S. Maedler, E. J. Reiner, et al.
2015. Lithium an emerging contaminant: bioavailability, effects on protein expression, and homeostasis disruption in short-term exposure of rainbow trout. Aquat. Toxicol. 161:85–93.

Tournois, J., A. M. Darnaude, F. Ferraton, C. Aliaume, L. Mercier, and D. J. McKenzie.
2017. Lagoon nurseries make a major contribution to adult populations of a highly prized coastal fish. Limnol. Oceanogr. 62:1219–1233.

Vasconcelos, R. P., P. Reis-Santos, S. Tanner, A. Maia, C. Latkoczy, D. Günther, M. J. Costa, and H. Cabral.
2008. Evidence of estuarine nursery origin of five coastal fish species along the Portuguese coast through otolith elemental fingerprints. Estuar. Coast. Shelf Sci. 79:317–327.

Venables, W. N., and B. D. Ripley.
2002. Modern applied swith S, 4th ed., 495 p. Springer, New York.

Vieira, J. P.
1991. Juvenile mullets (Pisces: Mugilidae) in the estuary of Lagoa dos Patos, RS, Brazil. Copeia 1991:409–418.

Vieira, J. P., and C. Scalabrin.
1991. Migração reprodutiva da “tainha” (*Mugil platanus* Gunther, 1980) no sul do Brasil. Atlântica 13:131–141.

Vrdoljak, D., S. Matić-Skoko, M. Peharda, H. Uvanović, K. Markulin, and R. Mertz-Kraus.
2020. Otolith fingerprints reveals [sic] potential pollution exposure of newly settled juvenile *Sparus aurata*. Mar. Pollut. Bull. 160:111695.

Walther, B. D., and S. R. Thorrold.
2006. Water, not food, contributes the majority of strontium and barium deposited in the otoliths of a marine fish. Mar. Ecol. Prog. Ser. 311:125–130.
2009. Inter-annual variability in isotope and elemental ratios recorded in otoliths of an anadromous fish. J. Geochem. Explor. 102:181–186.

Walther, B. D., M. J. Kingsford, M. D. O’Callaghan, and M. T. McCulloch.
2010. Interactive effects of ontogeny, food ration and temperature on elemental incorporation in otoliths of a coral reef fish. Environ. Biol. Fishes 89:441–451.

Warnes, G. R., B. Bolker, T, Lumley, A. Magnusson, B, Venables, G. Ryodan, S. Moeller, I. Wilson, M. Davis, N. Jain, et al.
2022. gtools: various R programming tools. R package, vers. 3.9.3. [Available from website, accessed August 2022.]

Wickham, H.
2016. ggplot2: elegant graphics for data analysis, 2nd ed., 260 p. Springer, New York.

Wickham H., R. François, L. Henry, K. Müller, and D. Vaughan.
2022. dplyr: a grammar of data manipulation. R package, vers. 1.0.10. [Available from website, accessed October 2022.]

National Marine
Fisheries Service
NOAA

Fishery Bulletin
established in 1881

Spencer F. Baird
First U.S. Commissioner
of Fisheries and founder
of *Fishery Bulletin*

Spatiotemporal dynamics of dolphinfish (*Coryphaena hippurus*) in the western Atlantic Ocean

Matthew D. Damiano (contact author)[1]
Mandy Karnauskas[2]
Wessley Merten[3]
Jie Cao[4]

Email address for contact author: matt.damiano@noaa.gov

[1] Cooperative Center for Marine and Atmospheric Studies
University of Miami
4600 Rickenbacker Causeway
Miami, Florida 33149
Present address: Southeast Fisheries Science Center
National Marine Fisheries Service, NOAA
75 Virginia Beach Drive
Miami, Florida 33149

[2] Southeast Fisheries Science Center
National Marine Fisheries Service, NOAA
75 Virginia Beach Drive
Miami, Florida 33149

[3] Beyond Our Shores Foundation
P.O. Box 3506
Newport, Rhode Island 02871

[4] Center for Marine Sciences and Technology
Department of Applied Ecology
North Carolina State University
303 College Circle
Morehead City, North Carolina 28557

Abstract—Dolphinfish (*Coryphaena hippurus*) are caught throughout the western Atlantic Ocean over varying spatial and temporal scales. Prior attempts to quantify the population dynamics of dolphinfish in this region have been inhibited by an inability to model the spatiotemporal dynamics of this stock. We fit a seasonal vector autoregressive spatiotemporal (VAST) model to quantify the spatiotemporal dynamics of western Atlantic dolphinfish, to estimate standardized relative indices of abundance during 1986–2022 at regional scales, and to estimate changes in spatial distribution. The magnitude of abundance was greatest during spring and summer in northern spatial strata and was comparable over seasons in southern spatial strata. Abundance of dolphinfish appeared to be stable during 1986–2018 and then declined during 2019–2022. This trend occurred in all regions, except for in Atlantic waters from Cape Hatteras, North Carolina, to the southern border of Georgia, where abundance remained stable during 2019–2022. No shift in the distribution of the population was detected, but regional patterns of abundance provide insight into changes in the timing of availability. This study resulted in the first standardized index of relative abundance to capture the spatiotemporal dynamics of western Atlantic dolphinfish. These results have increased our understanding of the population dynamics of this species in this region and should prove useful in future attempts to manage the population at different spatial and temporal scales.

Manuscript submitted 21 August 2023.
Manuscript accepted 18 March 2024.
Fish. Bull. 122:26–43 (2024).
Online publication date: 3 April 2024
doi: 10.7755/FB.122.1-2.3

The views and opinions expressed or implied in this article are those of the author (or authors) and do not necessarily reflect the position of the National Marine Fisheries Service, NOAA.

The dolphinfish (*Coryphaena hippurus*) is a mid-level trophic predator and migratory, cosmopolitan species of pelagic fish that is found throughout tropical and subtropical regions (Palko et al., 1982; Luckhurst, 2017; Moltó et al., 2020). The stock structure of dolphinfish caught in the western Atlantic Ocean, specifically in the southern extent of Food and Agriculture Organization of the United Nations (FAO) major fishing area 21 (the northwestern Atlantic Ocean) and FAO major fishing area 31 (the western Central Atlantic Ocean), is not precisely known (Damiano, 2023). Using analyses of size composition in catches over space, life history traits, and allelic frequencies, Oxenford and Hunte (1986) found evidence of a northern and southern stock in the western Central Atlantic Ocean and hypothesized that there are 2 unique seasonal migration patterns. The northern stock migration has been defined by seasonal movements into waters of Puerto Rico during late fall and early winter, movement along the Greater Antilles and Bahamas and into Florida waters during the spring, then into waters of the eastern United States during late spring and summer, and finally outward toward Bermuda during late summer (Oxenford and Hunte, 1986; Oxenford, 1999).

Tagging experiments conducted by Merten et al. (2014a, 2014b, 2016) revealed further complexity in the stock connectivity between dolphinfish caught along the eastern United States, in the Caribbean Islands, and in the Caribbean Sea, expanding the northeastern circuit to include coastal waters along the northeastern United States, and dolphinfish caught along an additional pathway to waters in Florida from the Caribbean Sea and through the Straits of Florida (Damiano, 2023). The connectivity between populations of dolphinfish in the western Atlantic Ocean and the Gulf of Mexico remains unclear (Damiano, 2023). Results from the DNA sequencing conducted by Merten et al. (2015) indicate shallow genetic differences among dolphinfish caught along the eastern United States and parts of the Caribbean Sea, and although the DNA sequencing results do not present conclusive evidence of a single stock, multiple subpopulations have been identified at smaller geographic scales in other ocean basins (Duarte-Neto et al., 2008; Ochoa-Zavala et al., 2022). Strong genetic separation of populations is likely driven by oceanographic barriers (Maggio et al., 2019), of which there are none known for the regions composing the western Atlantic Ocean (Damiano, 2023). However, despite this uncertainty, sufficient evidence exists of stock mixing and movement linkages in dolphinfish caught in the eastern United States and parts of the Caribbean Sea (Merten et al., 2014a, 2015, 2016), and that evidence indicates the need to model the spatiotemporal dynamics of a western Atlantic stock (Damiano, 2023).

According to a recent review of the condition of international dolphinfish fisheries in the western Central Atlantic Ocean that builds on the work of Mahon (1999), dolphinfish continue to support numerous high-value commercial, recreational, and artisanal fisheries at different seasonal and spatial scales (Merten et al., 2022a). Management of dolphinfish in the western Atlantic Ocean falls under the purview of the International Commission for the Conservation of Atlantic Tunas, but landings of this species are labeled as those of *other fishes* along with commercial bycatch taxa and therefore are not actively managed (Merten et al., 2022a).

In the eastern United States, the dolphinfish is managed under the Dolphin and Wahoo Fishery Management Plan by the South Atlantic Fishery Management Council (SAFMC, 2003). The annual catch limit for this species in the eastern United States is determined by using an average of past catches; this approach is a data-limited management procedure employed when biological reference points cannot be reliably estimated from an assessment model (Prager[1]). At the state level, effort-reducing and size-based management measures, such as bag limits and minimum size limits, are implemented for recreational and for-hire fisheries, but not all states implement both types of measures (SAFMC, 2003; Damiano, 2023).

The Caribbean Fishery Management Council, also a U.S. management body, and the Western Central Atlantic Fishery Commission, established by the FAO, do not have fishery management plans for dolphinfish, but they provide some monitoring and guidance for sustainable management of dolphinfish (Damiano, 2023). Practical management in Caribbean island waters and the Caribbean Sea falls to individual island nations and countries and territories of the Americas (Mahon, 1999; Merten et al., 2022a).

Such a lack of spatially consistent management measures is uncommon for transboundary stocks for which management and governance normally must adhere to an international policy (Levesque, 2008). Despite advances in spatiotemporal models and enhanced knowledge of the stock structure and movement connectivity of dolphinfish in the western Atlantic Ocean, no indices of relative abundance and no stock assessments are based on explicit modeling of the spatiotemporal dynamics of the population or subpopulations that make up this stock (Damiano, 2023). There are several other concerns regarding the western Atlantic stock. Lynch et al. (2018) reported a negative trend in estimated abundance of dolphinfish throughout the western Central Atlantic Ocean on the basis of catch per unit of effort (CPUE) data from the U.S. pelagic longline (U.S. PLL) logbook for the period 1987–2013. In addition, 23 nations still do not report landings of dolphinfish to the FAO (Merten et al., 2022a), and increases in sea-surface temperatures (SSTs) due to climate change may affect stock productivity and distribution (Barange et al., 2018; Damiano, 2023).

As is the case for highly migratory species, such as the swordfish (*Xiphias gladius*) and tuna species, catch and effort information come primarily from fishery-dependent sources (Forrestal et al., 2019), and apart from tagging programs, there are no fishery-independent data collection or monitoring programs for dolphinfish. Sources of fishery-dependent data, such as landings and CPUE data, also have mostly been disparate over both space and time for this species (Rose and Hassler, 1968; Mahon, 1999; Arocha et al., 2021; Merten et al., 2022a; Damiano, 2023). Consequently, past efforts to model the population dynamics of dolphinfish in the western Atlantic Ocean have generally been accomplished by using a surplus production model that has been fit to an index of relative abundance derived from fishery-dependent CPUE information for a discrete subsection of the stock's distribution (Damiano, 2023). Each of these cases has involved fitting standardization models to CPUE data (Prager[1]; Parker et al.[2]; Kleisner, 2008) in order to develop model-based indices that address the commonly violated assumption of constant catchability (Maunder and Punt, 2004), then fitting a surplus production model.

In each of these efforts, CPUE data were not sufficiently informative because of short time series, "one-way trip" patterns, or other common features of fishery-dependent data (Maunder et al., 2006; Magnusson and Hilborn, 2007), and their use resulted in highly uncertain estimates of biological reference points that could not be used to inform fisheries management. Kleisner (2008) accurately concluded that for assessment of dolphinfish to be successful, estimating robust indices of relative abundance must be employed with new techniques that account for spatiotemporal structure in observed catch data (Damiano, 2023).

---

[1] Prager, M. 2000. Exploratory assessment of dolphinfish, *Coryphaena hippurus*, based on U.S. landings from the Atlantic Ocean and Gulf of Mexico, 18 p. Southeast Fish. Sci. Cent., Natl. Mar. Fish. Serv., NOAA, Beaufort, NC. [Available from website.]

[2] Parker, C., K. M. Kleisner, and J. S. Nowlis. 2006. Preliminary assessment of the western Central Atlantic dolphinfish (*Coryphaena hippurus*) stock: a Caribbean regional fisheries mechanism project, 13 p. Sustainable Fisheries Division Contribution SFD-2005-041. [Available from Sustain. Fish. Div., Southeast Fish. Sci. Cent., Natl. Mar. Fish. Serv., NOAA, 75 Virginia Beach Dr., Miami, FL 33149.]

The spatiotemporal dynamics of dolphinfish in the western Atlantic Ocean are also likely linked to SST (Kleisner, 2008), given that dolphinfish reproduce year-round within their optimal thermal habitat (Schwenke and Buckel, 2008; Merten et al., 2015; Schlenker et al., 2021) and that high catch rates are associated with warm fronts with SSTs near 24–25C° (Farrell et al., 2014) and with mats of *Sargassum* macroalgae (Farrell et al., 2014; Rudershausen et al., 2019). Lynch et al. (2012) developed a 2-stage delta-generalized linear mixed model (GLMM) capable of modeling temperature regimes and habitat use of pelagic fish. They applied this method by fitting a delta-GLMM to CPUE data for highly migratory species, including dolphinfish, from the U.S. PLL logbook for the period 1987–2013 and by treating *year* as a random effect (Lynch et al., 2018). The indices derived by Lynch et al. (2018) are currently the most robust indices of relative abundance for dolphinfish in the western Atlantic Ocean. Although the majority of dolphinfish landings that are reported within the western Atlantic Ocean come from recreational fisheries (Merten et al., 2022a), the U.S. PLL logbook remains the most robust data set because of the long time series of observations of dolphinfish made at the fishing set level, which is a fine temporal resolution, throughout the western Atlantic Ocean.

Spatiotemporal autocorrelation is often present in commercial data because sampling (fishing) by fishing fleets is preferential and not random (Maunder and Punt, 2004). Spatiotemporal autocorrelation can lead to positively biased estimates of abundance (Xu et al., 2018), particularly for undersampled regions (Pennino et al., 2019). Lynch et al. (2018) noted that future work should consider other treatments of spatiotemporal data when estimating indices of relative abundance from fishery-dependent data and made specific reference to geostatistical delta-GLMMs (Thorson et al., 2015). Geostatistical delta-GLMMs include the use of vector autoregressive spatiotemporal (VAST) models that are built on a 2-stage modeling philosophy similar to that of a delta-GLMM. In a VAST model, covariates can be assigned specifically to effects related to environmental conditions or habitat and to catchability, spatial and spatiotemporal variation can be estimated explicitly as random effects, and spatiotemporal autocorrelation can be estimated (Thorson et al., 2015; Thorson, 2019) instead of implicitly assuming that sampling over space is independent (Conn et al., 2017). In the model in the R package VAST, the space over which spatial and spatiotemporal processes are measured can also be treated as being evenly distributed to address the unbalanced and preferential nature of sampling in fishery-dependent data (Thorson, 2019).

Findings from several studies indicate that spatiotemporal models can be used to reliably estimate indices of relative abundance from fishery-dependent data (Maunder et al., 2020; Ducharme-Barth et al., 2022; Hansell et al., 2022). The use of VAST models fit to data has generally resulted in improved estimation of abundance (Thorson et al., 2020; O'Leary et al., 2022) and of spatial population dynamics (Cao et al., 2017), with success demonstrated when models have been fit to fishery-dependent longline data for other highly migratory pelagic fish species, such as tunas (Maunder et al., 2020; Hansell et al., 2022). Our goals were to quantify the spatiotemporal dynamics of dolphinfish in the western Atlantic Ocean and to develop a model-based index of relative abundance that is unaffected by variation over space and time. Additionally, we sought to answer the following questions with our study:

1. Can the VAST model be used to estimate the seasonal patterns in the spatiotemporal dynamics of the density of the dolphinfish population in the western Atlantic Ocean?
2. How do the spatiotemporal dynamics of dolphinfish differ at regional scales?
3. Has a range shift occurred at the population level for dolphinfish in the western Atlantic Ocean?
4. Do estimates from use of the VAST package reveal spatiotemporal signals similar to those found in other data sources?

Materials and methods

Fishery data

For our analysis, we used U.S. PLL logbook data from the National Marine Fisheries Service (NMFS). Although the fishing effort of the U.S. PLL fleet is not uniform over space and time (Lynch et al., 2018), the logbook data contain 37 years of detailed catch and effort information on dolphinfish to the longline set level and compose the only data set with long-term observations collected over nearly the full extent of the geographic range of western Atlantic dolphinfish. Additionally, the dolphinfish, although targeted by the fleet, is not the primary target species of the U.S. PLL fleet, which primarily targets the swordfish and tunas (Luckhurst, 2017). Therefore, dolphinfish sampling (i.e., CPUE) is less likely to be biased by preferential sampling that results from the targeting behavior of the fleet. Vessels in the U.S. PLL fleet report the date and location of catch to the set level, SST, the type of gear and bait used, the number of hooks per set, whether dolphinfish were targeted or not, the number of dolphinfish caught, and the numbers of dolphinfish discarded dead and discarded alive. We used all logbook data from reports of catch in the western Atlantic Ocean for which latitude, longitude, SST, and CPUE information were available. The data we used contain approximately 255,000 observations, of which approximately 160,000 were observations in which zero encounters with dolphinfish were recorded.

Nominal catch calculation

We treated the number of hooks used in a longline set as the unit of effort (Lynch et al., 2012). We calculated the nominal CPUE as the number of dolphinfish caught per 1000 hooks, including any dolphinfish caught and retained or caught and discarded, whether dead or alive. We explored the number of set hours as an additional measure of effort; however, the results of analysis of catch versus hourly effort indicate a gear saturation effect in which CPUE declines exponentially after 5 h of soak time. This decrease in CPUE violates the assumption that the probability of catch is the same over every hour (Peterson et al., 2017; Hansell et al., 2022).

Spatial domain

The spatial domain included what we have defined as the western Atlantic Ocean, which extends approximately from 0°N to 55°N and from 25°W to 86°W. We stratified the spatial domain by using the discrete management areas for the U.S. PLL fishery described in the U.S. PLL logbook data set. These areas are defined, east to west and north to south, as follows: the region closest to the coast from Cape Cod, Massachusetts, to Cape Hatteras, North Carolina, which in the logbook data set is referred to as the *Mid-Atlantic Bight* (MAB); northeast coastal waters (NEC), farther to the north and east from the MAB; northeast distant waters on the Grand Banks (NED); the region closest to the coast from Cape Hatteras to the southern border of Georgia, described in the logbook data set as the *South Atlantic Bight* (SAB); waters off the Florida east coast and around the Florida Keys (FEC); the eastern part of the Sargasso Sea (SAR); the region in the north-central Atlantic Ocean that forms the western part of the Sargasso Sea (NCA); the Caribbean Sea (CAR); and offshore waters (OFS) (Fig. 1) (Damiano, 2023). To map data, we used a custom extrapolation grid to encompass all strata (Damiano, 2023).

Seasonality

The VAST model was configured to estimate indices for 4 seasons to capture the pattern of seasonal availability throughout the range of dolphinfish in the Western Atlantic Ocean. We assigned seasonal IDs to U.S. PLL logbook data at the monthly level: *winter* included December of a given year and January and February of the following year; *spring* included March, April, and May of the same year; *summer* included June, July, and August of the same year; and *fall* included September, October, and November of the same year (Damiano, 2023). The VAST model was configured with a total of 148 time steps over 4 seasons and 37 years. We also explored a monthly time step.

Spatiotemporal model description

The models implemented in the VAST package (vers. 3.5.0; Thorson and Barnett, 2017) in statistical software R (vers. 4.0.3; R Core Team, 2020) were fit to nominal CPUE values to derive standardized indices of relative abundance. The model in the VAST package functions like a delta-GLMM, also called a *hurdle* or *delta* model, that separately models the probability of non-zero catches (i.e., positive encounters) and positive catch rates from each encounter (i.e., positive catch rates) (Thorson et al., 2015; Lynch et al., 2018). We used the binomial GLMM with a logit link for the first linear predictor and explored lognormal, gamma, and Tweedie distributions for the second linear predictor. We chose the delta-lognormal configuration so that we could compare the results with those of Lynch et al. (2018) and could report the optimal model configuration, which was identified on the basis of model diagnostics, by using the following equations:

$$P_{1,\mathrm{i}} = \beta_1\left(t_\mathrm{i}\right) + \omega_1\left(s_\mathrm{i}\right) + \varepsilon_1\left(s_\mathrm{i}, t_\mathrm{i}\right) + \sum\nolimits_{p=1}^{n_\mathrm{p}} \gamma_1\left(p\right) X\left(p, s_\mathrm{i}, t_\mathrm{i}\right), \text{ and} \tag{1}$$

$$P_{2,\mathrm{i}} = \beta_2\left(t_\mathrm{i}\right) + \omega_2\left(s_\mathrm{i}\right) + \varepsilon_2\left(s_\mathrm{i}, t_\mathrm{i}\right) + \sum\nolimits_{p=1}^{n_\mathrm{p}} \gamma_2\left(p\right) X\left(p, s_\mathrm{i}, t_\mathrm{i}\right), \tag{2}$$

where $P_{1,\mathrm{i}}$ = the probability of positive dolphinfish encounter for observation *i*;
$P_{2,\mathrm{i}}$ = the positive dolphinfish catch rates (i.e., number of dolphinfish caught per 1000 hooks) given that they were encountered, for observation *i*;
$\beta(t_\mathrm{i})$ = the intercept for each time step *t* for observation *i*;
$\omega(s_\mathrm{i})$ = the spatial variation that is constant over time for knot *s* for observation *i*;
$\varepsilon(s_\mathrm{i}, t_\mathrm{i})$ = the time-varying spatiotemporal autocorrelation variation for knot *s* and time step *t* for observation *i*;
$\gamma(p)$ = the habitat effect *p* on the univariate response variable;
n_p = the number of habitat covariates; and
$X(p, s_\mathrm{i}, t_\mathrm{i})$ = the value of covariate *p* in knot *s* in time step *t* for observation *i*.

Note that $\beta(t_\mathrm{i})$ was treated as an independent and identically distributed random effect. Because of the seasonality in availability of dolphinfish to the U.S. PLL fishery over space, we included *season* as a spatially varying random effect of habitat; this treatment is also the standard for seasonal implementations of a VAST model. The spatial processes, $\omega_1(s_\mathrm{i})$ and $\omega_2(s_\mathrm{i})$, and spatiotemporal processes, $\varepsilon_1(s_\mathrm{i}, t_\mathrm{i})$ and $\varepsilon_2(s_\mathrm{i}, t_\mathrm{i})$, were modeled as Gaussian Markov random fields (random effects) (Lindgren et al., 2011) with an isotropic Matérn covariance function (i.e., correlation over a 2-dimensional spatial grid). We conducted correlation analyses by using the COR (vers. 0.0.1; Guo, 2020) and corrplot (vers. 0.92; Wei and Simko, 2021) packages in R with spatially stratified nominal CPUE for each season to determine the appropriate spatiotemporal structure for the second linear predictor. Although

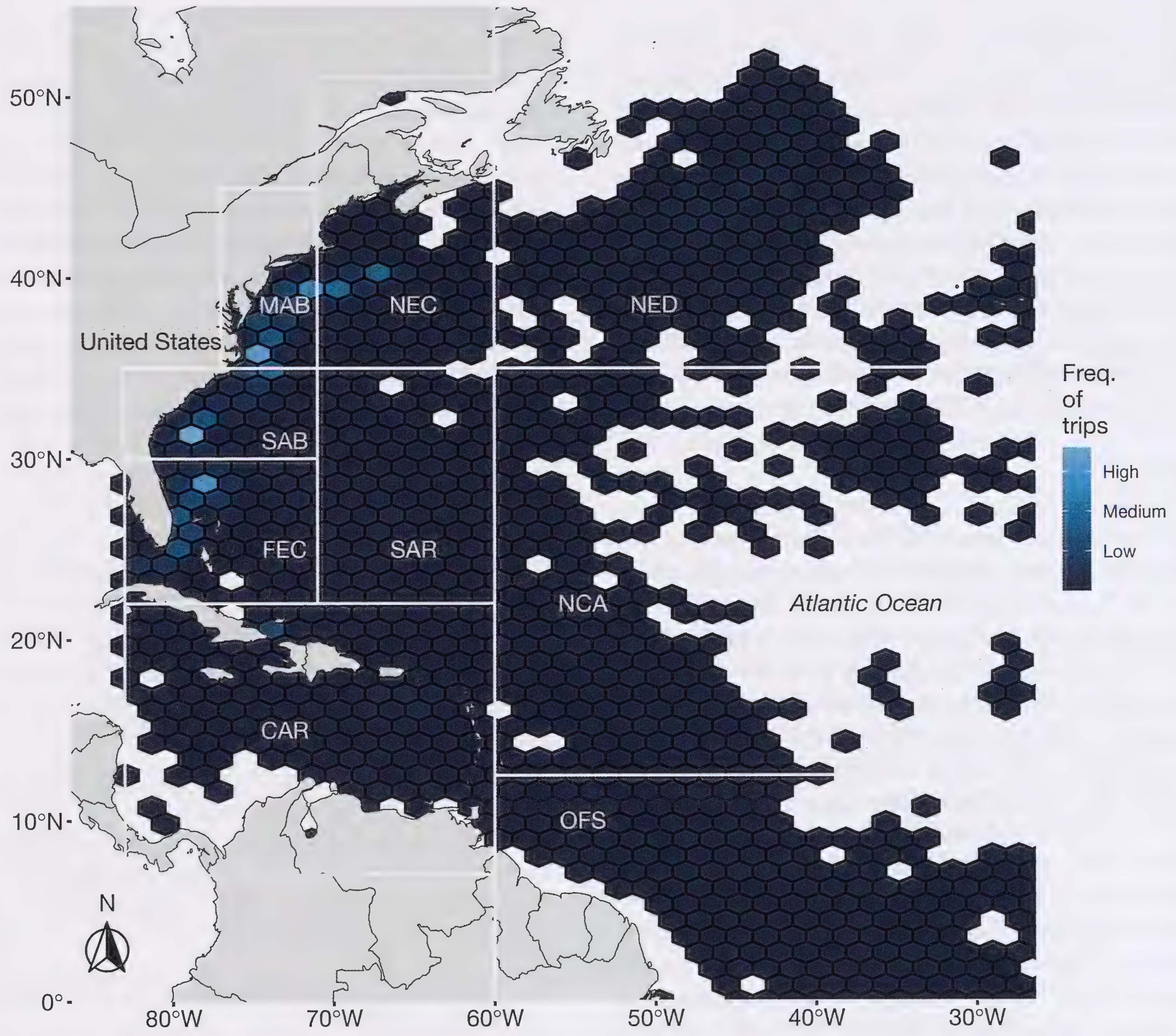

Figure 1

Map of the relative frequency of commercial trips in which dolphinfish (*Coryphaena hippurus*) were caught during 1986–2022, based on data from the U.S. pelagic longline logbook for the following management areas: the region closest to the coast from Cape Cod, Massachusetts, to Cape Hatteras, North Carolina, which in the logbook data set is referred to as the *Mid Atlantic Bight* (MAB); northeast coastal waters (NEC) farther to the north and east from the MAB; northeast distant waters on the Grand Banks (NED); the region closest to the coast from Cape Hatteras to the southern border of Georgia, referred to in the logbook data set as the *South Atlantic Bight* (SAB); waters off the Florida east coast and around the Florida Keys (FEC); the eastern part of the Sargasso Sea (SAR); the region in the north-central Atlantic Ocean that forms the western part of the Sargasso Sea (NCA); the Caribbean Sea (CAR); and offshore waters (OFS). Colors indicate relative frequency of trips made to the geographic coordinates within each hexagon.

correlation was high among some strata during specific seasons, there was no consistent pattern (Suppl. Fig. 1) (online only); therefore, we assumed that spatiotemporal random effects were independent and identically distributed. We fit the VAST model by using a mesh approach with 500 knots, the unit of measure over which to measure the spatial and spatiotemporal processes.

Parameters were determined through maximum likelihood estimation, in which fixed and random effects were integrated, by using the R package Template Model Builder (vers. 1.9.6; Kristensen et al., 2016). We used estimated log-scale densities to calculate indices as the predicted local density d for knots s and time step t multiplied by area a, summed over the total number of knots (n_s). In the VAST model, standardized indices of relative abundance are labeled as biomass in kilograms by default when the response is continuous CPUE (Thorson, 2019). However, we rescaled the index (I) estimates by using a constant so that the values would be unitless:

$$I\left(t\right) = \sum\nolimits_{s=1}^{n_s} \left(a\left(s\right) \times d\left(s,t\right)\right). \qquad (3)$$

We rescaled the index for each time step t as a product of local density and area a over knots s summed over the total number of knots. We calculated the change in spatial distribution using the center of gravity, which is the estimated centroid of the population's distribution:

$$Z(t) = \sum\nolimits_{s=1}^{n_s} \frac{\left(z(s) \times a(s) \times d(s,t)\right)}{I(t)}, \tag{4}$$

where $Z(t)$ = the center of gravity over time t that sums the center of gravity statistic z multiplied by area and density over the index I over the number of knots s.

The changes in population distribution were measured in kilometers in eastings and northings (Thorson et al., 2015). Following Li et al. (2014), we also calculated the center of gravity for the nominal effort data (Z_e), using the effort contained in the U.S. PLL logbook data set, as the sum of the product of seasonal effort (E_t) and space (i.e., latitude and longitude) (L_t) over the sum of total effort to explore spatial changes in the distribution of U.S. PLL effort:

$$Z_\mathrm{e} = \frac{\sum (E_\mathrm{t} L_\mathrm{t})}{\sum E_\mathrm{t}}. \tag{5}$$

Model selection, sensitivities, and diagnostics

We identified the optimal configuration of the model described in the previous section on the basis of the percentage of deviance explained and Akaike information criterion (AIC) (Akaike, 1973). In the "Results" section, we report these values in relation to the null model, which was constant intercept-only and required for calculating the percentage of deviance explained. We also provide results for a time-varying intercept-only model. Model fit was evaluated by using the R package for residual diagnostics, DHARMa (vers. 0.4.6; Hartig, 2022); diagnostics for all models were acceptable, and the optimal model diagnostics are provided in Supplementary Figure 2 (online only).

Correlation analysis

The final research question was whether the VAST estimates could pick up spatiotemporal signals in other sources of data on dolphinfish. In order to address this question, we used the COR and corrplot packages to analyze correlations between indices of estimated abundance by spatial strata and season with independent catch time series. These data include recreational catch and effort information for the period 2002–2019 from the Large Pelagics Survey of private and for-hire recreational vessels conducted by the Marine Recreational Information Program (NMFS, website), commercial landings for fishing operations that were not longline in spring and summer in North Carolina and Florida during 1991–2021 (M. Karnauskas, personal commun.), and recreational dolphinfish tournament data for the period 2000–2019 from the Marine Recreational Fishing Program of the Puerto Rico Department of Natural and Environmental Resources (Rodríguez-Ferrer[3]). Analysis of correlations with other fisheries data sets, especially those from recreational sources, will help to determine if an index fit to commercial data is consistent with noncommercial fishery trends (Damiano, 2023). A description of the indices and catch time series that were analyzed is provided in Table 1.

Results

Optimal model selection

We experimented with several model configurations to explore the effects of covariates and alternate distributions. Excluding intercept-only models, only 3 models

Table 1

The time series and seasons used to estimate the indices of abundance, of dolphinfish (*Coryphaena hippurus*) in the western Atlantic Ocean by spatial strata, for which correlation analyses were conducted. The spatial strata include the following regions: the region closest to the coast from Cape Cod, Massachusetts, to Cape Hatteras, North Carolina (NC), which in the U.S. pelagic longline (U.S. PLL) logbook data set is referred to as the *Mid-Atlantic Bight* (MAB); the region closest to the coast from Cape Hatteras to the southern border of Georgia, referred to in the U.S. PLL logbook data as the *South Atlantic Bight*; waters off the Florida east coast and around the Florida Keys (FEC); and the Caribbean Sea (CAR). The time series include data from the Large Pelagics Survey (LPS) of the Marine Recreational Information Program, commercial landings in NC and Florida (FL) from the NOAA Southeast Fisheries Science Center, and data from the Marine Recreational Fishing Program (MRFP) of the Puerto Rico Department of Natural and Environmental Resources.

Region	Catch time series	Period	Seasons
MAB	LPS recreational catch and effort	2002–2019	Summer and fall
SAB, FEC	Hook-and-line catch in FL and NC	1991–2021	Spring and summer
CAR	MRFP recreational tournament	2000–2019	Winter, spring, and fall

---

[3] Rodríguez-Ferrer, Y. 2022. Personal commun. Mar. Recreat. Fish. Progr., Puerto Rico Dep. Nat. Environ. Resour., 1375 Ave. Ponce de León, San Juan, Puerto Rico 00926.

converged to a solution. We attempted to fit set-level observations of SST using a 3-parameter basis spline function because of the association of dolphinfish with a relatively narrow, dome-shaped band of warm SSTs that varies over space and likely leads to positive catch rates (Farrell et al., 2014; Moltó et al., 2020; Schlenker et al., 2021). We also experimented with treating SST as a spatially varying random habitat effect. Given that the U.S. PLL targeted dolphinfish in only approximately 8% of observations during the period examined, we also tested one catchability covariate to account for variation in fleet behavior: a 3-level factor describing targeting behavior; in the U.S. PLL logbook data, most observations are assigned a *Yes* or *No* for targeting dolphinfish. For each observation with no targeting assignment, we added the letter *U*, for *Unknown*, in the blank cell. In this configuration, *targeting behavior* was treated as a spatially varying linear random effect. We considered *bait* as a potential catchability covariate, but bait type was nearly uniform throughout the data set. Therefore, it was not included.

We also attempted to model an individual *vessel* effect to account for spatiotemporal changes in fishing power (O'Leary et al., 2022). However, it either became computationally infeasible when used as a random effect, resulting in hundreds of thousands of new parameters, or resulted in computer memory allocation issues when treated as a fixed effect, likely because of approximately 700 individual vessels being treated as individual levels of a factor. We conducted a sensitivity analysis in which a geometric anisotropy spatial smoother was used in the optimal model; however, a solution could not be found with this model. We also experimented with gamma and Tweedie distributions for the observation model in the second linear predictor, but a solution could not be obtained with either model.

The optimal model (i.e., the basic seasonal spatiotemporal model) explained 30.8% of deviance and had an AIC of 880,221. The time-varying intercept model, which was used to explore the effect of temporal variation, explained 9.9% of deviance and had an AIC of 962,118. Adding SST as a spatially varying linear random effect resulted in a model with 31.6% of deviance explained and an AIC of 876,181. Although the percentage of deviance explained is greater and the AIC is lower for this model, the relationship between catch rates for dolphinfish and SST is not linear (Farrell et al., 2014). Furthermore, the relationship between catch rates and SST is likely confounded with seasonality, and the additional 0.8% of deviance explained may account for the variation in set-level SST observations.

The model that included both SST and *targeting behavior* as spatially varying random linear covariates related to habitat and catchability, respectively, explained 32.4% of deviance and had an AIC of 871,608. Although this model technically achieved the best performance metrics, using it did not result in different patterns in estimates of abundance or center of gravity. Still, use of this model did result in substantially larger standards for those estimated quantities, indicating that the addition of spatially varying random linear covariates, which added tens of thousands of additional random effects for estimation, did not alter the pattern and overall magnitude of trends obtained from the basic seasonal spatiotemporal model. This result further indicates that variation in estimates due to environmental effects or targeting behavior of fleets was confounded or "absorbed" by seasonal, spatial, and spatiotemporal process error. Therefore, we chose the basic spatiotemporal VAST model, which was the most parsimonious model, as the optimal configuration.

Spatiotemporal patterns in abundance

The total estimated seasonal index of relative abundance for the western Atlantic Ocean (Fig. 2) was defined by several peaks and troughs with no trend until 2018, after which the magnitude of subsequent peaks and troughs declined. Overall, the greatest levels of total abundance of dolphinfish occurred during 1986, 1995, and 2015, and abundance was generally highest in spring. The lowest abundance occurred in 2020. The trend of the total index among seasons was similar but stratified by magnitude; total relative abundance was greatest in spring, followed by summer and fall in some years, and then winter. Stratified by region, indices had considerable variability in trend and seasonality.

Estimates from northern coastal strata, such as the NEC, MAB, and SAB, had the highest variability among seasons, with higher abundances during spring and summer and lower abundances during fall and winter (Fig. 2); trends in abundance in spring and summer were similar through 2012 but began to deviate afterward. This pattern was most pronounced in the SAB, where abundance in summer declined to fall and winter levels after 2014 and abundance in spring remained relatively high and relatively stable during 2020–2022. Additionally, it is worth noting that the magnitude of abundance in fall increased relative to other seasons toward the north and the east (e.g., the magnitude of abundance in fall rose from the SAB to the MAB, from the MAB to the NEC, and from the NEC to the NED) (Fig. 2).

Estimates from the more southern strata and offshore strata (i.e., FEC, SAR, NCA, CAR, and OFS) indicate weaker or low variability in seasonality and mirror the index of estimated total abundance that has no trend until the decline during 2019–2022 (Fig. 2). Estimates were most certain (had the lowest standard errors) for abundance in the MAB and SAB, followed by those for abundance in the FEC and CAR, and were most uncertain (had the highest standard errors) for abundance in the offshore strata NED, SAR, and NCA (Fig. 2). These patterns in uncertainty were most likely due to higher and lower rates of sampling (i.e., fishing within those strata) respectively (Fig. 1). Furthermore, the highest estimates of abundance relative to the total index were found for the NCA, likely influencing the shape of the overall estimated trend in seasonal abundance.

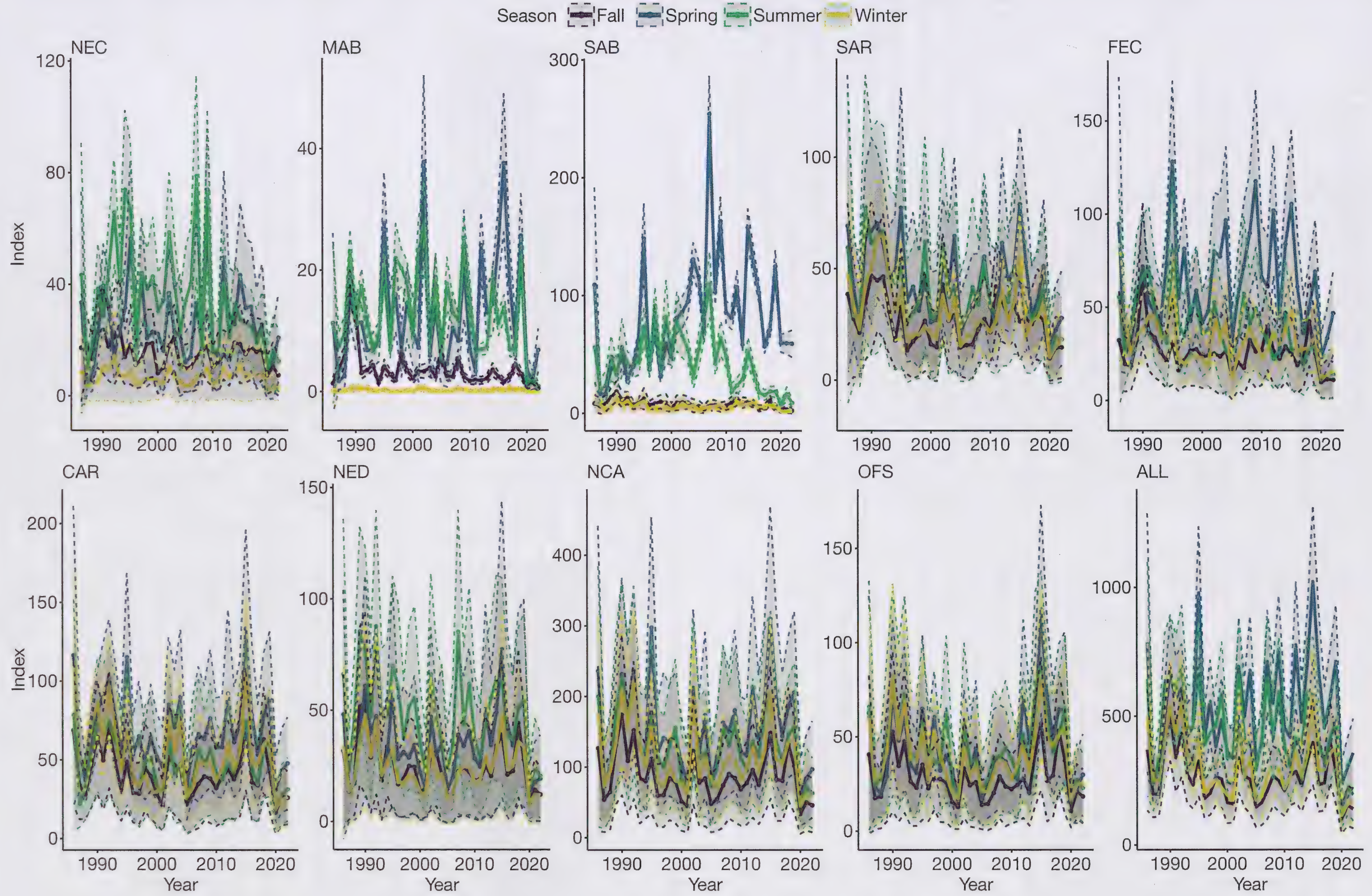

Figure 2

Standardized seasonal spatiotemporal indices of relative abundance for dolphinfish (*Coryphaena hippurus*) in the western Atlantic Ocean derived with data from the U.S. pelagic longline logbook. Indices were estimated for the period 1986–2022, by season, for all regions combined (ALL) and for each of the following management areas: northeast coastal waters (NEC), the region along the Atlantic coast referred to in the logbook data set as the *Mid-Atlantic Bight* (MAB), the region along the coast of the southeastern United States referred to in the logbook data set as the *South Atlantic Bight* (SAB), the eastern part of the Sargasso Sea (SAR), the east coast of Florida and the Florida Keys (FEC), the Caribbean Sea (CAR), northeast distant waters (NED), the western part of the Sargasso Sea in the north-central Atlantic Ocean (NCA), and offshore waters (OFS). For each season, a gray area outlined with colored dashed lines indicates the 95% confidence interval.

Shift in center of gravity

For the indices of estimated abundance, the eastings that approximate the spatial distribution from west to east from the bottom of the *y*-axis have no obvious trend (Fig. 3A). The northings that approximate the spatial distribution from south to north from the bottom of the *y*-axis also have no trend (Fig. 3B). For the nominal CPUE, the center of gravity in eastings indicates a strong westward shift (~120 km) during 1986–1994, then a gradual eastward shift during 1995–2022 (~90 km) that was consistent among seasons (Fig. 3C). The center of gravity in northings for nominal CPUE indicates an overall southern shift during 1993–2022 (~40 km), with some seasonal stratification: trends were similar between summer and winter and between spring and fall (Fig. 3D). We used box plots to visualize the average seasonal pattern in centers of gravity for the index of estimated abundance and for nominal CPUE (Fig. 4, A–D). The average seasonal pattern in the center of gravity for the estimated abundance index was defined by abundance shifting north and west as winter transitions to spring, slightly south and east during the transition to summer, and then south and east during fall (Fig. 4, A and B). For the nominal CPUE, the average seasonal pattern in the box plots more closely mirrored the time series shown in Figure 3, C and D, with a net southeastern movement throughout the year (Fig. 4, C and D).

Correlation analysis

Correlations among the VAST-estimated index and indices based on data sources independent of the U.S. PLL logbook, by spatial strata, were consistent with the timing of large migrations of dolphinfish and the overall seasonal pattern in the center of gravity (Fig. 4, A and B). The strong positive correlations between the Marine Recreational Fishing Program tournament catches in fall and the abundance estimates for winter and spring in the CAR (Fig. 5) are consistent with the timing of the movement of dolphinfish through the Antilles Current, which flows along the archipelago that separates the Caribbean Sea from the Atlantic Ocean, and with lower seasonal variation in abundance in this region compared with the variation in other regions (Fig. 3). Similarly, hook-and-line catches in North Carolina and Florida had the strongest correlations with estimates of abundance in the FEC and SAB during spring and summer months, and the CPUE data from the Large Pelagics Survey was most correlated with the estimate of abundance for the MAB in the fall (Fig. 5). Weak or negative correlations generally occurred between the estimated abundance index and the indices

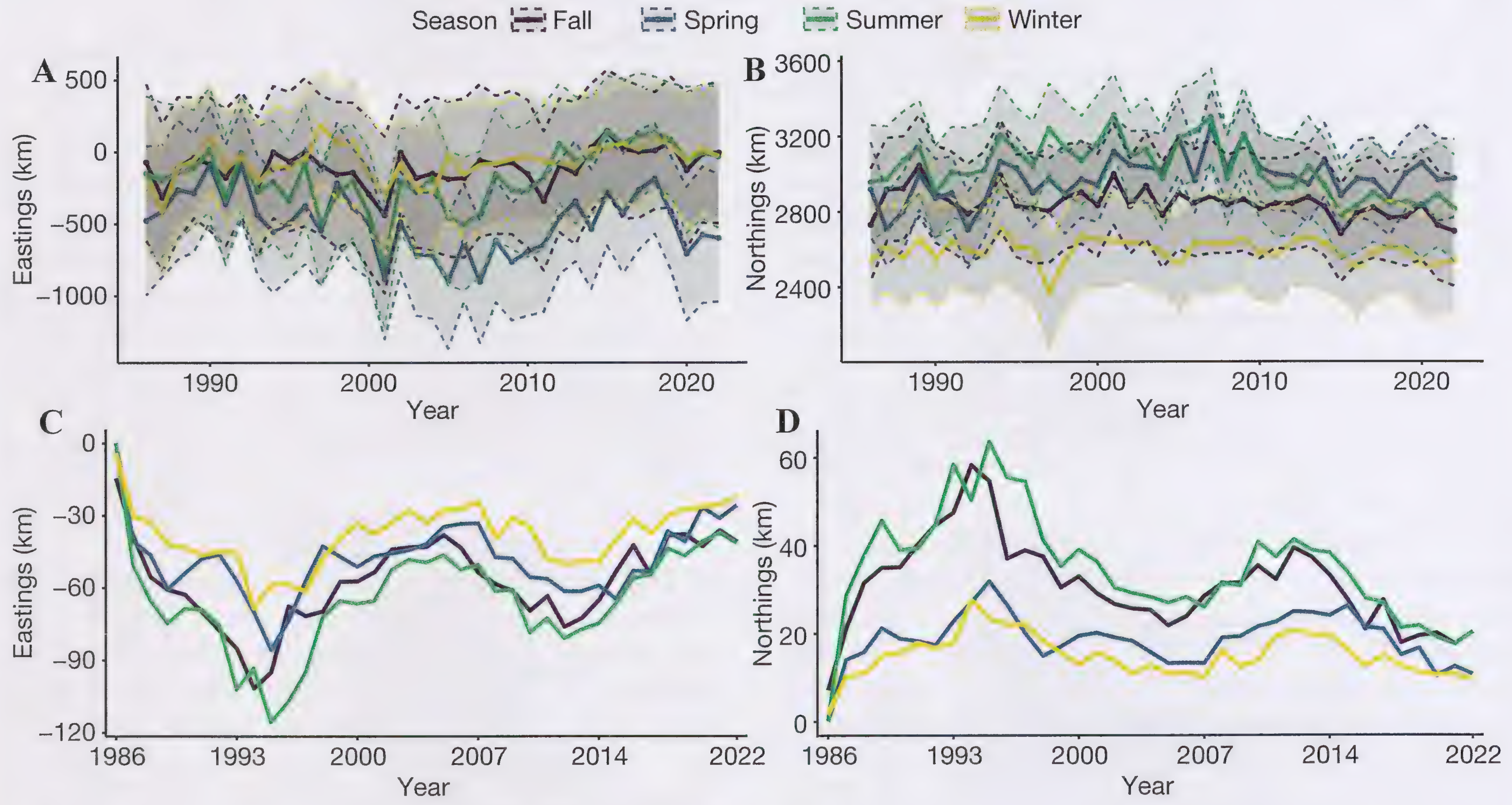

Figure 3

Seasonal estimates of the centroid or center of gravity of the distribution of dolphinfish (*Coryphaena hippurus*), by (**A**) eastings and (**B**) northings, in the western Atlantic Ocean during 1986–2022, based on abundance indices created with a vector autoregressive spatiotemporal model. Also shown are the seasonal centers of gravity calculated for nominal catch per unit of effort from the U.S. pelagic longline logbook for the same period, by (**C**) eastings and (**D**) northings. In the top panels, a gray area for each season outlined with colored dashed lines indicates the 95% confidence interval for that season.

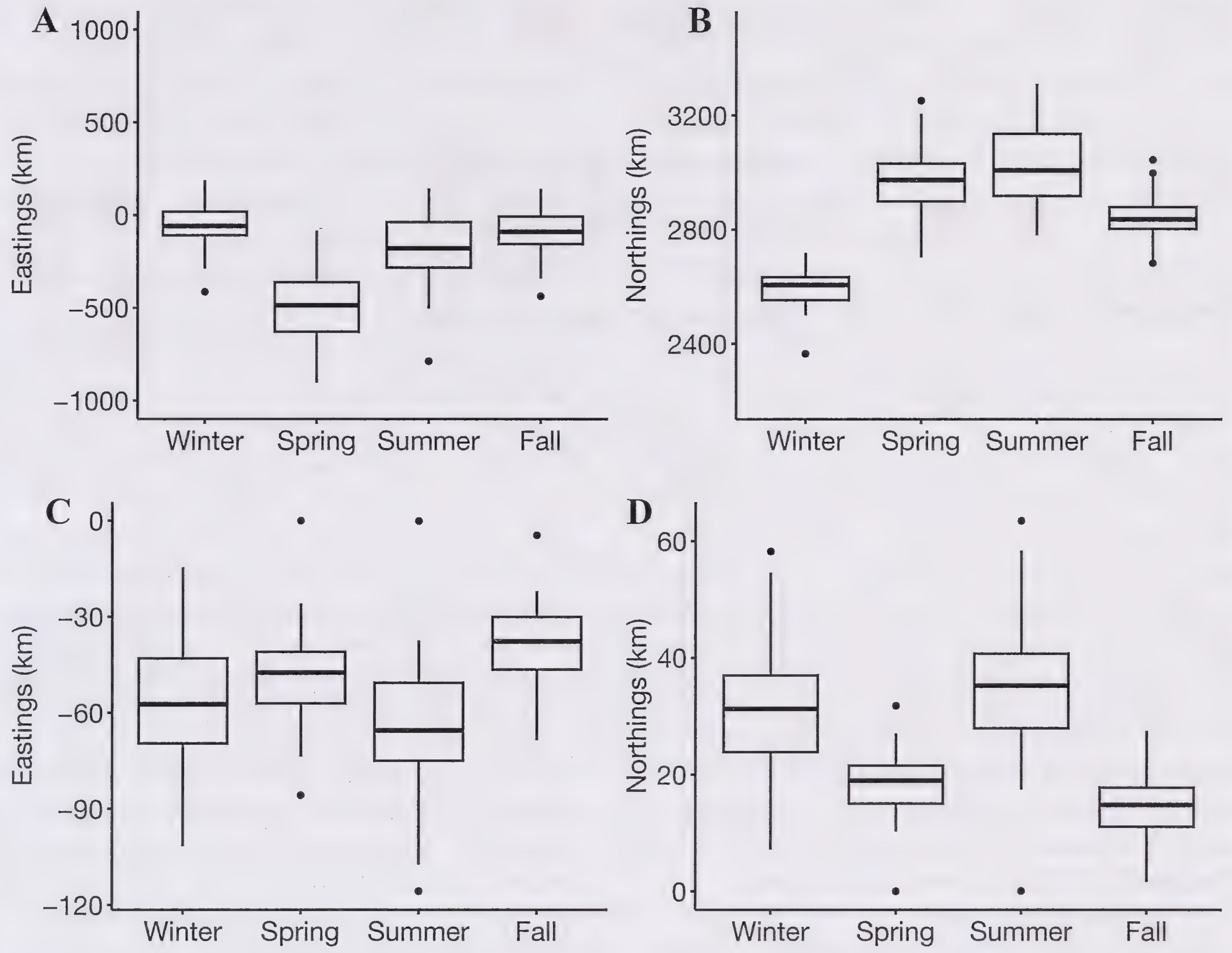

Figure 4

Box plots of seasonal estimates of the centroid or center of gravity of the distribution of dolphinfish (*Coryphaena hippurus*), by (**A**) eastings and (**B**) northings, in the western Atlantic Ocean during 1986–2022, based on abundance indices created with a vector autoregressive spatiotemporal model. Also shown are the seasonal centers of gravity calculated for the nominal catch per unit of effort from the U.S. pelagic longline logbook for the same time period, by (**C**) eastings and (**D**) northings. The thick line within the box indicates the median, the upper and lower parts of the box represent the first and third quartiles (the 25th and 75th percentiles), the whiskers extending above and below the box correspond to 1.5 times the interquartile range, and points represent values outside this range.

based on other data sources when season or region did not overlap (Fig. 5). Additionally, results of the correlation analysis provide some validation for estimated spatiotemporal patterns in abundance and indicate that using a VAST model to estimate spatial and spatiotemporal random effects can reveal broader spatiotemporal signals in the population dynamics of dolphinfish.

Discussion

Our model results reveal several important features of the population dynamics for western Atlantic dolphinfish. The overall abundance of dolphinfish in the western Atlantic Ocean was relatively stable during 1986–2018, followed by a decline during 2019–2022; seasonal patterns in abundance vary at different spatial scales. The stable trend in estimated abundance for 1986–2018 was somewhat surprising given the more pronounced negative trends found by Kleisner (2008) and Lynch et al. (2018). However, as of 2023, the U.S. PLL logbook has become a much larger data set than the one that was available during either of these previous studies, and in light of the results of our study (Fig. 2), the negative trends identified previously may have been driven by natural downward fluctuations in abundance that happened to occur during the terminal year of each analysis. Apart from the overall negative trend, our results are consistent with the general pattern in estimated abundance of dolphinfish that has been reported for the periods 1987–2005 (Kleisner, 2008) and 1987–2013 (Lynch et al., 2018). Furthermore, because we modeled spatial and spatiotemporal process errors, our results likely explain variation in numerous albeit aggregated latent processes (e.g., variation due to the behavior of the Gulf Stream or changes in fleet composition and behavior) that could not be explicitly modeled in previous research efforts.

Movement of dolphinfish generates seasonally and spatially explicit availability of abundance to many fisheries (Oxenford and Hunte, 1986; Mahon, 1999). Our results (Fig. 4, A and B) matched expectations for both the

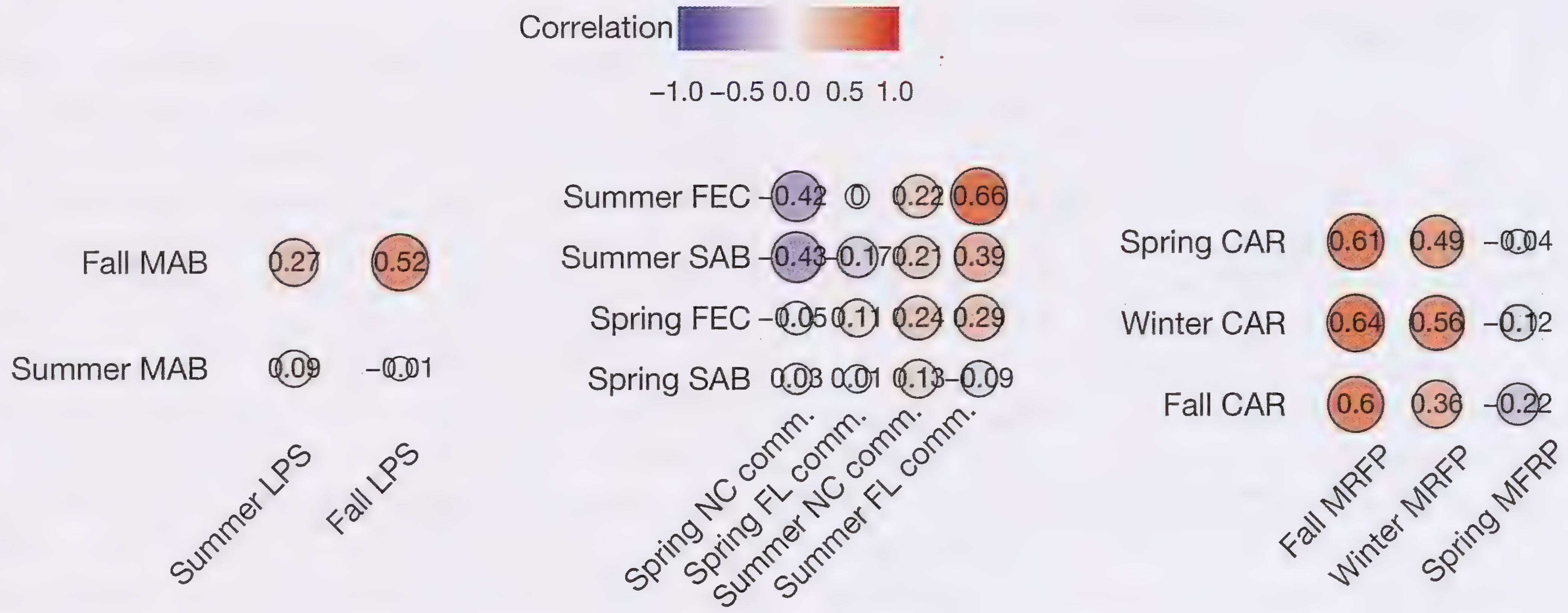

Figure 5

Correlations between indices of estimated abundance of dolphinfish (*Coryphaena hippurus*) in the western Atlantic Ocean and independent catch time series, by spatial strata and season. The correlations on the left side are between the indices of estimated abundance in summer and fall in the region closest to the coast from Cape Cod, Massachusetts, to Cape Hatteras, North Carolina, which in the U.S. pelagic longline logbook data set is referred to as the *Mid-Atlantic Bight* (MAB), and catch and effort data for the period 2002–2019 from the Marine Recreational Information Program's Large Pelagics Survey (LPS). The correlations in the middle are between estimated abundance indices for spring and summer in the region closest to the coast from Cape Hatteras to the southern border of Georgia, referred to in the logbook data set as the *South Atlantic Bight* (SAB), and in waters on the east coast of Florida and around the Florida Keys (FEC) and commercial catches (comm.) in spring and summer in North Carolina (NC) and Florida (FL) during 1991–2021. The correlations on the right side are between indices of estimated abundance in the fall, winter, and spring in the Caribbean Sea (CAR) and recreational tournament catch data for the same seasons during 2000–2019 from the Marine Recreational Fishing Program (MRFP) of the Puerto Rico Department of Natural and Environmental Resources.

seasonal distribution of abundance of dolphinfish and the spatiotemporal pattern of movement outlined by Oxenford and Hunte (1986) for the northern stock and expanded on by Merten et al. (2014a, 2014b, 2016). The estimates of abundance during spring and summer within strata along the East Coast of the United States were consistent with documented patterns of seasonal abundance (Merten et al., 2014a, 2015, 2016). Additionally, movement rates of dolphinfish slow in the SAB because of the Charleston Gyre (Merten et al., 2014a), an eddy off the coast of Charleston, South Carolina, that may be responsible for increased availability for extended pulses of fishing effort in spring and summer (Damiano, 2023). In the northern regions, the magnitude of abundance in spring and summer is substantially greater than in fall and winter, but this seasonal difference in magnitude (i.e., inter-seasonal variability) is lower in the southern regions.

The timing of the movement of the northern stock through the Caribbean Sea generates broad seasonal availability of dolphinfish to fisheries (Oxenford and Hunte, 1986), as reflected in estimates of abundance for southern spatial strata (Damiano, 2023). For example, although estimates of abundance in spring in the CAR were still the greatest among seasons, the magnitude of abundance in fall and winter were comparable with that of abundance in spring. These peaks in abundance in fall and winter may coincide with the movement of dolphinfish traveling to and from the Strait of Florida (Merten et al., 2014b, 2015) and the appearance of large dolphinfish (>90 cm in total length) in the waters of Caribbean islands (such large dolphinfish are caught in recreational tournaments; W. Merten, personal commun.), but these peaks may be more indicative of patterns in abundance of dolphinfish in certain U.S. territories in the Caribbean region than patterns in the broader CAR stratum (Damiano, 2023).

The increases in abundance in spring in the MAB and SAB during 2010–2018 and the associated decrease in abundance in summer in the SAB are also consistent with perceptions of commercial, recreational, and for-hire fishermen regarding local availability of dolphinfish in waters of North Carolina, including those north of the Outer Banks; they have observed either an increase in or stable catches of dolphinfish during the period approximately from 2015 through 2018 or 2019 (McPherson et al., 2022). The linear negative trend in abundance in the FEC region during 2015–2022 is similarly consistent with observations by stakeholders from eastern Florida and the Florida Keys of lower catches of dolphinfish in recent years leading up to a workshop held in 2021 (McPherson et al., 2022). Some local perceptions of abundance in Puerto Rico also have matched the recent decrease in estimated abundance in the CAR (Merten et al., 2022a; W. Merten, personal commun.).

These stakeholder observations provide some validation for the regional estimates of spatiotemporal indices of relative abundance (Damiano, 2023). Additionally, it is worth noting that the estimated trends in total abundance, and in abundance in the MAB, SAB, and FEC, strongly resemble those of the catch time series for dolphinfish from the Marine Recreational Information Program (NMFS, website). Further, the results of our correlation analysis indicate that the modeled spatial and spatiotemporal processes are identifying signals observed in data for other fisheries and in the Large Pelagics Survey that are independent of the U.S. PLL fleet. However, additional information, specifically from other Caribbean island nations and countries bordering the Caribbean Sea, would be required to determine if the index for the CAR is sufficiently representative of spatiotemporal dynamics of dolphinfish in the western extent of the Caribbean Sea where the U.S. PLL fleet fishes less than it does in U.S. territories (Fig. 1) (Damiano, 2023).

We suggest that there are 2 potential explanations (which are not mutually exclusive) for the recent decrease in abundance of dolphinfish during 2019–2022. The recent decline may be a lagged effect of a protracted period of high fishing pressure by commercial, recreational, and artisanal sectors throughout the western Atlantic Ocean (Damiano, 2023). Private recreational fishing in the coastal United States has been the dominant source of reported removals of dolphinfish in the western Atlantic Ocean (Merten et al., 2022a), and recreational effort linearly increased during 1986–2010 and then plateaued (NMFS, website). In the northeastern states located within the NEC and MAB, recreational catches have remained high (NMFS, website) despite the estimated decreases in abundance (Fig. 2). Consequently, these increases in recreational exploitation rates in specific areas may explain the recent reductions in abundance (Fig. 2, Suppl. Fig. 3 [online only]).

With respect to commercial effort, although the number of trips of the U.S. PLL fleet has decreased since 1994 and effort has linearly declined (senior author, personal observ.), commercial fishing throughout the northwest Atlantic and western Central Atlantic Oceans in numerous countries in aggregate has linearly increased (FAO FishStat, website); this trend does not include those countries where fishing occurs but landings of dolphinfish are not reported (Merten et al., 2022a). In Barbados, landings of dolphinfish have slowly decreased while CPUE has remained relatively stable during 1994–2018 (Oxenford et al.[4]), with higher sustained effort coupled with reduced landings (i.e., availability of fish), indicating the possibility of an effect on stock productivity.

Concerning the effect of artisanal fisheries, artisanal fishing in Venezuela also is reportedly a large source of removals of dolphinfish in the Caribbean Sea (Arocha et al., 2021), and other Caribbean island countries are reportedly developing artisanal fleets that target pelagic fish, including dolphinfish, for which data are not available (W. Merten, personal commun.). Cumulatively, a scenario in which overexploitation is occurring throughout the western Atlantic Ocean is plausible, although this notion is subject to a high degree of uncertainty because of the lack of reporting.

Alternatively, or in concert with fishing activity, environmental effects may explain the overall trend and recent decline in estimated abundance. Mean SST is rising throughout the world (Garcia-Soto, 2021) and in the large marine ecosystems that compose the western Atlantic Ocean (Kessler et al., 2022). Within the western Atlantic Ocean, the most pronounced rates of increased warming are occurring in the North and northwest Atlantic Oceans (Saba et al., 2016; Kessler et al., 2022) due to a combination of natural climate variability and anthropogenic climate change (Chen et al., 2020). Consequently, northward shifts in the distribution of abundance have been observed for many species along the continental shelf of the Atlantic coast of the United States (Kleisner et al., 2017; Morley et al., 2018). Additionally, the heat transported northward by the Gulf Stream that had normally been quite variable has steadily declined since 2008 (Bryden et al., 2020), with a pronounced decrease occurring in 2020 that has since been followed by a period of uncharacteristically low heat transport (NOAA Atlantic Oceanographic and Meteorological Laboratory, website).

Dolphinfish appear to prefer warm water within a relatively narrow band (Moltó et al., 2020), and like individuals of other marine fishes, they will seek to remain within their optimal thermal habitat (Schlenker et al., 2021). However, temperature preferences of populations of dolphinfish are not geographically uniform; for example, dolphinfish prefer waters with temperatures of 22–24°C off the coast of Peru (Torrejón-Magallanes et al., 2019), but dolphinfish have been caught in waters as warm as 36–37°C in the Gulf of Oman, an arm of the Arabian Sea (W. Merten, personal commun.). A recent lab experiment conducted by Heuer et al. (2021) off eastern Florida confirmed that a dolphinfish's ability to physically move was optimal within the well-documented preference of western Atlantic dolphinfish for waters with temperatures of 24–29°C (Farrell et al., 2014; Merten et al., 2014b; Schlenker et al., 2021). However, exposure to temperatures beyond 31°C has resulted in reduced mobility or death for this species (Heuer et al., 2021). These results may explain the reduction in abundance of dolphinfish in spring in the FEC during 2015–2022 and subsequent divergence in abundance in spring and summer in the SAB (Fig. 2); the timing of fish migrating north from the Antilles may be occurring earlier during the year so that dolphinfish can avoid inhospitable temperatures. Salvadeo et al. (2020) estimated a northward shift in the population of dolphinfish in the eastern Pacific Ocean at similar latitudes. These distribution changes across different ocean basins are consistent with the broadscale effects of climate change on marine species globally (Poloczanska et al., 2013; Damiano, 2023).

---

[4] Oxenford, H. A., D. Johnson, S.-A. Cox, and J. Franks. 2019. Report on the relationships between *Sargassum* events, oceanic variables, and dolphinfish and flyingfish fisheries, 25 p. Cent. Resour. Manage. Environ. Stud., Univ. West Indies, Cave Hill Campus. Bridgetown, Barbados. [Available from website.]

A shift in population distribution is also consistent with stakeholder observations in the FEC region: fishermen from the Florida Keys could not find dolphinfish in waters warmer that than the temperatures preferred by dolphinfish (>29°C), and fishermen from more northern regions (e.g., NEC, MAB, and SAB) have perceived more stable abundance and availability and done so earlier in the year (McPherson et al., 2022). Although it is highly plausible that dolphinfish exposed to near-lethal temperatures (>31°C) would move, the overall pattern in estimated abundance closely mirrors that of an SST "fingerprint" that indicates the recent weakening of the Atlantic Meridional Overturning Circulation and consists of cooling in the subpolar Atlantic Ocean and warming in the Gulf Stream region (Caesar et al., 2018; Ditlevsen and Ditlevsen, 2023). The behavior of these oceanographic features may indicate a more complex relationship between the Gulf Stream and spatiotemporal dynamics of dolphinfish.

Changes in fishing pressure and in the environment are likely contributing to the observed patterns in abundance, and data gaps make it challenging to discern the drivers of shifts with more accuracy. Additionally, some of the changes in fishing pressure and in the environment are aligned spatially and temporally, making it more challenging to disentangle the forces. For example, increases in landings from the Eastern Caribbean in 2014 coincided with significant changes in temperature, upwelling, and productivity in the region from Cape Hatteras through the Florida Keys (Craig et al., 2021). Sudden warming of the Florida Straits (Volkov et al., 2019), which connects the Gulf of Mexico and Atlantic Ocean and is a major migration pathway for dolphinfish, may also have contributed to changes in presence of dolphinfish. Most of the variation in these overlapping processes is likely absorbed by the estimation of spatial and spatiotemporal process errors with small contributions to deviance (i.e., variation) explained by modeling explicit habitat and catchability covariates. Differentiating between the drivers related to habitat and catchability will require more intensive analysis of patterns in ocean conditions and fishing exploitation in relation to patterns in the abundance discussed herein.

We recommend further investigation into the relationship between SST anomalies and the behavior of the Atlantic Meridional Overturning Circulation and Gulf Stream and the abundance of western Atlantic dolphinfish by using fine-scale fishery-independent oceanographic and movement data. Such an analysis would allow further differentiation between changes in fishing pressure and changes in the environment as drivers of distribution patterns and would provide some insight into whether these patterns will continue in the future given the shifts in temperature and current systems that are predicted to occur with climate change (Alexander et al., 2020; Damiano, 2023). Spatiotemporal models may not be appropriate for these analyses because of the tendency to aggregate estimated spatial and spatiotemporal process errors. Furthermore, although the seasonal patterns in the estimated center of gravity (Fig. 4, A and B) indicate that a generalized movement circuit was captured with the VAST model, we acknowledge that movement of dolphinfish is likely much more complex than the patterns described herein, potentially with patterns markedly different from those reported in the literature (Peterson[5]) and may include connectivity with regions not included in this analysis (e.g., the Gulf of Mexico and West Africa).

The configuration of the VAST model used in this study and described herein does not include any age or size structure in the population. Therefore, any spatiotemporal differences in ontogeny (e.g., documented differences in feeding habits) (Pincay-Espinoza and Varela, 2022), in spawning and larval distribution (Park et al., 2017), in changes in growth rate with size and age, or in vertical habitat use (i.e., association with fish aggregating devices or *Sargassum*) (Ortega-Garcia et al., 2022) were also likely to have been absorbed by the estimation of spatial and spatiotemporal random effects. No relationship was detected between influxes of *Sargassum* and CPUE for dolphinfish in the Eastern Caribbean (Oxenford et al.[5]), but large quantities of *Sargassum* may make fishing more difficult (i.e., fishing methods are negatively affected and fish are harder to detect and, therefore, less likely to be encountered). This notion warrants some investigation into the precise nature of the effects of *Sargassum* on catchability. We recommend that future research prioritize collection of age- or length-structure information sufficient for estimating age or size bins by using VAST or other spatiotemporal modeling techniques (Cao et al., 2020; Hansell et al., 2022).

The U.S. PLL logbook data have substantial spatial limitations and, therefore, uncertainty in eastern areas outside of the U.S. exclusive economic zone and the western extent of the Caribbean Sea (Fig. 1). This uncertainty is evidenced by stronger extrapolation to the CAR and OFS regions and by larger standard errors and confidence intervals for regionally stratified indices from those regions (Fig. 3). Furthermore, although the average pattern of the seasonal center of gravity (Fig. 4, A and B) appears to have captured the movement circuit of the northern stock, the dynamics of a purported southern stock found in the CAR and OFS strata are likely confounded (Oxenford and Hunte, 1986). Despite this caveat, fitting a VAST model to these data may help inform the estimation of abundance in neighboring cells in the model's extrapolation grid if both stocks occur. Future efforts to quantify the spatiotemporal dynamics of western Atlantic dolphinfish may benefit from calibrating the CPUE data from the U.S. PLL logbook with foreign longline fleet data sets from areas with low U.S. PLL fleet activity (O'Leary et al., 2022). Such an exercise will also help to determine the accuracy of this study's model extrapolations to undersampled regions and consistency with signals appearing in other data sets. Lastly, we acknowledge that the optimal VAST model was sensitive to different configurations, smoothers, and assumptions concerning the second linear predictor's error structure. Future efforts dedicated to teasing apart fishery and environmental drivers of the population dynamics of western Atlantic dolphinfish by using models that are not spatiotemporal may help elucidate reasons for these sensitivities.

---

[5] Peterson, C. 2023. Personal commun. Southeast Fish. Sci. Cent., Natl. Mar. Fish. Serv., NOAA, 101 Pivers Island Rd., Beaufort, NC 28516-9722.

The development of an index of relative abundance for western Atlantic dolphinfish through modeling with spatiotemporal variation is a vital step toward understanding the population dynamics of western Atlantic dolphinfish and improving the robustness of management measures (Damiano, 2023). Ideally, a spatially explicit stock assessment would be the next step toward determining stock status. However, despite advances in modeling software and in technology available for data collection and despite a growing citizen science data collection program (Merten et al., 2022b), the quality and temporal resolution of most data sources for western Atlantic dolphinfish have not changed radically since previous assessments were conducted in 2000 and 2006. Therefore, assessments would likely continue to be confined to surplus production models. Kleisner (2008) found that fitting surplus production models to geostatistical indices did not improve the ability to obtain reference points. Although McDonald et al. (2021) demonstrated that a spatially explicit biomass dynamics model can capture time-varying spatial patterns in both population processes and fishing effort, most removal data are available only at an annual time step, precluding modeling of the seasonal dynamics reported in this study.

If improved data collection or monitoring are not possible or stock status cannot be determined from an assessment, an alternative and perhaps more realistic use of the spatiotemporal index of relative abundance could be to guide an index-based management approach to setting catch advice (Apostolaki and Hillary, 2009; Little et al., 2011; Fischer et al., 2020; Sánchez-Maroño et al., 2021; Damiano, 2023). Indeed, empirical index-based management procedures that have been simulation-tested through a management strategy evaluation have been shown to have promise for data-limited stocks (Geromont and Butterworth[6]; Sagarese et al., 2019). For western Atlantic dolphinfish, correlations at various time lags should be analyzed to identify appropriate lead times, and rigorous evaluation through simulations or a management strategy evaluation should be pursued to test the robustness of such management procedures to alternative spatial and temporal scopes (Bosley et al., 2019; Cadrin et al., 2020) and to the substantial uncertainty found in this study and described herein. Additionally, a management strategy evaluation would be useful in determining if an empirical management procedure will be more or less responsive than, or as responsive as, the current catch-averaging strategy for quantifying the spatiotemporal dynamics of western Atlantic dolphinfish (Walter et al., 2023).

Conclusions

The dolphinfish possesses a unique life history characterized by fast growth and early maturation (Oxenford, 1999; Perrichon et al., 2019) that hypothetically makes individuals of this species capable of withstanding high levels of fishing pressure (Schwenke and Buckel, 2008; Damiano, 2023). The population abundance and distribution of dolphinfish in the western Atlantic Ocean appear to have been relatively stable during 1986–2018, but that period was followed by one of declining abundance during 2019–2022. High fishing pressure in concert with changing ocean conditions may be responsible for the recent decline in and changes to abundance at finer spatial scales (Damiano, 2023). Having used VAST models in our study, we provide the first spatiotemporal index of relative abundance for dolphinfish caught in the western Atlantic Ocean at seasonally and spatially explicit scales. The general consistency of our results with those of past studies and with stakeholder observations and the relatively strong spatiotemporal correlations with recreational catch time series indicate that our index is robust and reliably captures the spatiotemporal dynamics of western Atlantic dolphinfish (Damiano, 2023). This research addressed the need for a reliable index of relative abundance and improved upon the work of Kleisner (2008) and Lynch et al. (2018) by accounting for spatial and spatiotemporal variation in abundance of dolphinfish. Spatiotemporal modeling techniques, although complex and data-intensive, provide more information than nonspatial configurations (Berger et al., 2017) and are especially useful for standardizing fishery-dependent data (Maunder et al., 2020; Izquierdo et al., 2022) when improved monitoring programs are too costly (Damiano, 2023).

Resumen

El dorado (*Coryphaena hippurus*) se captura en todo el océano Atlántico occidental a distintas escalas espaciales y temporales. Los intentos previos de cuantificar la dinámica poblacional del dorado en la región se han visto inhibidos por la incapacidad de modelar la dinámica espaciotemporal de esta población. Ajustamos un modelo vectorial espaciotemporal, estacional y autorregresivo (VAST) para cuantificar la dinámica espaciotemporal del dorado del Atlántico occidental, para estimar los índices abundancia relativos estandarizados de durante 1986–2022 a escalas regionales y estimar los cambios en la distribución espacial. La magnitud de la abundancia fue mayor durante la primavera y el verano en los estratos espaciales del norte y fue comparable a lo largo de las estaciones en los estratos espaciales del sur. La abundancia del dorado pareció estabilizarse durante 1986–2018y luego disminuyó durante 2019–2022. Esta tendencia ocurrió

---

[6] Geromont, H., and D. Butterworth. 2015. A review of assessment methods and the development of management procedures for data-poor fisheries, 198 p. University of Cape Town, Cape Town, South Africa. [Report produced for the FAO.] [Available from website.]

en todas las regiones, excepto en las aguas del Atlántico desde el cabo Hatteras, Carolina del Norte, hasta la frontera sur de Georgia, donde la abundancia se mantuvo estable durante 2019–2022. No se detectó ningún cambio en la distribución de la población, pero los patrones regionales de abundancia proporcionan información sobre los cambios en el momento de la disponibilidad. En el presente estudio se reporta el primer índice de abundancia relativa estandarizado que capta la dinámica espaciotemporal del dorado del Atlántico occidental. Estos resultados incrementaron nuestra comprensión sobre la dinámica poblacional de esta especie en la región y deberían resultar útiles en futuros intentos de manejar la población a diferentes escalas espaciales y temporales.

Acknowledgments

We would like to thank the NMFS and North Carolina Sea Grant for funding this research through the NMFS-Sea Grant Fellowship in Population and Ecosystem Dynamics (award no. NA20OAR4170468), J. Buckel and M. Karp for their insights during the development of this manuscript, and the peer reviewers for their helpful feedback.

Literature cited

Akaike, H.
1973. Information theory and an extension of the maximum likelihood principle. *In* Proceedings of the 2nd International Symposium on Information Theory; Tsahkadsor, 2–8 September 1971 (B. N. Petrov and F. Csaki eds.), p. 267–281. Akadémiai Kiadó, Budapest, Hungary.

Alexander, M. A., S. Shin, J. D. Scott, E. Curchitser, and C. Stock.
2020. The response of the northwest Atlantic Ocean to climate change. J. Clim. 33:405–428.

Apostolaki, P., and R. Hillary.
2009. Harvest control rules in the context of fishery-independent management of fish stocks. Aquat. Living Resour. 22:217–224.

Arocha, F., X. Gutierrez, and E. Evaristo.
2021. Revised and updated catches of the common dolphinfish (*Coryphaena hippurus*) from Venezuelan fisheries. Collect. Vol. Sci. Pap. ICCAT 77(10):1–4. [Available from website.]

Barange, M., T. Bahri, M. C. M. Beveridge, K. L. Cochrane, S. Funge-Smith, and F. Poulain (eds.).
2018. Impacts of climate change on fisheries and aquaculture: synthesis of current knowledge, adaptation and mitigation options. FAO Fish. Aquac. Tech. Pap. 627, 628 p. FAO, Rome.

Berger, A. M., D. R. Goethel, and P. D. Lynch.
2017. Introduction to "space oddity: recent advances incorporating spatial processes in the fishery stock assessment and management interface." Can. J. Fish. Aquat. Sci. 74:1693–1697.

Bryden, H. L., W. E. Johns, B. A. King, G. McCarthy, E. L. McDonagh, B. I. Moat, and D. A. Smeed.
2020. Reduction in ocean heat transport at 26°N since 2008 cools the eastern subpolar gyre of the North Atlantic Ocean. J. Clim. 33:1677–1689.

Bosley, K. M., D. R. Goethel, A. M. Berger, J. J. Deroba, K. H. Fenske, D. H. Hanselman, B. J. Langseth, and A. M. Schueller.
2019. Overcoming challenges of harvest quota allocation in spatially structured populations. Fish. Res. 220:105344.

Cadrin, S. X., M. N. Maunder, and A. E. Punt.
2020. Spatial structure: theory, estimation and application in stock assessment models. Fish. Res. 229:105608.

Caesar, L., S. Rahmstorf, A. Robinson, G. Feulner, and V. Saba.
2018. Observed fingerprint of a weakening Atlantic Ocean overturning circulation. Nature 556:191–196.

Cao, J., J. T. Thorson, R. A. Richards, and Y. Chen.
2017. Spatiotemporal index standardization improves the stock assessment of northern shrimp in the Gulf of Maine. Can. J. Fish. Aquat. Sci. 74:1781–1793.

Cao, J., J. T. Thorson, A. E. Punt, and C. Szuwalski.
2020. A novel spatiotemporal stock assessment framework to better address fine-scale species distributions: development and simulation testing. Fish Fish. 21:350–367.

Chen, Z., Y.-O. Kwon, K. Chen, P. Fratantoni, G. Gawarkiewicz, and T. M. Joyce.
2020. Long-term SST variability on the Northwest Atlantic continental shelf and slope. Geophys. Res. Lett. 47:e2019GL085455.

Conn, P. B., J. T. Thorson, and D. S. Johnson.
2017. Confronting preferential sampling when analysing population distributions: Diagnosis and model-based triage. Methods Ecol. Evol. 8:1535–1546.

Craig, J. K., G. T. Kellison, S. M. Binion-Rock, S. D. Regan, M. Karnauskas, S.-K. Lee, R. He, D. M. Allen, N. M. Bacheler, H. Blondin, et al.
2021. Ecosystem status report for the U.S. South Atlantic region. NOAA Tech. Memo. NMFS-SEFSC-753, 145 p.

Damiano, M. D.
2023. In search of novel solutions to emerging challenges in quantitative fisheries management. Ph.D. diss., 170 p. North Carolina State Univ., Raleigh, NC. [Available from website.]

Ditlevsen, P., and S. Ditlevsen.
2023. Warning of a forthcoming collapse of the Atlantic meridional overturning circulation. Nat. Commun. 14:4254.

Duarte-Neto, P., R. Lessa, B. Stosic, and E. Morize.
2008. The use of sagittal otoliths in discriminating stocks of common dolphinfish (*Coryphaena hippurus*) off northeastern Brazil using multishape descriptors. ICES J. Mar. Sci. 65:1144–1152.

Ducharme-Barth, N. D., A., Grüss, M. T. Vincent, H. Kiyofuji, Y. Aoki, G. Pilling, J. Hampton, and J. T. Thorson.
2022. Impacts of fisheries-dependent spatial sampling patterns on catch-per-unit-effort standardization: a simulation study and fishery application. Fish. Res. 246:106169.

Farrell, E. R., A. M. Boustany, P. N. Halpin, and D. L. Hammond.
2014. Dolphinfish (*Coryphaena hippurus*) distribution in relation to biophysical ocean conditions in the northwest Atlantic. Fish. Res. 151:177–190.

Fischer, S. H., J. A. A. De Oliveira, and L. T. Kell.
2020. Linking the performance of a data-limited empirical catch rule to life-history traits. ICES J. Mar. Sci. 77:1914–1926.

Forrestal, F. C., C. P. Goodyear, and M. Schirripa.
2019. Applications of the longline simulator (LLSIM) using US pelagic longline logbook data and Atlantic blue marlin. Fish. Res. 211:331–337.

Garcia-Soto, C., L. Cheng, L. Caesar, S. Schmidtko, E. B. Jewett, A. Cheripka, I. Rigor, A. Caballero, S. Chiba, J. C. Báez, et al.
2021. An overview of ocean climate change indicators: sea-surface temperature, ocean heat content, ocean pH,

dissolved oxygen concentration, arctic sea ice extent, thickness and volume, sea level and strength of the AMOC (Atlantic Meridional Overturning Circulation). Front. Mar. Sci. 8:642372.

Guo, G.
2020. A block bootstrap for quasi-likelihood in sparse functional data. Statistics 54:909–925.

Hartig, F.
2022. DHARMa: residual diagnostics for hierarchical (multi-level / mixed) regression models. R package, vers. 0.4.6. [Available from website, accessed March 2023.]

Hansell, A. C., S. L. Becker, S. X. Cadrin, M. Lauretta, J. F. Walter III, and L. A. Kerr.
2022. Spatio-temporal dynamics of bluefin tuna (*Thunnus thynnus*) in US waters of the northwest Atlantic. Fish. Res. 255:106460.

Heuer, R. M., J. D. Stieglitz, C. Pasparakis, I. C. Enochs, D. D. Benetti, and M. Grosell.
2021. The effects of temperature acclimation on swimming performance in the pelagic mahi-mahi (*Coryphaena hippurus*). Front. Mar. Sci. 8:654276.

Izquierdo, F., R. Menezes, L. Wise, A. Teles-Machado, and S. Garrido.
2022. Bayesian spatio-temporal CPUE standardization: case study of European sardine (*Sardina pilchardus*) along the western coast of Portugal. Fish. Manage. Ecol. 29:670–680.

Kessler, A., N. Goris, and S. K. Lauvset.
2022. Observation-based Sea surface temperature trends in Atlantic large marine ecosystems. Prog. Oceanogr. 208:102902.

Kleisner, K. M.
2008. A spatio-temporal analysis of dolphinfish; *Coryphaena hippurus*, abundance in the western Atlantic: implications for stock assessment of a data-limited pelagic resource. Ph.D. diss., 234 p. Univ. Miami, Coral Gables, FL. [Available from website.]

Kleisner, K. M., M. J. Fogarty, S. McGee, J. A. Hare, S. Moret, C. T. Perretti, and V. S. Saba.
2017. Marine species distribution shifts on the U.S. Northeast Continental Shelf under continued ocean warming. Prog. Oceanogr. 153:24–36.

Kristensen, K., A. Nielsen, C. W. Berg, H. Skaug, and B. M. Bell.
2016. TMB: automatic differentiation and Laplace approximation. J. Stat. Softw. 70(5):1–21.

Levesque, J. C.
2008. International fisheries agreement: review of the International Commission for the Conservation of Atlantic Tunas: case study—shark management. Mar. Policy 32:528–533.

Li, G., X. Chen, L. Lin, and W. Guan.
2014. Distribution of hotspots of chub mackerel based on remote-sensing data in coastal waters of China. Int. J. Remote Sens. 35:4399–4421.

Lindgren, F., H. Rue, and J. Lindström.
2011. An explicit link between Gaussian fields and Gaussian Markov random fields: the stochastic partial differential equation approach. J. R. Stat. Soc., B 73:423–498.

Little, L. R., S. E. Wayte, G. N. Tuck, A. D. M. Smith, N. Klaer, M. Haddon, A. E. Punt, R. Thomson, J. Day, and M. Fuller.
2011. Development and evaluation of a cpue-based harvest control rule for the southern and eastern scalefish and shark fishery of Australia. ICES J. Mar. Sci. 68:1699–1705.

Luckhurst, B. E.
2017. Aspects of the migration, seasonality and habitat use of two mid-trophic level predators, dolphinfish (*Coryphaena hippurus*) and wahoo (*Acanthocybium solandri*), in the pelagic ecosystem of the western Atlantic including the Sargasso Sea. Collect. Vol. Sci. Pap. ICCAT 73:3163–3174. [Available from website.]

Lynch, P. D., K. W. Shertzer, and R. J. Latour.
2012. Performance of methods used to estimate indices of abundance for highly migratory species. Fish. Res. 125–126:27–39.

Lynch, P. D., K. W. Shertzer, E. Cortés, and R. J. Latour.
2018. Abundance trends of highly migratory species in the Atlantic Ocean: accounting for water temperature profiles. ICES J. Mar. Sci. 75:1427–1438.

Maggio, T., A. Allegra, F. Andaloro, J. Pedro Barreiros, P. Battaglia, C. M. Butler, A. Cuttitta, M. R. J. Fontes, R. Freitas, M. Gatt, et al.
2019. Historical separation and present-day structure of common dolphinfish (*Coryphaena hippurus*) populations in the Atlantic Ocean and Mediterranean Sea. ICES J. Mar. Sci. 76:1028–1038.

Magnusson, A., and R. Hilborn.
2007. What makes fisheries data informative? Fish Fish. 8:337–358.

Mahon, R.
1999. Dolphinfish fisheries in the Caribbean region. Sci. Mar. 63:411–420.

Maunder, M. N., and A. E. Punt.
2004. Standardizing catch and effort data: a review of recent approaches. Fish. Res. 70:141–159.

Maunder, M. N., J. R. Sibert, A. Fonteneau, J. Hampton, P. Kleiber, and S. J. Harley.
2006. Interpreting catch per unit effort data to assess the status of individual stocks and communities. ICES J. Mar. Sci. 63:1373–1385.

Maunder, M. N., J. T. Thorson, H. Xu, R. Oliveros-Ramos, S. D. Hoyle, L. Tremblay-Boyer, H. H. Lee, M. Kai, S.-K. Chang, T. Kitakado, et al.
2020. The need for spatio-temporal modeling to determine catch-per-unit effort based indices of abundance and associated composition data for inclusion in stock assessment models. Fish. Res. 229:105594.

McDonald, R. R., D. M. Keith, J. A. Sameoto, J. A. Hutchings, and J. M. Flemming.
2021. Explicit incorporation of spatial variability in a biomass dynamics assessment model. ICES J. Mar. Sci. 78:3265–3280.

McPherson, M., M. Karnauskas, J. Byrd, J. Hadley, S. Sagarese, C. Peterson, K. Craig, A. Mastitski, and S. Crosson.
2022. Participatory modeling of dolphin and wahoo fisheries in the U.S. South Atlantic: final report from a workshop series. NOAA Tech. Memo. NMFS-SEFSC-755, 18 p.

Merten, W., R. Appeldoorn, and D. Hammond.
2014a. Movements of dolphinfish (*Coryphaena hippurus*) along the U.S. east coast as determined through mark and recapture data. Fish. Res. 151:114–121.
2014b. Spatial differentiation of dolphinfish (*Coryphaena hippurus*) movements relative to the Bahamian archipelago. Bull. Mar. Sci. 90:849–864.
2016. Movement dynamics of dolphinfish (*Coryphaena hippurus*) in the northeastern Caribbean Sea: evidence of seasonal re-entry into domestic and international fisheries throughout the western central Atlantic. Fish. Res. 175:24–34.

Merten, W. B., N. V. Schizas, M. T. Craig, R. S. Appeldoorn, and D. L. Hammond.
2015. Genetic structure and dispersal capabilities of dolphinfish (*Coryphaena hippurus*) in the western central Atlantic. Fish. Bull. 113:419–429.

Merten, W., R. Appeldoorn, A. Grove, A. Aguilar-Perera, F. Arocha, and R. Rivera.
2022a. Condition of the international fisheries, catch and effort trends, and fishery data gaps for dolphinfish (*Coryphaena hippurus*) from 1950 to 2018 in the Western Central Atlantic Ocean. Mar. Policy 143:105189.

Merten, W., R. Appeldoorn, J. Latour, C. Glaser, E. Becker, and D. Hammond.
2022b. A citizen science approach to enhance dolphinfish (*Coryphaena hippurus*) data collection to improve species management. Fish. Manage. Ecol. 29:502–515.

Moltó, V., P. Hernández, M. Sinopoli, A. Besbes-Benseddik, R. Besbes, A. Mariani, M. Gambin, F. Alemany, B. Morales-Nin, A. M. Grau, et al.
2020. A global review on the biology of the dolphinfish (*Coryphaena hippurus*) and its fishery in the Mediterranean Sea: advances in the last two decades. Rev. Fish. Sci. Aquac. 28:376–420.

Morley, J. W., R. L. Selden, R. J. Latour, T. L. Frölicher, R. J. Seagraves, and M. L. Pinsky.
2018. Projecting shifts in thermal habitat for 686 species on the North American continental shelf. PLoS ONE 13(5):e0196127.

Ochoa-Zavala, M., P. Diaz-Jaimes, S. Ortega-García, and F. Galván-Magaña.
2022. Genetic divergence at species boundaries of the dolphinfish (*Coryphaena hippurus*) in the Tropical Eastern Pacific. PeerJ 10:e14389.

O'Leary, C. A., L. B. DeFilippo, J. T. Thorson, S. Kotwicki, G. R. Hoff, V. V. Kulik, J. N. Ianelli, and A. E. Punt.
2022. Understanding transboundary stocks' availability by combining multiple fisheries-independent surveys and oceanographic conditions in spatiotemporal models. ICES J. Mar. Sci. 79:1063–1074.

Ortega-Garcia, S., C. R. Perle, N. M. Whitney, R. Rodriguez-Sanchez, J. O'Sullivan, and S. S. Koch.
2022. Vertical distributions of dolphinfish (*Coryphaena hippurus*) in the Eastern Pacific Ocean suggest variability in potential associations with floating objects. PLoS ONE 17(11):e0276873.

Oxenford, H. A.
1999. Biology of the dolphinfish (*Coryphaena hippurus*) in the western central Atlantic: a review. Sci. Mar. 63:277–301.

Oxenford, H. A., and W. Hunte.
1986. A preliminary investigation of the stock structure of the dolphin, *Coryphaena hippurus*, in the western central Atlantic. Fish. Bull. 84:451–460.

Palko, B. J., G. L. Beardsley, and W. J. Richards.
1982. Synopsis of the biological data on dolphin-fishes, *Coryphaena hippurus* and *Coryphaena equiselis*. NOAA Tech. Rep. NMFS Circ. 443, 28 p.

Park, J. M., S.-H. Huh, H. C. Choi, and S. N. Kwak.
2017. Larval distribution of the common dolphinfish *Coryphaena hippurus* Linnaeus, 1758 (Coryphaenidae) in the East Sea/Sea of Japan. J. Appl. Ichthyol. 33:815–818.

Pennino, M. G., I. Paradinas, J. B. Illian, F. Muñoz, J. M. Bellido, A. López-Quílez, and D. Conesa.
2019. Accounting for preferential sampling in species distribution models. Ecol. Evol. 9:653–663.

Perrichon, P., J. D. Stieglitz, E. G. Xu, J. T. Magnuson, C. Pasparakis, E. M. Mager, Y. Wang, D. Schlenk, D. D. Benetti, Roberts, et al.
2019. Mahi-mahi (*Coryphaena hippurus*) life development: morphological, physiological, behavioral and molecular phenotypes. Dev. Dyn. 248:337–350.

Peterson, C. D., J. Gartland, and R. J. Latour.
2017. Novel use of hook timers to quantify changing catchability over soak time in longline surveys. Fish. Res. 194:99–111.

Pincay-Espinoza, J. E., and J. L. Varela.
2022. Spatial- and size-related shifts in feeding habits of the common dolphinfish (*Coryphaena hippurus*) in the Southeast Pacific Ocean. Environ. Biol. Fishes 105:313–326.

Poloczanska, E. S., C. J. Brown, W. J. Sydeman, W. Kiessling, D. S. Schoeman, P. J. Moore, K. Brander, J. F. Bruno, L. B. Buckley, M. T., Burrows, et al.
2013. Global imprint of climate change on marine life. Nat. Clim. Change Lond. 3:919–925.

R Core Team.
2021. R: a language and environment for statistical computing. R Foundation for Statistical Computing, Vienna, Austria. [Available from website, accessed February, 2021.]

Rose, C. D., and W. W. Hassler.
1968. Age and growth of the dolphin, *Coryphaena hippurus* (Linnaeus), in North Carolina waters. Trans. Am. Fish. Soc. 97:271–276.

Rudershausen, P. J., S. J. Poland, W. Merten, and J. A. Buckel.
2019. Estimating discard mortality for dolphinfish in a recreational hook-and-line fishery. North Am. J. Fish. Manage. 39:1143–1154.

Saba, V. S., S. M. Griffies, W. G. Anderson, M. Winton, M. A. Alexander, T. L. Delworth, J. A. Hare, M. J. Harrison, A. Rosati, G. A. Vecchi, et al.
2016. Enhanced warming of the Northwest Atlantic Ocean under climate change. J. Geophys. Res. Oceans 121:118–132.

South Atlantic Fishery Management Council (SAFMC).
2003. Fishery management plan for the dolphin and wahoo fishery of the Atlantic, including a final environmental impact statement, regulatory impact review, initial regulatory flexibility analysis, and social impact assessment/ fishery impact statement, 308 p. SAFMC, Charleston, SC. [Available from website.]

Sagarese, S. R., W. J. Harford, J. F. Walter, M. D. Bryan, J. J. Isely, M. W. Smith, D. R. Goethel, A. B. Rios, S. L. Cass-Calay, C. E. Porch, et al.
2019. Lessons learned from data-limited evaluations of data-rich reef fish species in the Gulf of Mexico: implications for providing fisheries management advice for data-poor stocks. Can. J. Fish. Aquat. Sci. 76:1624–1639.

Salvadeo, C., D. M. Auliz-Ortiz, D. Petatán-Ramírez, H. Reyes-Bonilla, A. Ivanova-Bonchera, and E. Juárez-León.
2020. Potential poleward distribution shift of dolphinfish (*Coryphaena hippurus*) along the southern California Current System. Environ. Biol. Fishes 103:973–984.

Sánchez-Maroño, S., A. Uriarte, L. Ibaibarriaga, and L. Citores.
2021. Adapting simple index-based catch rules for data-limited stocks to short-lived fish stocks' characteristics. Front. Mar. Sci. 8:662942.

Schlenker, L. S., R. Faillettaz, J. D. Stieglitz, C. H. Lam, R. H. Hoenig, G. K. Cox, R. M. Heuer, C. Pasparakis, D. D. Benetti, C. B. Paris, et al.
2021. Remote predictions of mahi-mahi (*Coryphaena hippurus*) spawning in the open ocean using summarized accelerometry data. Front. Mar. Sci. 8:626082.

Schwenke, K. L., and J. A. Buckel.
2008. Age, growth, and reproduction of dolphinfish (*Coryphaena hippurus*) caught off the coast of North Carolina. Fish. Bull. 106:82–92.

Thorson, J. T.
2019. Guidance for decisions using the Vector Autoregressive Spatio-Temporal (VAST) package in stock, ecosystem, habitat and climate assessments. Fish. Res. 210:143–161.

Thorson, J. T., and L. A. K Barnett.
2017). Comparing estimates of abundance trends and distribution shifts using single- and multispecies models of fishes and biogenic habitat. ICES J. Mar. Sci. 74:1311–1321.

Thorson, J. T., A. O. Shelton, E. J. Ward, and H. J. Skaug.
2015. Geostatistical delta-generalized linear mixed models improve precision for estimated abundance indices for West Coast groundfishes. ICES J. Mar. Sci. 72:1297–1310.

Thorson, J. T., M. N. Maunder, and A. E. Punt.
2020. The development of spatio-temporal models of fishery catch-per-unit-effort data to derive indices of relative abundance. Fish. Res. 230:105611.

Torrejón-Magallanes, J., D. Grados, and W. Lau-Medrano.
2019. Spatio-temporal distribution modeling of dolphinfish (*Coryphaena hippurus*) in the Pacific Ocean off Peru using artisanal longline fishery data. Deep Sea Res., II 169–170:104665.

Walter, J. F., III, C. D. Peterson, K. Marshall, J. J. Deroba, S. Gaichas, B. C. Williams, S. Stohs, D. Tommasi, and R. Ahrens.
2023). When to conduct, and when not to conduct, management strategy evaluations. ICES J. Mar. Sci. 80:719–727.

Wei, T., and V. Simko.
corrplot: visualization of correlation matrix. R package, vers. 0.92. [Available from website, accessed March 2021.]

Volkov, D. L., S.-K. Lee, R. Domingues, H. Zhang, and M. Goes.
2019. Interannual sea level variability along the southeastern seaboard of the United States in relation to the gyre-scale heat divergence in the North Atlantic. Geophys. Res. Lett. 46:7481–7490.

Xu, L., X. Chen, W. Guan, S. Tian, and Y. Chen.
2018. The impact of spatial autocorrelation on CPUE standardization between two different fisheries. J. Oceanol. Limnol. 36:973–980.

National Marine
Fisheries Service
NOAA

Fishery Bulletin
established in 1881

Spencer F. Baird
First U.S. Commissioner
of Fisheries and founder
of *Fishery Bulletin*

Chemical clocks: using otolith geochemistry to enhance estimation of age and growth of white hake (*Urophycis tenuis*)

Benjamin R. LaFreniere (contact author)[1,2]
Briony Donahue[2]
Jillian E. Price[3]
Alicia Cruz-Uribe[4]
Nate Miller[5]
Benjamin T. Manard[6]
Richard McBride[3]
John A. Mohan[1]

Email address for contact author: benjamin.r.lafreniere@maine.gov

[1] School of Marine and Environmental Programs
University of New England
11 Hills Beach Road
Biddeford, Maine 04005

[2] Maine Department of Marine Resources
P.O. Box 8
West Boothbay Harbor, Maine 04575-0008

[3] Population and Ecosystems Monitoring and Analysis Division
Northeast Fisheries Science Center
National Marine Fisheries Service, NOAA
166 Water Street
Woods Hole, Massachusetts 02543

[4] School of Earth and Climate Sciences
University of Maine
5790 Bryand Global Sciences Center
Orono, Maine 04469-5790

[5] Department of Earth and Planetary Sciences
Jackson School of Geosciences
University of Texas at Austin
2275 Speedway, Stop C9000
Austin, Texas 78712-1722

[6] Chemical Sciences Division
Oak Ridge National Laboratory
1 Bethel Valley Road
Oak Ridge, Tennessee 37830

Abstract—The white hake (*Urophycis tenuis*) is a groundfish distributed throughout the Gulf of Maine. Catch advice is based on stock assessments done with age-based population dynamics models; however, otolith aging is challenging because of unclear growth increments. To address this concern, we compared the consistency of aging with counts of visual annuli to that of aging with cycles of elemental concentrations measured by using laser ablation inductively coupled plasma mass spectrometry. We tested the hypothesis that oscillations in both environmental conditions and internal physiology through time influence uptake of elements during otolith mineralization. Concentrations of manganese, in comparison with those of the other investigated trace elements (magnesium, strontium, and barium), had the most promising correlation with visual growth increments (~100% age agreement, ±1 year), offering an additional tool to enhance increment identification. In our examination of 550 otoliths collected during 2007–2021, we found that white hake lived a maximum of 10.3 years and exhibited sexual dimorphism in maximum length and age. By using generated von Bertalanffy growth functions, $L(t)=110(1-e^{-0.113(t+0.45)})$ for males and $L(t)=140(1-e^{-0.113(t-0.30)})$ for females (where $L(t)$ is length at time t), size and age at maturity were calculated for males (37.4 cm in total length (TL), 3.3 years) and females (47.4 cm TL, 4.2 years). These results demonstrate that otolith geochemistry can be used to improve the accuracy and precision of the estimation of fish age and maturity, even for challenging species.

Manuscript submitted 5 September 2023.
Manuscript accepted 28 March 2024.
Fish. Bull. 122:44–57 (2024).
Online publication date: 2 May 2024.
doi: 10.7755/FB.122.1-2.4

The views and opinions expressed or implied in this article are those of the author (or authors) and do not necessarily reflect the position of the National Marine Fisheries Service, NOAA.

The use of biological hard structures, such as otoliths, is the most common method of aging bony fish (Pannella, 1971; Gauldie and Nelson, 1990; Stevenson and Campana, 1992), dating back to the late 18th century (Hederström, 1959; Jones, 1992). Otoliths are made of the biomineral calcium carbonate and form part of the mechanoreceptor system in bony fish (Campana, 1999). These biomineral structures are well established aging tools because they grow in proportion to the individual with continuous accretion (Pannella, 1971; Stevenson and Campana, 1992; Vigliola and Meekan, 2009).

Like the fish itself, the rate at which the otolith grows is not always constant, changing because of a range of internal (age, sex, metabolism, and reproductive status) and external (environmental conditions and prey availability) factors (Campana and Neilson, 1985; Neilson and Geen, 1985; Wright, 1991; Yamamoto et al., 1997; Wright et al., 2001; Hüssy, 2008). Such variability in growth rate by an individual is transcribed into otolith formation through physiological processes, linking otolith growth to time (Pannella, 1971). For species that inhabit temperate climates, seasonal oscillations in environmental conditions translate to variations in growth, which are observed as distinct translucent (winter) and opaque (summer) growth increments (visible under reflected light) that, as a pair, represent a single year of growth (Victor and Brothers, 1982; Campana, 1999; Wright et al., 2002a). Although well studied, the drivers of seasonal growth increments are still debated and have been shown to be highly species specific (Ding et al., 2020). Species-specific studies that validate that one annulus spans one year of growth are required for accurate age estimation through otolith annuli counting.

Although this process of counting growth increments in otoliths is well established, it remains challenging in application for certain species like the white hake (*Urophycis tenuis*), whose age has been validated in waters of Canada (Hunt, 1982) but not in the Gulf of Maine (GOM). In past research, white hake were observed to have a combination of false and weak growth increments consistent among sexes, sizes, and populations (Clay and Clay, 1991). Unlike true growth increments, false growth increments do not form a full ring around the otolith core (Katayama, 2018). The biological mechanism for false growth increment deposition is still debated, with research results indicating that a combination of physiological (feeding and lifestyle transitions) or environmental (temperature, salinity, and oxygen) conditions are typically responsible (Watson, 1967; Berghahn, 2000; (Cappo et al., 2000; Wright et al., 2002b; Katayama and Isshiki, 2007; Katayama, 2018). Weak growth increments are true growth increments that are indistinct between the opaque and translucent zones, likely because of decreased metabolism between seasons with age, and are ultimately difficult to identify. The occurrence of either false or weak growth increments raises the potential for both overestimating and underestimating ages, resulting in bias in growth models.

For white hake, the appearance of the first annulus has been characterized in detail by Lang et al. (1996), and identification of the first several annuli has been corroborated by the modes in length–frequency plots (Hunt, 1982). Although these 2 studies serve as a foundation for the validation of the frequency of annulus formation in white hake, continued research efforts are needed to provide evidence that assigned ages can be validated through aging with the entire otolith section.

The white hake is an ecologically and economically important groundfish species found within the GOM (Ames, 2012; Ames and Lichter, 2013) and is managed by the New England Fishery Management Council. With a full range from Florida to Iceland, this species has been found along the eastern coast of North America and primarily inhabits muddy substrates along the continental shelf and slope (Musick, 1974; Ames, 2012). Limited age and growth research has been conducted for the neighboring northern stock of white hake in the Gulf of St. Lawrence (Clay and Clay, 1991), but the GOM stock has not been fully explored because of the difficulty in aging this species (Penttila, and Dery, 1988), limiting age-based fishery management efforts. For a comparable species for which ages have been difficult to assign, the Atlantic cod (*Gadus morhua*), analysis of otolith geochemistry has been applied recently as a new tool (Heimbrand et al., 2020; Hüssy et al., 2021).

Otolith core-to-edge geochemistry has been used to determine life history information for a range of species. Otoliths are metabolically inert; therefore, incorporated trace elements are retained permanently during growth throughout the life of a fish (Campana and Neilson, 1985). Such chemical histories have been shown to correspond to both environmental and physiological conditions experienced by individuals during life (Campana, 1999). Heimbrand et al. (2020) demonstrated that the uptake of certain trace elements, magnesium (Mg) and phosphorus (P), in otoliths of Atlantic cod had seasonal oscillations, resulting in distinct elemental peaks that were correlated with age. Hüssy et al. (2021) found similar results for the uptake of Mg, P, and manganese (Mn) and proposed counting of enrichment peaks for select elements as a means of age determination. Also, age estimates from the use of 2-dimensional (2D) geochemical maps of the entire surface of otoliths have been shown to correlate with those from the use of visual annuli (Ulrich et al., 2009), providing confidence in the use of elemental peak counting techniques for age determination (Heimbrand et al., 2020). Methods for counting peaks in uptake of trace elements in otoliths show promise as alternative aging techniques for species for which the traditional method of counting growth increments is prone to error because of false or weak annuli, as has been the case for the white hake.

The purpose of this study was to develop models for estimation of age and growth of male and female white hake by using traditional growth increment counting informed by core-to-edge geochemistry and by using 2D geochemical mapping. We hypothesized that growth trends for white hake would be sex specific, with females growing larger than males as a reproductive benefit, on the basis of the results of previous studies in waters of Canada (Hunt, 1982; Markle et al., 1982). From the use of our generated growth models, we also report estimates for both length and age at maturity for both sexes. Overall, our results can be used to inform decisions concerning techniques for aging white hake in the future, with regard to factors including time, operation scale, and the costs associated with laser ablation inductively coupled plasma mass spectrometry (LA-ICP-MS).

Materials and methods

Sample collection

White hake are sampled by the Maine Department of Marine Resources (DMR) during the biannual Maine–New Hampshire Inshore Trawl Survey. Conducted since the spring of 2000, this fishery-independent, multispecies trawl survey involves sampling inshore waters out 12 nautical miles from the coast from Seabrook, New Hampshire, to the Canada–United States border. Data from the surveys in inshore waters of New Hampshire and Maine are used to generate species abundance indices and enhance management practices across fisheries, and specimens caught during the surveys are used in biological studies. Survey gear consists of a modified shrimp net, selected to minimize habitat disruption and sample multiple species of varying sizes. Fishermen in this region collaborated with the DMR on the trawl survey design and selection of gear type. The aim for tows of the trawl net is a period of 20 min (mean: 18.8 min [standard deviation (SD) 2.2]), with distances of tows ranging from 0.29 to 1.51 nautical miles. Although the survey is conducted biannually, sagittal otoliths are collected from sampled white hake only during the fall, when white hake are primarily (~87%) caught. The sampled white hake are measured for total length (TL) to the nearest 1 cm and for weight to the nearest whole gram, their sex is determined, and their maturity status is assessed (see the "Maturity" section) prior to extraction of otoliths.

Otolith preparation

Otoliths were mounted in Buehler EpoThin 2[1] epoxy resin (Buehler Ltd., Lake Bluff, IL), then transversely cut, with a target thickness of 0.5–0.75 mm, by using an IsoMet Low Speed Saw (Buehler Ltd.) with a diamond blade. After cross-sectioning, otolith samples were polished with a range of low-grit sandpaper (300–60,000 grit), to smooth the surface and increase optical clarity for counting of growth increments and to prepare otoliths for trace elemental analysis.

All otoliths were assigned an age by the primary reader (see the "Aging" section) prior to elemental analysis. Otolith samples were mounted to glass petrographic slides with Crystalbond thermoplastic cement (Aremco Products Inc., Valley Cottage, NY), then sent off for trace elemental analysis. In this study, we used 3 different approaches for trace elemental analysis: line transects (number of otolith samples [n]=43), partial 2D maps (n=30), and complete 2D maps (n=7). This analysis was conducted at 3 separate geochemistry facilities: University of Texas at Austin, University of Maine, and Oak Ridge National Laboratory. Line transects consisted of a single line scan run from the otolith core to the edge, along the primary aging axis. Partial 2D maps delineated a region consisting of the otolith's core and dorsal surface, and complete 2D maps delineated the entire otolith's surface. The high-resolution 2D elemental maps provide spatial detail to better understand the regional compositional context of the elemental time series obtained with the single core-to-edge line scans. These 3 approaches for trace elemental analysis varied in effort (time) and were selected as a means to accurately identify chemical increments. We chose multiple geochemistry facilities because of logistical concerns about funding and equipment availability.

Aging

The primary reader for this study (senior author) assigned ages for all otoliths (n=550). Samples were selected across a range of years, from 2007 to 2021 (Suppl. Table 1) (online only), in which the DMR fall inshore trawl survey was conducted, with the assumption that variation in growth patterns between years sampled was negligible. Aging of white hake was conducted by using a Leica S9 D microscope and LAS X imaging software (Leica Microsystems, Wetzlar, Germany), following techniques outlined by Hunt (1982). Samples were submerged, with the sulcus groove facing down and the dorsal side to the right (Fig. 1), in a small, blacked-out, water-filled petri dish that sat on the microscope stage during the aging process. Otoliths were illuminated by using reflected light, then imaged with a gray scale to increase growth increment contrast. Additional band-clarifying methods, such as baking, burning, and staining, have not been proven to enhance contrast between growth increments (Hunt, 1982) and were not used in this study.

The most consistent counts of growth increments were done along the primary aging axis, which starts at the otolith core and runs along the dorsal axis (Fig. 1) (Clay and Clay, 1991). Attempts to assign ages by counting in other core-to-edge directions, such as the secondary aging axis that runs parallel to the sulcus groove (Fig. 1), were necessary when poor growth incrementing on the dorsal plane occurred. Following previous research on white hake (Beacham and Nepszy, 1980; Hunt, 1982; Clay and Clay, 1991) and other groundfish species (Gauldie and Nelson, 1990); Stevenson and Campana, 1992; Ferri, 2023), we assumed that a pair of translucent and opaque growth increments represents 1 year of growth.

The secondary reader (J. Price) assigned ages for a random subset (n=130) of otoliths. The precision of agreements between reader-assigned ages were evaluated with 2 indices, percent agreement and Chang's coefficient of variation (CV) (Chang, 1982), and bias of disagreements was evaluated with 3 tests of symmetry, Evans and Hoenig's (1998), Bowker's (1948), and McNemar's (1947) tests, following the recommendations of McBride (2015). Comparisons between ages assigned by the primary reader and ages estimated by analyzing otolith geochemistry (see the "Elemental data analysis" section) used the same 2 precision indices and 3 bias tests. All such analyses and data plotting were done by using the FSA package (vers. 0.9.1; Ogle et al., 2021) in RStudio (vers. 2022.07.2; RStudio Team, 2022) (Ogle, 2016).

The final age assignments, which involved adjustments for age differences between sampling months, were determined after accounting for between-reader discrepancies. Although spawning seasonality of white hake in the GOM has not been observed, juveniles of this species are thought to hatch in the late spring or early summer months in the GOM (Ames, 2012); therefore, birthdates were assigned as 1 June and their date of capture was factored into the age estimate by using the following equation:

$$\begin{aligned} Age &= Age\ assignment \\ &\quad + ((Month\ of\ capture - 6)/12). \end{aligned} \tag{1}$$

By using these final age estimates, von Bertalanffy growth curves for male and female white hake were fit.

---

[1] Mention of trade names or commercial companies is for identification purposes only and does not imply endorsement by the National Marine Fisheries Service, NOAA.

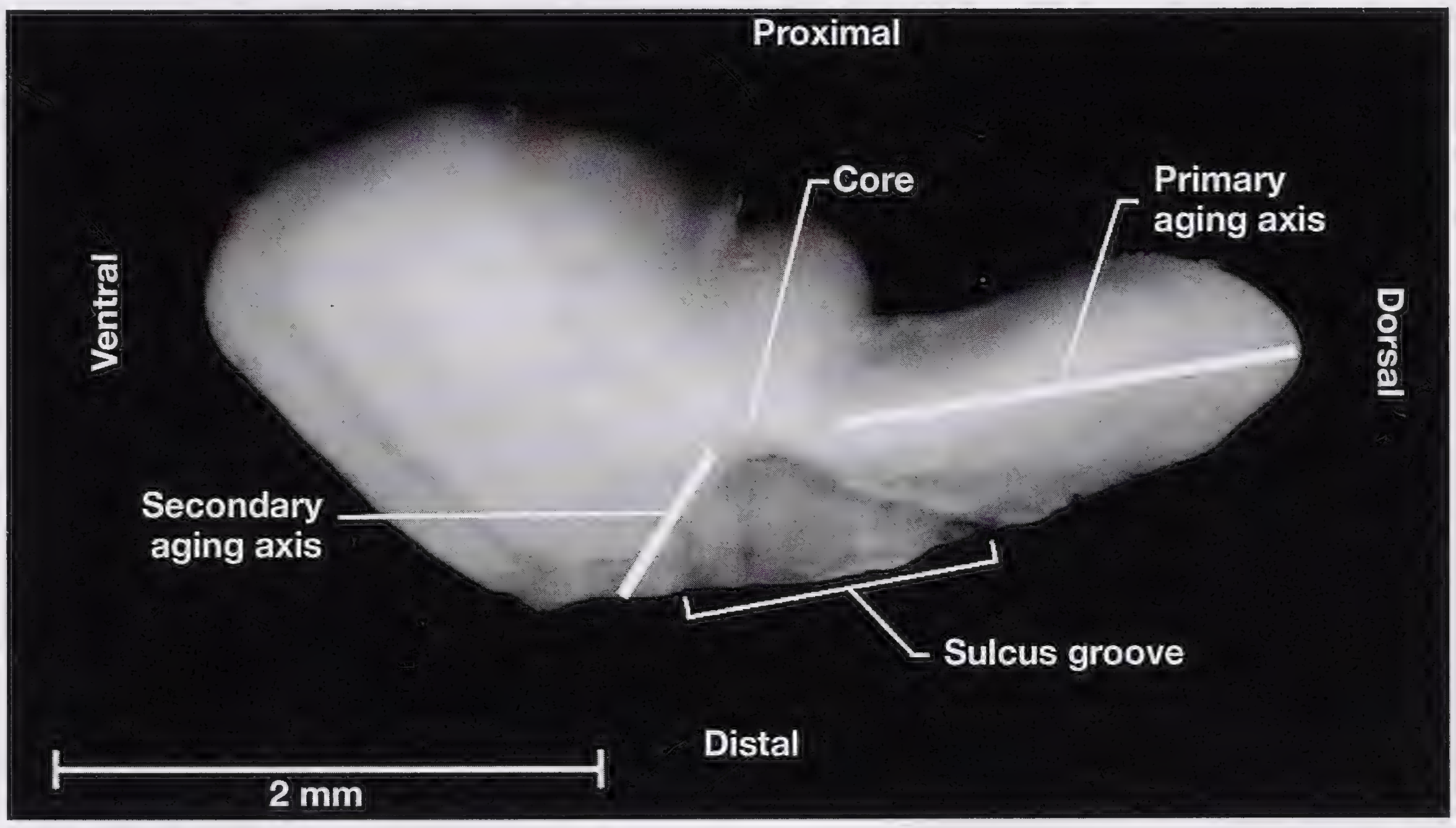

Figure 1

Image of a transversely sectioned sagittal otolith from a female white hake (*Urophycis tenuis*) sampled on 26 September 2012 in inshore waters of southern Maine, with proper orientation for aging. This fish had a total length of 42 cm, a weight of 0.5 kg, and an estimated age of 3.3 years. The primary aging axis is the axis where growth increments were primarily sampled, and the secondary aging axis is the axis where growth increments were sampled if the primary axis was difficult to interpret or to check the count of increments on the primary axis.

These growth equations were modeled using the following formula (von Bertalanffy, 1934):

$$L(t) = L_\infty\left(1 - e^{-k(t-t_0)}\right), \qquad (2)$$

where $L(t)$ = the length (in centimeters) of an individual at a certain time t (in years);
L_∞ = the hypothetical average maximum length;
k = the rate of growth to L_∞; and
t_0 = the age at which length is zero.

The Gompertz growth curve was also explored for these age estimates but produced a weaker model fit (AIC: 1460 for males and 1726 for females) compared with that of the von Bertalanffy growth curve (AIC: 1457 for males and 1579 for females), and it was not investigated further. A full combination of fixed variables from growth equations for both males and females was explored with the von Bertalanffy growth function, as well (Table 1).

Table 1

Comparison of the various configurations of the von Bertalanffy growth function used in this study. Models differed in which, if any, parameters were fixed. The parameters include the hypothetical average maximum length (L_∞), the rate of growth (k), and the age at which length is zero (t_0). The asterisk (*) indicates the model with the lowest Akaike information criterion (AIC) and, therefore, the selected model. Models were fit to data from analysis of otoliths from white hake (*Urophycis tenuis*) captured in New Hampshire and Maine during fall from 2007 through 2021.

Fixed parameters	df	AIC
None	7	176
L_∞	6	300
k*	6	164
t_0	6	256
L_∞, t_0	5	431
k, t_0	5	199
L_∞, k	5	187
All	4	267

Trace element analysis

For trace elemental analysis, a random subset of 73 otolith samples was chosen from the 550 samples for which traditional aging was done in this study. This subset was from fish that ranged in sex (40 females and 33 males), maturity stage, age, sampling year, and age readability of their otoliths. Across laboratories, analytes included isotopes of Mg, calcium (Ca), Mn, strontium (Sr), and barium (Ba): ^{24}Mg, ^{43}Ca, ^{55}Mn, ^{88}Sr, and ^{138}Ba. Our analyses entailed otolith core-to-edge line scans along the primary aging axis (Fig. 1), as well as partial (from the core to the dorsal surface only) and complete 2D maps. For complete 2D mapping, contiguous parallel line scans were run over the entire sample surface, allowing for observation of elemental patterns, such as oscillations in concentrations of elements consistent with growth increments (Heimbrand et al., 2020). The 2D maps clearly show high enrichment at the otolith core across elements (Fig. 2); therefore, line scans were trimmed from the first growth increment to the edge, in an effort to reduce the potential for misreading the highly enriched core as a growth increment.

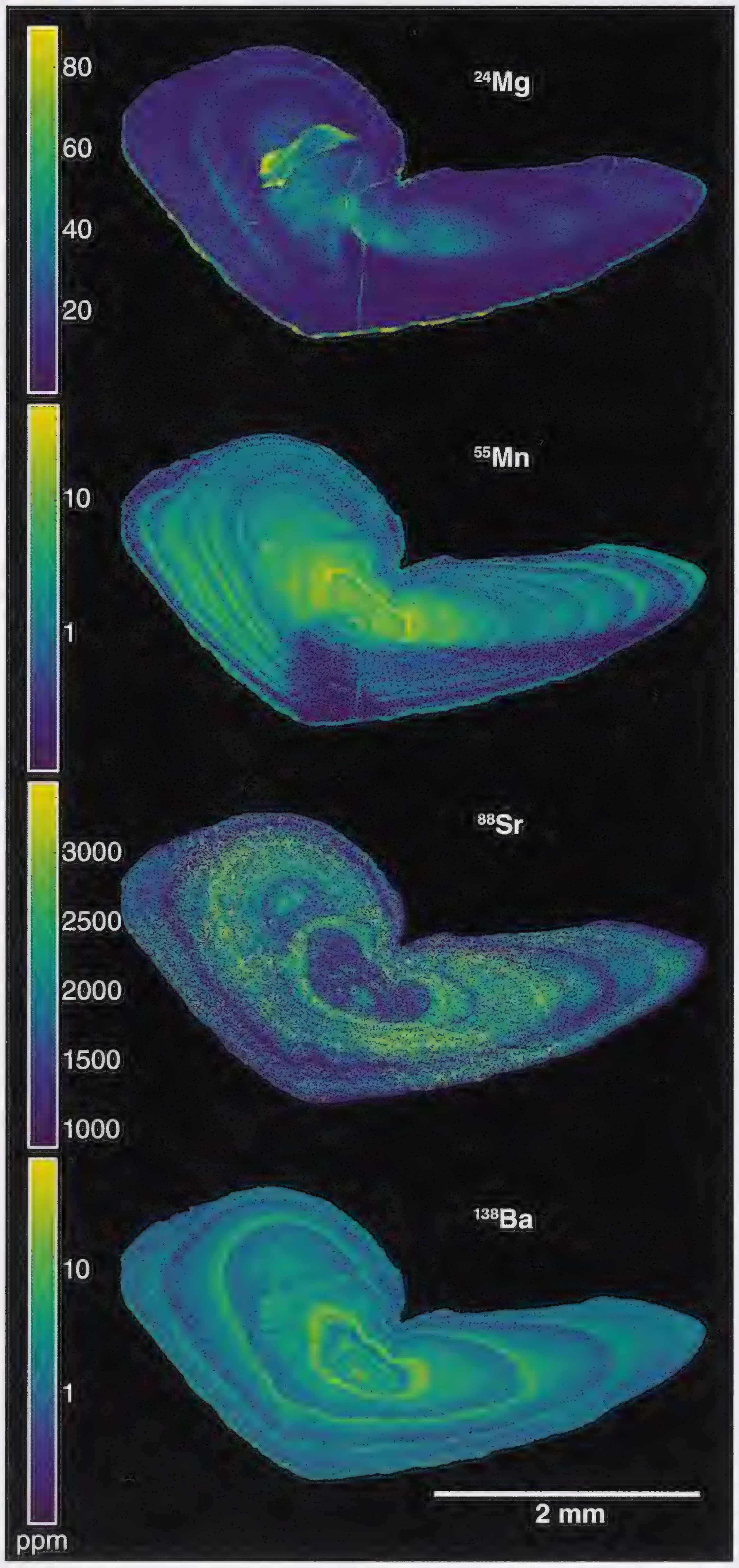

Figure 2

2D maps of the geochemistry of the otolith of a female white hake (*Urophycis tenuis*) sampled on 24 October 2012 in inshore waters of northern Maine. Peaks in concentrations of isotopes of magnesium (Mg), calcium (Ca), manganese (Mn), strontium (Sr), and barium (Ba)—^{24}Mg, ^{55}Mn, ^{88}Sr, and ^{138}Ba—in parts per million (ppm) were analyzed. This fish had a total length of 85 cm, a weight of 5.1 kg, and an estimated age of 7.3 years.

University of Texas at Austin Elemental variations along a line transect on each otolith (n=43) of white hake were measured through LA-ICP-MS, by using an ESI NWR193 excimer LA system (193-nm wavelength and 4-ns pulse width; Elemental Scientific Inc., Omaha, NE) coupled with an Agilent 7500ce ICP-MS (Agilent Technologies, Santa Clara, CA). The LA-ICP-MS system is equipped with a large format, 2-volume sample cell with fast washout (<1 s) that accommodated all samples and standards (ECRM-752-NP, USGS MACS-3, and NIST 612) in a single cell loading. The system was optimized daily for sensitivity across the atomic mass unit range and for low oxide production (mean ratio of thorium oxide to thorium [ThO/Th]: 0.40 [SD 0.01]) by tuning on a reference material (NIST 612), and these parameters were checked with trial transects on representative samples.

Following pre-ablation (75-µm spot, 50-µm/s scan rate, 2-J/cm energy density [fluence]) to remove shallow surface contaminants, scans along transect lines on sectioned otoliths were run from the core to the marginal edge, by using a 25-by-50-µm rectangular aperture, with a long axis perpendicular to the radial growth axis, a 5-µm/s scan rate, a fluence of 2.73 J/cm (SD 0.05), a 20-Hz repetition rate, and a carrier gas flow of 0.80 L/min for both argon and helium. The quadrupole duty cycle of 0.4152 s corresponded to 94% of measurement time, with a corresponding linear sampling rate of 2.08 µm/s, equivalent to 12 measurements within the 25-µm-high aperture footprint.

Measured intensities were converted to elemental concentrations (in parts per million) by using iolite 4 software (Paton et al., 2011); ^{43}Ca was used as the internal standard element with the assumption of a Ca index weight percentage of 38.3% (Serre et al., 2018; Hüssy et al., 2021). Carbonate pressed pellet USGS MACS-3 was used as the primary calibration material, and NIST 612 and ECRM-752-NP were measured as external reference materials. Analyte recoveries were typically within 7% and 9% of the reference values for NIST 612 (n=33) and ECRM-752-NP (n=32), respectively. The grand average of secondary standard (n=27) recovery fractions for all elements was typically within 7% of preferred values in the GeoReM database (Jochum et al., 2005) for NIST 612 and within 14% of values for USGS MACS-3. Typical (mean) analyte concentrations over otolith transects were tens to hundreds of times higher than the limits of detection for all elements.

University of Maine Elemental variations along multiple line transects covering the core and dorsal surface of otoliths of white hake for partial 2D maps (n=27) and covering the entire surface of otoliths for complete 2D maps (n=4) were measured through LA-ICP-MS at the Micro-Analytical Geochemistry and Isotope Characterization Laboratory, by using an ESI NWR193UC excimer LA system (Elemental Scientific Inc.) coupled to an Agilent 8900 triple quadrupole ICP-MS (Agilent Technologies) and following the methods described in Cruz-Uribe et al. (2021) and Walters et al. (2022). The fast washout mapping setup in the MicroAnalytical Geochemistry and Isotope Characterization Laboratory consisted of 1-mm ID tubing connected directly from the analytical cup of a TwoVol3 LA chamber to a dual concentric injector ICP-MS torch (DCI1) from Elemental Scientific Inc.. A 10-by-10-µm square spot was rastered in parallel lines across the sample surface at a repetition rate of 200 Hz and a scan speed of 500 µm/s with a fluence of 2 J/cm.

Two lines of NIST SRM 610 glass were ablated at the beginning and end of map acquisition. The USGS GSD-1G basalt glass and a speleothem nano-powder pressed pellet (KCSp-1NP) from the International Association of Geoanalysts (IAG) were used as quality control materials. Element recoveries were within 10% of preferred values for GSD-1G in the GeoReM database. Measured trace element values for KCSp-1NP were within the uncertainty (SD of 2 on replicate analyses) of the preferred values in the IAG report for this material. Time-resolved signals were processed by using the Trace Elements data reduction scheme in iolite 4, and trace element maps were produced by using the CellSpace module in iolite 4 (Woodhead et al., 2007; Paton et al., 2011; Paul et al., 2012; Petrus et al., 2017). Trace element mass fractions were determined relative to the NIST SRM 610 reference glass with the assumption of an internal standard of a mass fraction of Ca of 40.04%.

Oak Ridge National Laboratory Elemental variations on the entire surface of otoliths of white hake for complete 2D maps (*n*=3) were measured through LA-ICP-MS, by using an ESI imageGEO193 laser (Elemental Scientific Inc.) equipped with a TV3 ablation cell coupled to a Thermo Scientific iCAP TQ ICP-MS (Thermo Fisher Scientific, Waltham, MA). A 10-by-10-µm square spot was rastered in parallel lines across the sample surface at a repetition rate of 200 Hz and a scan speed of 125 µm/s with a fluence of 5 J/cm. The USGS GSD-2G basalt glass and a speleothem nano-powder pressed pellet (KCSp-1NP) from the IAG were used as quality control materials. Measured trace element values for GSD-2G and KCSp-1NP were within the uncertainty (SD of 2 on replicate analyses) of the preferred values in the IAG reports for these materials.

Elemental data analysis

Generated 2D maps (partial and complete) were analyzed by using iolite 4 to investigate spatial variations in elemental concentrations. In these 2D maps, only Mn had patterns of growth incrementing across individuals (Fig. 3); therefore, only Mn was investigated in the line scan analysis.

Line scan elemental data were analyzed by using the ggplot2 package (vers. 3.3.6; Wickham, 2016) in RStudio. All derived elemental time series were smoothed by consecutive moving median and average filters with a 25-point boxcar width (equivalent to a distance of 175 µm), resulting in smooth, locally weighted signals free from high-frequency outliers. Signals were converted to distances (in micrometers) from the core on the basis of the scan rate and duty cycle. Concentrations of Mn were normalized across individuals, to apply the same parameters for counting peaks in elemental concentrations across individuals. Peaks in concentrations of elements were counted by using the stat_peak and stat_valley functions in RStudio, with a peak width (span) of 101, peak height (threshold) of 0.15, valley span of 151, and valley threshold of 0.80 (see the R script in Supplementary Material [online only]), as has been done similarly in previous research (Hüssy et al., 2021). Peaks in concentrations of elements between 2 valleys were counted as 1 growth increment, with multiple peaks between 2 valleys considered a single growth increment (Fig. 3). As was done previously for agreements in age assignments between the primary and secondary readers, tests of both precision and symmetry were conducted between age estimates based on assignments of the primary reader and counts of peaks in Mn concentrations, generating an age bias plot for both males and females. The methods used were the same as those used in the previous precision and symmetry analysis.

Maturity

Classification of the maturity of white hake followed the protocol of Burnett et al. (1989), with a final designation of either immature or mature male or female. The maturity of a few fish (*n*=4) could not be classified. The maturity for the remaining aged white hake (*n*=546) was analyzed. The median length (L_{50}) and age (A_{50}) at maturity were estimated by fitting binomial logistic models to sex-specific data with the sizeMAT package (vers. 1.1.2; Torrejon-Magallanes, 2020) in RStudio, and 95% confidence intervals were estimated by using bootstrapping (Torrejon-Magallanes, 2020). Sexual dimorphism, which had not been reported for this species in the GOM prior to our study, was investigated for both the *y*-intercept and slope by using a chi-square distribution summarized in an analysis of variance table.

Results

From 2007 through 2021, 550 of the white hake caught during the fall as part of the Maine–New Hampshire Inshore Trawl Survey were sampled for this study (Suppl. Fig. 1) (online only). Sampled white hake ranged in age between 0.3 and 10.3 years for females (*n*=291) and between 0.3 and 9.3 years for males (*n*=259) (Suppl. Table 2) (online only). The average female in this study was 41.6 cm TL, 0.9 kg, and 3.5 years old, and males were on average 32.3 cm TL, 0.4 kg, and 2.7 years old. The primary and secondary readers did not discern growth variation among years sampled, lending confidence to our initial assumption that growth variation between year classes is negligible.

The precision of paired age comparisons between age readers is acceptable but indicates the difficulty of aging

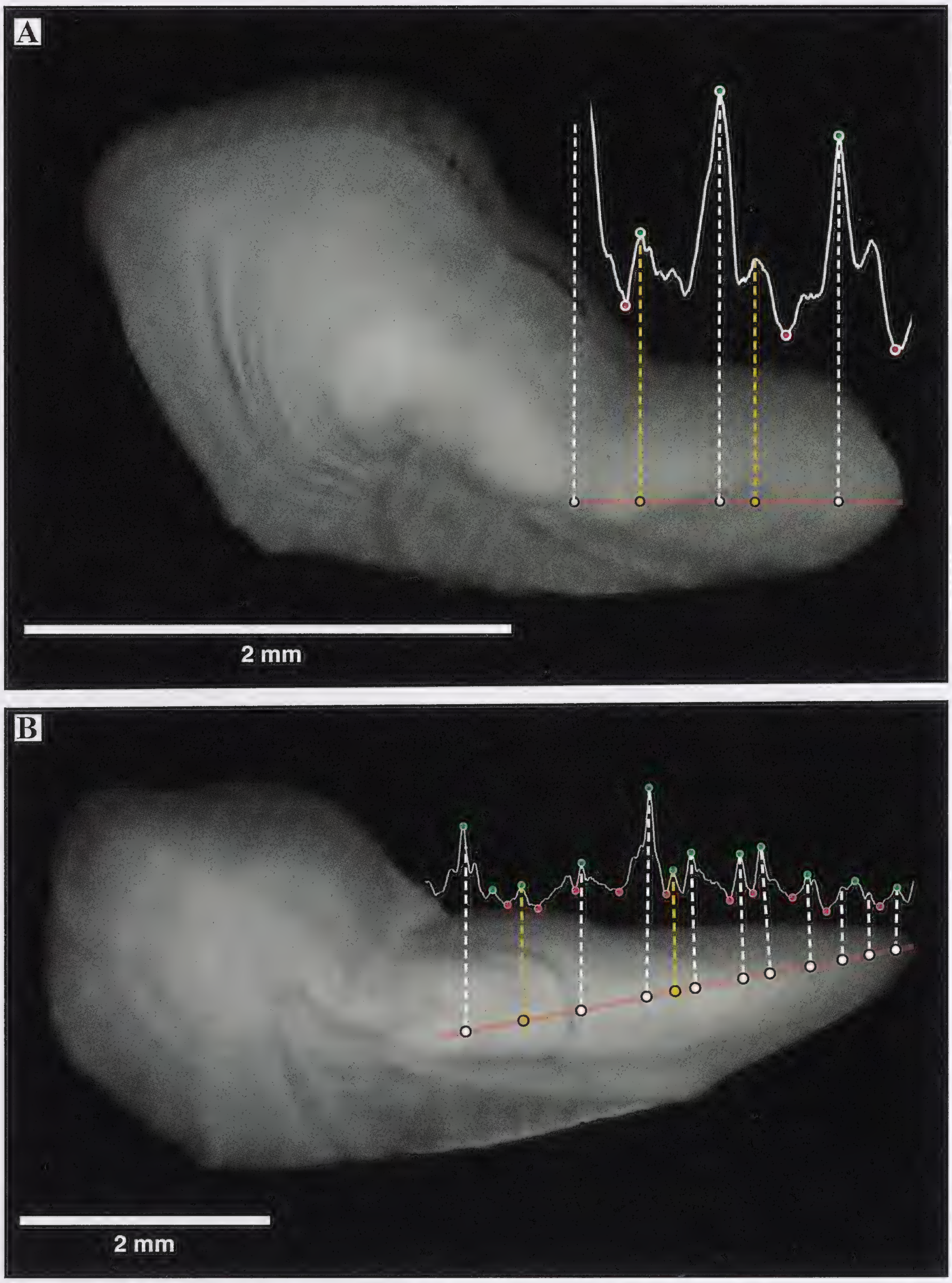

Figure 3

Normalized concentrations of the manganese isotope ^{55}Mn in the otoliths of (**A**) a male and (**B**) a female white hake (*Urophycis tenuis*) sampled on 4 October 2021 and 28 September 2012, respectively, in inshore waters of northern Maine. Concentrations are based on data from laser ablation line scans. Green (peaks) and red (valleys) dots are annotated on the transect of the line scan. The red line on the otolith identifies the line scan path, and the white and yellow dots are counted winter and false winter growth increments identified by the primary reader. The male had a total length of 33 cm, a weight of 0.3 kg, and an estimated age of 3.3 years, and the female had a total length of 102 cm, a weight of 9.3 kg, and an estimated age of 10.3 years.

both sexes of white hake (e.g., Chang's CVs between 5 and 10) (Table 2). Statistically significant bias was evident between ages assigned by readers (e.g., $P<0.01$ from Evans and Hoenig's test of symmetry), but the average differences by age class were small and without trend (Fig. 4, A and B).

Of all trace elements for which concentrations were quantified, only Mn had concentration patterns that corresponded to presumed summer and winter growth incrementing (Figs. 2 and 3). The precision of paired age comparisons between counts of peaks in concentrations of Mn and counts of growth increments by the primary

Table 2

Results from evaluation of precision and symmetry of age estimates for white hake (*Urophycis tenuis*) captured in inshore waters of New Hampshire and Maine from 2007 through 2021 in the fall. Age assignments made by the primary reader of growth increments on otoliths were compared either to age assignments made by the secondary reader (Secondary) or to age estimates based on peaks in concentrations of manganese in otoliths (Mn peaks). Precision was examined with 2 indices: percent agreement (PA), which is reported for both the exact year of the estimate and ±1 year of the estimate, and Chang's coefficient of variation (CV). Three symmetry tests were used. *n*=number of otoliths.

Sex	Method	*n*	PA (%)	PA (%) (±1 year)	CV	Symmetry test	*P*
Male	Secondary	69	71.01	98.55	9.38	McNemar's	<0.01
						Evans and Hoenig's	<0.01
						Bowker's	0.18
	Mn peaks	33	66.67	100.00	9.25	McNemar's	0.13
						Evans and Hoenig's	0.13
						Bowker's	0.14
Female	Secondary	61	72.13	100.00	5.79	McNemar's	<0.01
						Evans and Hoenig's	<0.01
						Bowker's	0.01
	Mn peaks	40	62.50	97.50	9.98	McNemar's	0.80
						Evans and Hoenig's	0.61
						Bowker's	0.07

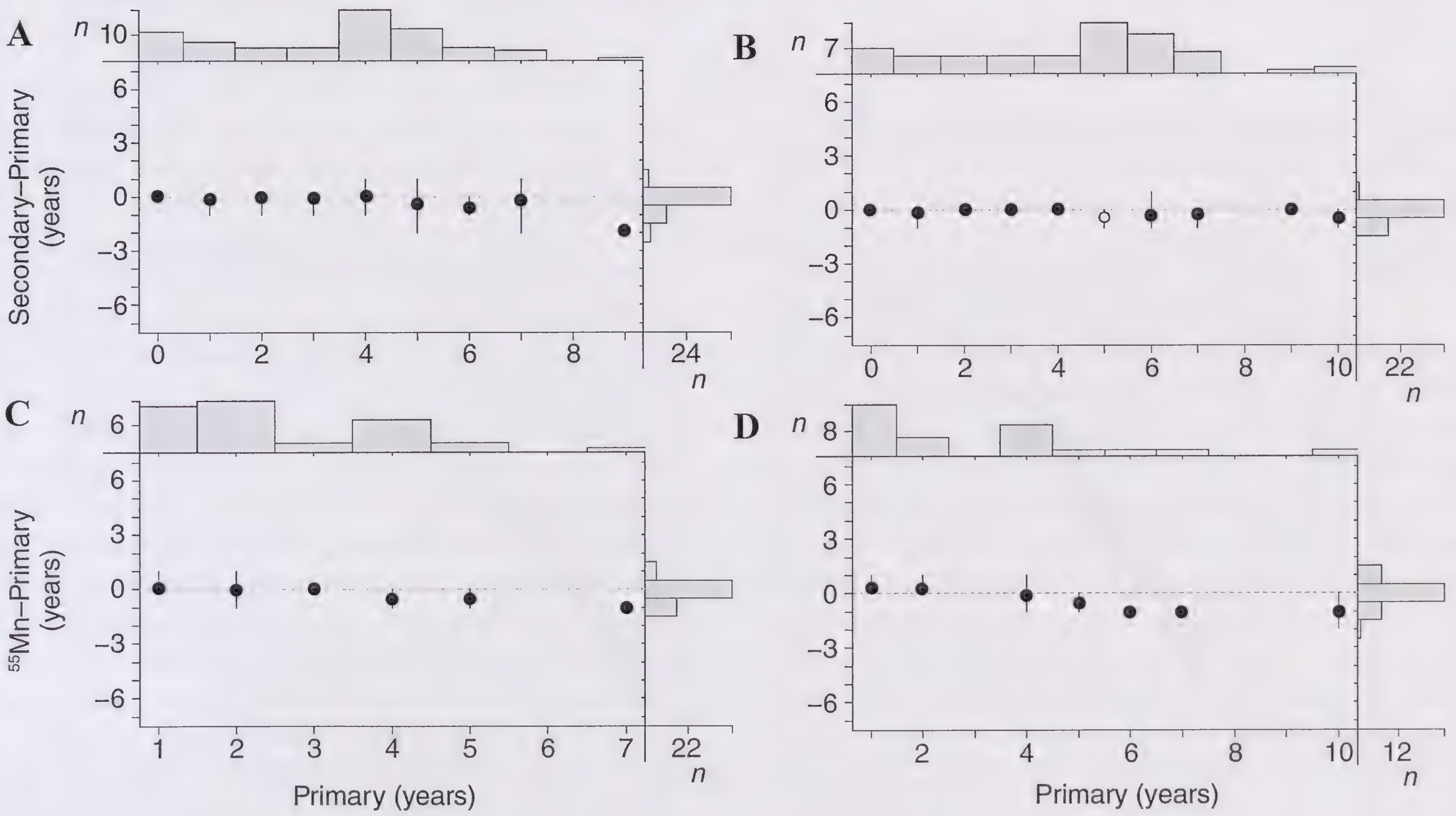

Figure 4

Age bias plots of the differences in ages between assignments by the primary and secondary readers of otoliths from (**A**) male (number of otoliths [*n*]=69) and (**B**) female (*n*=61) white hake (*Urophycis tenuis*) and between assignments by the primary reader and estimates based on counts of peaks in the concentration of the manganese istotope ^{55}Mn for otoliths of (**C**) male (*n*=33) and (**D**) female (*n*=40) white hake. Fish were captured in inshore waters of New Hampshire and Maine from 2007 through 2021 in the fall.

reader is acceptable but also indicates the difficulty of aging both sexes of white hake (e.g., Chang's CVs between 9 and 10) (Table 2). No statistically significant bias is evident (e.g., $P>0.05$ from Evans and Hoenig's test of symmetry), with minor disagreement in age assignments across lengths for both sexes (Fig. 4, C and D).

The estimated growth curves differed by sex. The growth curve was $L(t)=110(1-e^{-0.113(t+0.45)})$ for males and $L(t)=140(1-e^{-0.113(t-0.30)})$ for females. The von Bertalanffy growth function is best described with a fixed value for k (0.113), a smaller t_0 value for males (−0.45 year [SD 0.16]) than for females (0.30 year [SD 0.13]), and a larger L_∞ value for females (140 cm TL [SD 29.0]) than for males (110 cm TL [SD 19.0]) (Table 1, Fig. 5).

Median length and age at maturity also differed by sex. Female L_{50} was 10 cm longer than male L_{50} (47.4 cm TL [SD 2.3] versus 37.4 cm TL [SD 2.4]). Female A_{50} was 0.9 year older than male A_{50} (4.2 years [SD 0.2] versus 3.3 years [SD 0.3]) (Fig. 6). Model slopes were not significantly different between sexes ($P>0.05$), although y-intercepts were ($P<0.01$).

Discussion

This study is the first to demonstrate that sex-specific growth models are most suitable for white hake in U.S. waters of the GOM and the first to formally test the hypothesis of sexually dimorphic growth with an AIC approach. In previous work in the Gulf of St. Lawrence, Hunt (1982) found that females attained a larger size at age than males, with estimates for the parameter L_∞ very similar to estimates from our study (Suppl. Table 2) (online only).

The variation in L_∞ between females (140 cm TL) and males (110 cm TL) aligns with previous reports of the lifespan of females exceeding 20 years and that of males never exceeding 8 years (Burnett et al., 1984; Langton et al., 1994). Although in our study females reached a maximum age of only 10.3 years and maximum sizes of only 102 cm TL and 9.3 kg, larger and older individuals in the population likely exist. The age of a male white hake sampled in our study exceeds the previous maximum age observed for this species (8 years) (Burnett et al., 1984; Langton et al., 1994), with an estimate of 9.3 years and measured sizes of 85 cm TL and 5.0 kg. This individual was ~2 years older and 17 cm TL longer than the next largest male in our study, indicating that this specimen was anomalous in the inshore environment. The DMR, as part of the inshore trawl survey, does not sample beyond 12 nautical miles from shore, into areas possibly inhabited by white hake that are larger and older than those found in shallow waters (Chang et al., 1999; Ames, 2012). Overall, our results support the notion of sexually dimorphic growth that has been previously suggested for this species (Burnett et al., 1984; Langton et al., 1994; Haedrich, 2003) but not previously modeled for the GOM (Suppl. Table 2) (online only).

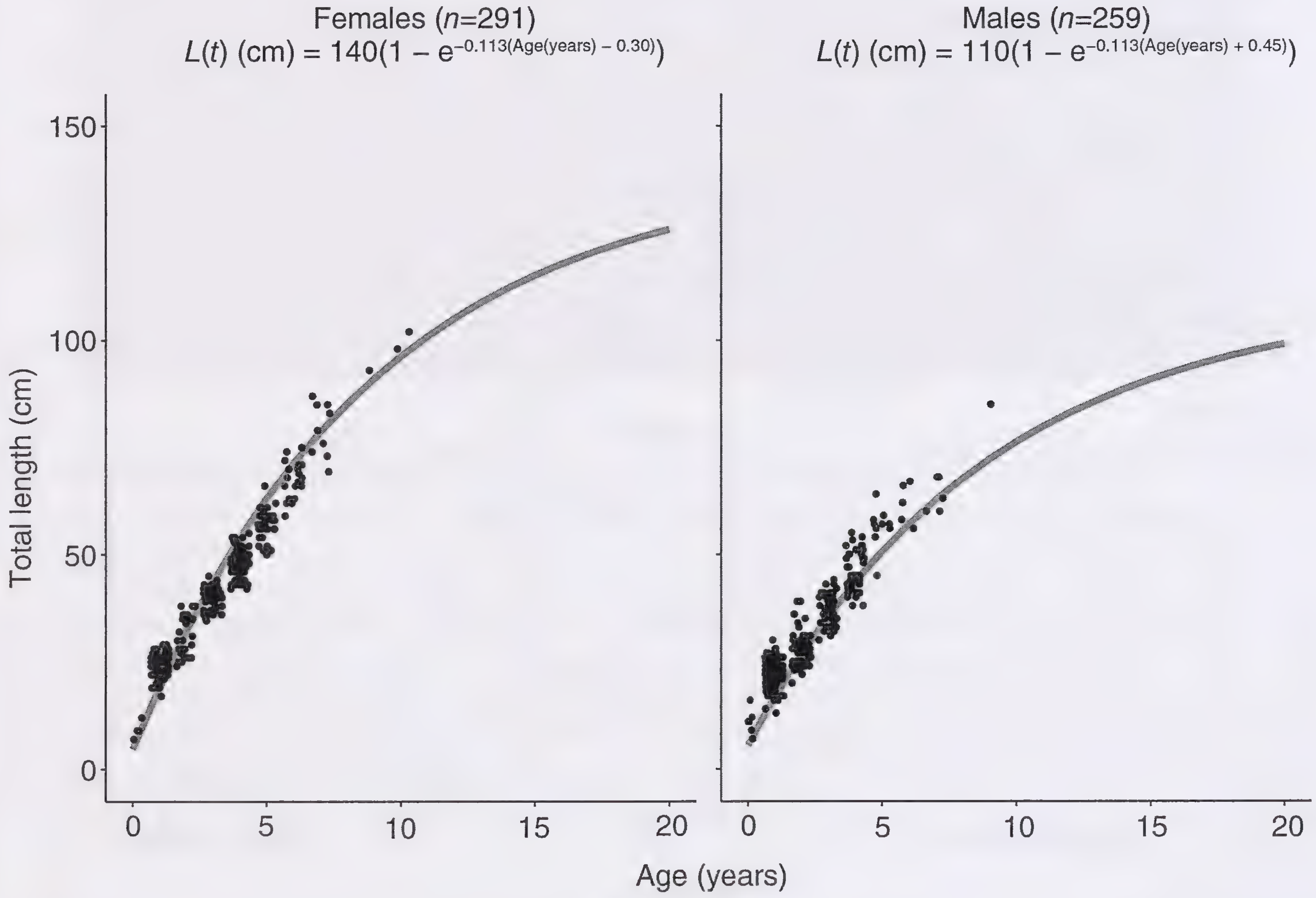

Figure 5

von Bertalanffy growth curves for both male (number of fish [n]=259) and female (n=291) white hake (*Urophycis tenuis*) caught in New Hampshire and Maine during 2007–2021 in the fall, based on age estimates from counting of visual growth increments in otoliths. Sex-specific von Bertalanffy growth functions are also provided. $L(t)$=length at time t.

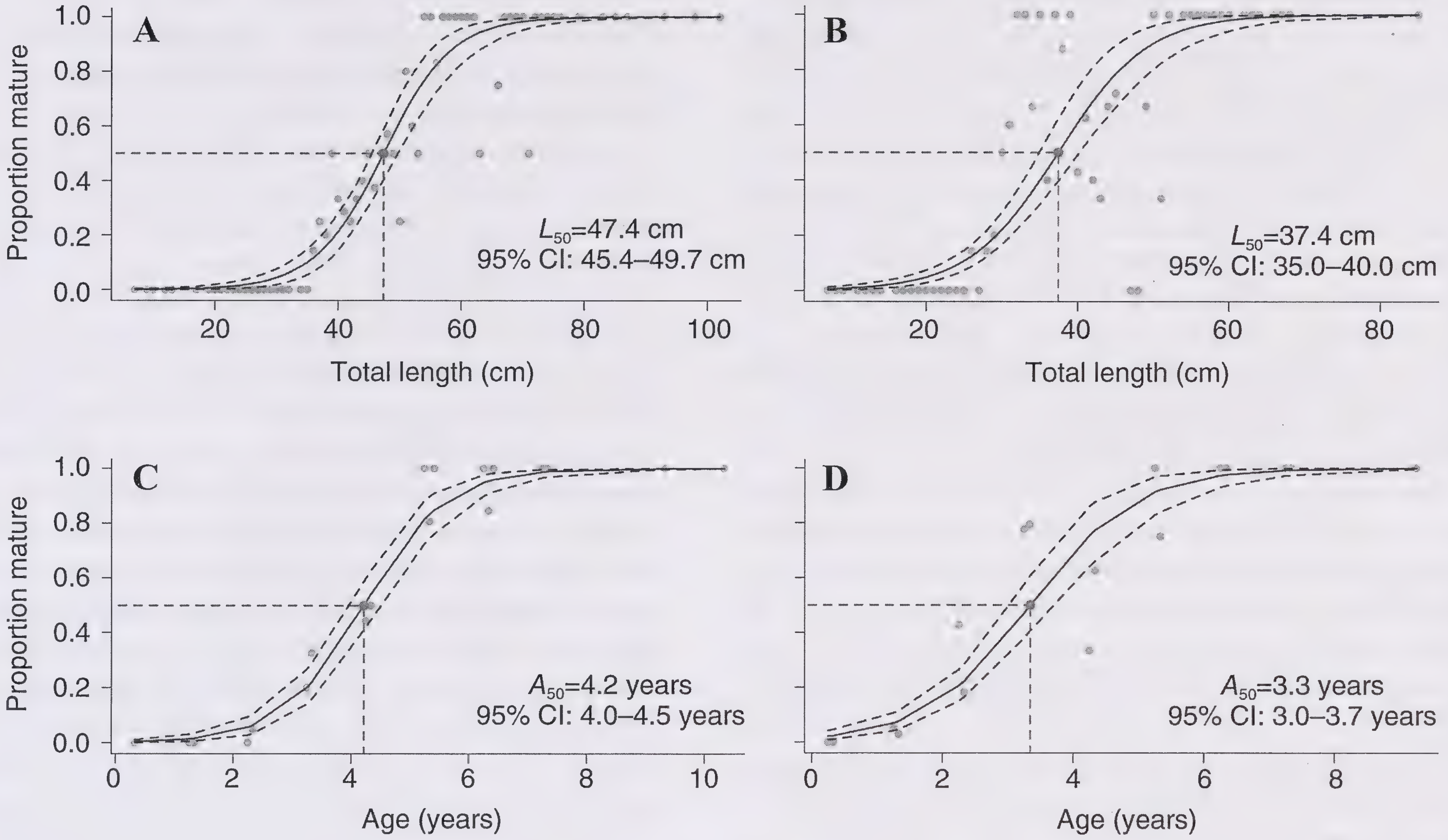

Figure 6

Maturity at length for (**A**) female (number of fish [n]=289) and (**B**) male (n=257) white hake (*Urophycis tenuis*) and maturity at age for (**C**) female and (**D**) male white hake captured in New Hampshire and Maine from 2007 through 2021 in the fall. The curved dashed lines indicate 95% confidence intervals (CIs). The vertical and horizontal dashed lines indicate the median length or (L_{50}) or age (A_{50}) at maturity.

We investigated the possible seasonal and annual patterns of concentrations of Mg, Mn, Sr, and Ba in otoliths of white hake by using 2D maps. These elements were chosen because of their prominence in previous otolith age and growth studies. We hypothesized that distinguishable variation in the concentration of one or more of these elements over time may be used as an indicator of age. Our hypothesis is supported by the finding that oscillations in the concentration of Mn, among those of other elements, most clearly had patterns in 2D maps similar to those of growth increments in otoliths, and we inferred that the patterns correspond to changes in Mn concentration in otoliths between seasonal growth increments (summer and winter). Variation in concentrations of Ba, Mg, and Sr each had varying patterns similar to those of growth increments, but the patterns were not consistent across individuals and, therefore, could not be attributed to growth (Suppl. Fig. 2, Suppl. Table 3) (online only). We speculate that variations in the concentration of these elements across individuals may be due to a combination of environmental (e.g., temperature and water chemistry) and physiological (e.g., diet and reproduction) factors. Research into these variations is ongoing, and we selected only Mn for line scan and peak counting as a means of estimating ages that could be later compared to age assignments by the primary reader of growth increments on otoliths. We made these comparisons by using symmetry and precision analyses, finding that age estimates from analysis of Mn concentration were ~100% in agreement, ±1 year, with ages assigned by readers. Again, we highlight the lack of age validation for this species and note that validation would allow increased confidence in the notion that Mn oscillations align with age.

Uptake of Mn into otoliths occurs as a substitute for Ca during biomineralization (Thomas et al., 2017; Hüssy et al., 2021), with reports from previous research also describing correlations between Mn and matrix proteins (Thomas et al., 2017). The element Mn has been shown to be a cofactor of extracellular serine and threonine protein kinase (Fam20C) (Tagliabracci et al., 2012), a biomineralization matrix protein. Growth increment patterns observed in 2D maps led us to hypothesize that Mn is a tracer of historical protein content, with seasonal oscillations in protein incorporation driven by growth, accounting for consistent age estimations across size classes.

In previous studies, elevated levels of Mn in otoliths cores have decreased through time, possibly in relation to maternal offloading and metabolism (Brophy et al., 2004; Ruttenberg et al., 2005; Miller, 2009; Friedrich and Halden, 2010; Clarke et al., 2011; Limburg et al., 2015; Hughes et al., 2016). Our 2D maps and data from line scans indicate comparable spatial variations on otoliths, with otolith cores enriched with Mn and the concentration of this element decreasing toward the edge of otoliths over successive inferred summer and winter growth increments.

In previous trace element research, Mn concentration has been shown to correlate with both hypoxic redox conditions that promote solubility of aqueous Mn^{2+} and somatic growth (Limburg et al., 2011; Mohan and Walther, 2015, 2016). Hypoxia is uncommon in the GOM, as its waters are cold and well mixed and its substrates are rocky (Hale and Heltshe, 2008; Irish et al., 2008); therefore, we attribute patterns of Mn concentration in otoliths of white hake to somatic growth. Heimbrand et al. (2020) made similar conclusions, ranking signals of Mn in otoliths with a high readability score for Atlantic cod and attributing distinct oscillations in concentration to growth. Variations in readability of Mn signals has been theorized to be a result of major influx in oxygen in the Baltic Sea, making Mn mineralization less reliable as a recorder of age compared with uptake of Mg and P, as substitution for Ca becomes altered (Heimbrand et al., 2020; Hüssy et al., 2021). Unlike in the Baltic Sea, hypoxic redox conditions do not regularly occur in the GOM, which has stable oxygen availability (Hale and Heltshe, 2008; Irish et al., 2008); therefore, somatic growth, which influences the seasonal incorporation of Mn in otoliths, is theorized to be less disrupted in white hake. In our investigation of concentration of Mg in otoliths of white hake, we found no discernable patterns indicative of growth, a result that varies from those of Heimbrand (2020) and Hüssy (2021). We interpret this result as a potential species (white hake versus Atlantic cod) or ecosystem (GOM versus Baltic Sea) effect.

Our analyses did not include P because of a lack of access to a standard to calibrate LA, and we strongly advocate for continued investigations into the concentration of P, and other trace elements, in otoliths and into environmental drivers of incorporation not examined in this study, for white hake in the GOM and for other species and ecosystems.

Similar to results from our examination of age estimates and growth, maturity schedules differed by sex. Previously, white hake had been reported to reach L_{50} at 32.7 cm TL for males and at 35.1 cm TL for females, with an estimated A_{50} of 1.4 years for both sexes (O'Brien et al., 1993). In comparison to those previously described differences, our observations indicate a high degree of sexual dimorphism in both length (L_{50} differed by 10 cm TL) and age (A_{50} differed by 1 year). Larger sizes of females, in comparison to the sizes of males, may indicate that female white hake increase fecundity with size, as noted by Beacham and Nepszy (1980). Delayed length and age at maturity has been reported previously as a sign of stock recovery, declining fishing pressure, or increased reproductive success for northern pike (*Esox lucius*) or chum salmon (*Oncorhynchus keta*) (Carlson et al., 2007; Edeline et al., 2007; Fukuwaka and Morita, 2008). The current understanding of the reproduction of white hake is limited; therefore, continued research is necessary to be able to pinpoint population trajectories. Although white hake have been previously described as highly fecund (Han and Kulka, 2008), significant spawning in the GOM has yet to be observed (Fahay and Able, 1989; O'Brien et al., 1993). Continued investigations into the maturity patterns of white hake by using historical data sets may help describe the future trajectory of stocks.

In this study, we compared techniques of aging otoliths from white hake, a traditional method of counting visual growth increments and a more recent method of analyzing geochemical markers. We found no variation in cost, effort, and time related to otolith preparation for each method. The traditional method of aging was more accessible (had lower costs and was faster) at a high volume of samples than the other investigated method. Aging through the use of otolith geochemistry was done quickly once elemental data were received from laboratories, but data collection and processing requires specialized instruments (had higher costs and was slower). The cost of LA-ICP-MS varies greatly between laboratories and equipment used, but results from using it have been promising in aging difficult species, like white hake. On the basis of our findings, we suggest that geochemical aging be considered for species for which aging through traditional reading of growth increments has proven difficult. Our approach of selecting white hake in a range of varying sizes provided us the ability to discern which elements had oscillations in their concentrations in otoliths that correlated to age, and the age estimates from analysis of these oscillations can be used moving forward as a reference for aging white hake by using traditional methods. With advancements in LA-ICP-MS technology, lowering of operation costs, and continued research, we see the potential for this approach to become an increasingly popular alternative method of aging.

Conclusions

Results from this study of white hake indicate the usefulness of analyzing otolith geochemistry as an alternative method of assigning age. Herein, we report accepted measures of precision and bias from a traditional comparison of between-reader agreement in age estimates and from comparisons of annulus counts of one reader to age estimates inferred from peaks in concentrations of Mn discerned through 2D mapping of otolith geochemistry. This expanded approach is likely to become more common (e.g., Heimbrand et al., 2020; Hüssy et al., 2021), although we cannot predict which elements will produce reliable annual patterns for different species, especially among different ecosystems. We emphasize that analysis of otolith geochemistry is worth consideration as a means to gain confidence in age assignments for difficult to age species; of course, growth validation, cost, and effort requirements of this method must be part of such consideration. The ability to increase certainty in age estimates for a species allows fishery managers to confidently determine growth rates, longevity, and reproductive output, all critical information for accurate stock assessment.

Resumen

La merluza blanca (*Urophycis tenuis*) es un pez de fondo distribuido por todo el Golfo de Maine. Las capturas se recomiendan con base en la evaluación de stock utilizando modelos de dinámica de poblaciones estructurados por edad; sin embargo, datar los otolitos es un reto debido a la falta de claridad de los incrementos de crecimiento. Para abordar esta preocupación, comparamos la consistencia entre las edades de recuentos visuales de anillos con las edades asignadas con ciclos de las concentraciones de elementos medidos utilizando ablación láser mediante espectrometría de masas con plasma acoplado inductivamente. Probamos la hipótesis de que las oscilaciones tanto en las condiciones ambientales como en la fisiología interna a lo largo del tiempo influyen en la absorción de elementos durante la mineralización del otolito. Las concentraciones de manganeso, en comparación con las de otros elementos traza investigados (magnesio, estroncio y bario), tuvieron la correlación más prometedora con los incrementos visuales de crecimiento (~100% de acuerdo con la edad, ±1 año), ofreciendo una herramienta adicional para mejorar la identificación de los incrementos. Examinamos 550 otolitos colectados durante 2007–2021, encontrando que la merluza blanca vivía un máximo de 10.3 años con dimorfismo sexual en longitud y edad máxima. Utilizando funciones de crecimiento de von Bertalanffy, $L(t)=110(1-e^{-0.113(t+0.45)})$ para machos y $L(t)=140(1-e^{-0.113(t-0.30)})$ para las hembras (donde $L(t)$ es la longitud en el tiempo t), se calcularon la talla y la edad de madurez de los machos (37.4 cm de longitud total [LT], 3.3 años) y las hembras (47.4 cm LT, 4.2 años). Estos resultados demuestran que la geoquímica de los otolitos puede utilizarse para mejorar la exactitud y precisión de la estimación de la edad y madurez de los peces, incluso en especies difíciles.

Acknowledgments

This project was prepared by the senior author under a grant from the National Marine Fisheries Service (award number NA22NMF4540361).

Literature cited

Ames, E. P.
2012. White hake (*Urophycis tenuis*) in the Gulf of Maine: population structure insights from the 1920s. Fish. Res. 114:56–65.

Ames, E. P., and J. Lichter.
2013. Gadids and alewives: structure within complexity in the Gulf of Maine. Fish. Res. 141:70–78.

Beacham, T. D., and S. J. Nepszy.
1980. Some aspects of the biology of white hake, *Urophycis tenuis*, in the southern Gulf of St. Lawrence. J. Northwest Atl. Fish. Sci. 1:49–54.

Berghahn, R.
2000. Response to extreme conditions in coastal areas: biological tags in flatfish otoliths. Mar. Ecol. Prog. Ser. 192:277–285.

Bowker, A. H.
1948. A test for symmetry in contingency tables. J. Am. Stat. Assoc. 43:572–574.

Brophy, D., T. E. Jeffries, and B. S Danilowicz.
2004. Elevated manganese concentrations at the cores of clupeid otoliths: possible environmental, physiological, or structural origins. Mar. Biol. 144:779–786.

Burnett, J., S. H. Clark, and L. O'Brien.
1984. A preliminary assessment of white hake in the Gulf of Maine–Georges Bank area. Nat. Mar. Fish. Serv., Northeast Fish. Cent., Woods Hole Lab. Ref. Doc. 84–31, 33 p.

Burnett, J., L. O'Brien, R. K. Mayo, J. A. Darde, and M. Bohan.
1989. Finfish maturity sampling and classification schemes used during Northeast Fisheries Center bottom trawl surveys, 1963–89. NOAA Tech. Memo. NMFS-F/NEC-76, 13 p.

Campana, S. E.
1999. Chemistry and composition of fish otoliths: pathways, mechanisms and applications. Mar. Ecol. Prog. Ser. 188:263–297.

Campana, S. E., and J. D. Neilson.
1985. Microstructure of fish otoliths. Can. J. Fish. Aquat. Sci. 42:1014–1032.

Cappo, M., P. Eden, S. J. Newman, and S. Robertson.
2000. A new approach to validation of periodicity and timing of opaque zone formation in the otoliths of eleven species of *Lutjanus* from the central Great Barrier Reef. Fish. Bull. 98:474–488.

Carlson, S. M., E. Edeline, L. A. Vøllestad, T. O. Haugen, I. J. Winfield, J. M. Fletcher, J. Ben James, and N. C Stenseth.
2007. Four decades of opposing natural and human-induced artificial selection acting on Windermere pike (*Esox lucius*). Ecol. Lett. 10:512–521.

Chang, S., W. W. Morse, and P. L. Berrien.
1999. Essential fish habitat source document: white hake, *Urophycis tenuis*, life history and habitat characteristics. NOAA Tech. Memo. NMFS-NE-136, 23 p.

Chang, W. Y. B.
1982. A statistical method for evaluating the reproducibility of age determination. Can. J. Fish. Aquat. Sci. 39:1208–1210.

Clarke, L. M., S. R. Thorrold, and D. O. Conover.
2011. Population differences in otolith chemistry have a genetic basis in *Menidia menidia*. Can. J. Fish. Aquat. Sci. 68:105–114.

Clay, D., and H. Clay.
1991. Determination of age and growth of white hake (*Urophycis tenuis* Mitchell) from the southern Gulf of St. Lawrence, Canada (including techniques for commercial sampling). Can. Tech. Rep. Fish. Aquat. Sci 1828, 29 p.

Cruz-Uribe, A. M., F. Z. Page, E. Lozier, M. D. Feineman, T. Zack, R. Mertz-Kraus, D. E. Jacob, and K. Kitajima.
2021. Trace element and isotopic zoning of garnetite veins in amphibolitized eclogite, Franciscan Complex, California, USA. Contrib. Miner. Pet. 176, article 14.

Ding, C., D. He, Y. Chen, Y. Jia, and J. Tao.
2020. Otolith microstructure analysis based on wild young fish and its application in confirming the first annual increment in Tibetan *Gymnocypris selincuoensis*. Fish. Res. 221:105386.

Edeline, E., S. M. Carlson, L. C. Stige, I. J. Winfield, J. M. Fletcher, J. B. James, T. O. Haugen, L. A. Vøllestad, and N. C. Stenseth.
2007. Trait changes in a harvested population are driven by a dynamic tug-of-war between natural and harvest selection. Proc. Natl. Acad. Sci. USA 104:15,799–15,804.

Evans, G. T., and J. M. Hoenig.
1998. Testing and viewing symmetry in contingency tables, with application to readers of fish ages. Biometrics 54:620–629.

Fahay, M. P., and K. W. Able.
1989. White hake, *Urophycis tenuis*, in the Gulf of Maine: spawning seasonality, habitat use, and growth in young of the year and relationships to the Scotian Shelf population. Can. J. Zool. 67:1715–1724.

Ferri, J.
2023. Otoliths and their applications in fishery science. Fishes 8, article 35.

Friedrich, L. A., and N. M. Halden.
2010. Determining exposure history of northern pike and walleye to tailings effluence using trace metal uptake in otoliths. Environ. Sci. Technol. 44:1551–1558.

Fukuwaka, M.-A., and K. Morita.
2008. Increase in maturation size after the closure of a high seas gillnet fishery on hatchery-reared chum salmon *Oncorhynchus keta*. Evol. Appl. 1:376–387.

Gauldie, R. W., and D. G. A Nelson.
1990. Otolith growth in fishes. Comp. Biochem. Physiol. A 97:119–135.

Haedrich, R. L.
2003. Bigelow and Schroeder's Fishes of the Gulf of Maine. Copeia 2003:422–423.

Hale, S. S., and J. F. Heltshe,.
2008. Signals from the benthos: development and evaluation of a benthic index for the nearshore Gulf of Maine. Ecol. Indic. 8:338–350.

Han, G., and D. W. Kulka.
2008. Dispersion of eggs, larvae and pelagic juveniles of white hake (*Urophycis tenuis*) in relation to ocean currents of the Grand Bank: a modelling approach. J. Northwest Atl. Fish. Sci. 41:183–196.

Hederström, H.
1959. Observations on the age of fishes. Inst. Freshw. Res. Drottningholm Rep. 40:161–164.

Heimbrand, Y., K. E. Limburg, K. Hüssy, M. Casini, R. Sjöberg, A.-M. Palmén Bratt, S.-E. Levinsky, A. Karpushevskaia, K. Radtke, and J. Öhlund.
2020. Seeking the true time: exploring otolith chemistry as an age-determination tool. J. Fish Biol. 97:552–565.

Hughes, J. M., J. Stewart, B. M. Gillanders, D. Collins, and I. M. Suthers.
2016. Relationship between otolith chemistry and age in a widespread pelagic teleost *Arripis trutta*: influence of adult movements on stock structure and implications for management. Mar. Freshw. Res. 67:224–237.

Hunt, J. J.
1982. Age determination of white hake (*Urophycis tenuis*) in the Gulf of St. Lawrence. Dep. Fish. Oceans, Can. Atl. Fish. Sci. Advis. Comm., Res. Doc. 1982/25,16 p. [Available from website.]

Hüssy, K.
2008. Otolith accretion rates: does size really matter? J. Exp. Mar. Biol. Ecol. 362:131–136.

Hüssy, K., M. Krüger-Johnsen, T. B. Thomsen, B. D. Heredia, T. Næraa, K. E. Limburg, Y. Heimbrand, K. McQueen, S. Haase, U. Krumme, et al.
2021. It's elemental, my dear Watson: validating seasonal patterns in otolith chemical chronologies. Can. J. Fish. Aquat. Sci. 78:551–566.

Irish, J. D., L. G. Ward, and S. Boduch.
2008. Correcting and validating moored oxygen time-series observations in the Gulf of Maine. *In* OCEANS 2008; Quebec City, 15–18 September, 6 p. [Proceedings.] [Available from website.]

Jochum, K. P., U. Nohl, K. Herwig, E. Lammel, B. Stoll, and A. W. Hoffman.
2005. GeoReM: a new geochemical database for reference materials and isotopic standards. Geostand. Geoanal. 29:333–338.

Jones, C. M.
1992. Development and application of the otolith increment technique. *In* Otolith microstructure examination and analysis. Can. Spec. Publ. Fish. Aquat. Sci. 117 (D. K. Stevenson and S. E. Campana, eds.), p. 1–11. [Available from website.]

Katayama, S.
2018. A description of four types of otolith opaque zone. Fish. Sci. 84:735–745.

Katayama, S., and T. Isshiki.
2007. Variation in otolith macrostructure of Japanese flounder (*Paralichthys olivaceus*): a method to discriminate between wild and released fish. J. Sea. Res. 57:180–186.

Lang, K. L., F. P. Almeida, G. R. Bolz, and M. P. Fahay.
1996. The use of otolith microstructure in resolving issues of first year growth and spawning seasonality of white hake, *Urophycis tenuis*, in the Gulf of Maine–Georges Bank region. Fish. Bull. 94:170–175.

Langton, R. W., J. B. Pearce, and J. A. Gibson.
1994. Selected living resources, habitat conditions, and human perturbations of the Gulf of Maine: environmental and ecological considerations for fishery management. NOAA Tech. Memo. NMFS NE-106, 70 p.

Limburg, K. E., C. Olson, Y. Walther, D. Dale, C. P. Slomp, and H. Høie.
2011. Tracking Baltic hypoxia and cod migration over millennia with natural tags. Proc. Natl. Acad. Sci. USA 108:E177–E182.

Limburg, K. E., B. D. Walther, Z. Lu, G. Jackman, J. Mohan, Y. Walther, A. Nissling, P. K. Weber, and A. K. Schmitt.
2015. In search of the dead zone: use of otoliths for tracking fish exposure to hypoxia. J. Mar. Syst. 141:167–178.

Markle, D. F., D. A. Methven, and L. J. Coates-Markle.
1982. Aspects of spatial and temporal cooccurrence in the life history stages of the sibling hakes, *Urophycis chuss* (Walbaum 1792) and *Urophycis tenuis* (Mitchill 1815) (Pisces: Gadidae). Can. J. Zool. 60:2057–2078.

McBride, R. S.
2015. Diagnosis of paired age agreement: a simulation of accuracy and precision effects. ICES J. Mar. Sci. 72:2149–2167.

McNemar, Q.
1947. Note on sampling error of the difference between correlated proportions of percentages. Psychometrika 12:153–157.

Miller, J. A.
2009. The effects of temperature and water concentration on the otolith incorporation of barium and manganese in black rockfish *Sebastes melanops*. J. Fish. Biol. 75:39–60.

Mohan, J. A., and B. D. Walther.
2015. Spatiotemporal variation of trace elements and stable isotopes in subtropical estuaries: II. regional, local, and seasonal salinity–element relationships. Estuaries Coasts 38:769–781.
2016. Out of breath and hungry: natural tags reveal trophic resilience of Atlantic croaker to hypoxia exposure. Mar. Ecol. Prog. Ser. 560:207–221.

Musick, J. A.
1974. Seasonal distribution of sibling hakes, *Urophycis chuss* and *Urophycis tenuis* (Pisces, Gadidae) in New England. Fish. Bull. 72:481–495.

Neilson, J. D., and G. H. Geen.
1985. Effects of feeding regimes and diel temperature cycles on otolith increment formation in juvenile chinook salmon, *Oncorhynchus tshawytscha*. Fish. Bull. 83:91–101.

O'Brien, L., J. Burnett, and R. K. Mayo.
1993. Maturation of nineteen species of finfish off the northeast coast of the United States, 1985–1990. NOAA Tech. Rep. NMFS 113, 66 p.

Ogle, D. H.
2016. Introductory fisheries analyses with R, 333 p. Chapman and Hall, Boca Raton, FL.

Ogle, D. H, J. C. Doll, A. P. Wheeler, and A. Dinno.
2021. FSA: simple fisheries stock assessment methods. R package, vers. 0.9.1. [Available from website, accessed December 2021.]

Pannella, G.
1971. Fish otoliths: daily growth layers and periodical patterns. Science 173:1124–1127.

Paton, C., J. Hellstrom, B. Paul, J. Woodhead, and J. Hergt.
2011. Iolite: freeware for the visualisation and processing of mass spectrometric data. J. Anal. Atomic Spectrom. 26:2508–2518.

Paul, B., C. Paton, A. Norris, J. Woodhead, J. Hellstrom, J. Hergt, and A. Greig.
2012. CellSpace: a module for creating spatially registered laser ablation images within the Iolite freeware environment. J. Anal. Atomic Spectrom. 27:700–706.

Penttila, J. A., and L. M. Dery (eds.).
2004. Age determination methods for northwest Atlantic species. NOAA Tech. Rep. NMFS 72, 132 p.

Petrus, J. A., D. M. Chew, M. I. Leybourne, and B. S. Kamber.
2017. A new approach to laser-ablation inductively-coupled-plasma mass-spectrometry (LA-ICP-MS) using the flexible map interrogation tool 'Monocle.' Chem. Geol. 463:76–93.

RStudio Team.
2022. RStudio: integrated development for R. RStudio, PBC, Boston, MA. [Available from website.]

Ruttenberg, B. I., S. L. Hamilton, M. J. H. Hickford, G. L. Paradis, M. S. Sheehy, J. D. Standish, O. Ben-Tzvi, and R. R. Warner.
2005. Elevated levels of trace elements in cores of otoliths and their potential for use as natural tags. Mar. Ecol. Prog. Ser. 297:273–281.

Serre, S. H., K. E. Nielsen, P. Fink-Jensen, T. B. Thomsen, and K. Hüssy.
2018. Analysis of cod otolith microchemistry by continuous line transects using LA-ICP-MS. Geol. Surv. Den. Greenl. Bull. 41:91–94.

Stevenson, D. K., and S. E. Campana (eds.).
1992. Otolith microstructure examination and analysis. Can. Spec. Publ. Fish. Aquat. Sci. 117, 126 p. Dep. Fish. Oceans, Ottawa, Canada. [Available from website.]

Tagliabracci, V. S., J. L. Engel, J. Wen, S. E. Wiley, C. A. Worby, L. N. Kinch, J. Xiao, N. V. Grishin, and J. E. Dixon.
2012. Secreted kinase phosphorylates extracellular proteins that regulate biomineralization. Science 336:1150–1153.

Thomas, O. R. B., K. Ganio, B. R. Roberts, and S. E. Swearer.
2017. Trace element–protein interactions in endolymph from the inner ear of fish: implications for environmental reconstructions using fish otolith chemistry. Metallomics 9:239–249.

Torrejon-Magallanes, J.
2020. sizeMat: estimate size at sexual maturity. R package, vers. 1.1.2. [Available from website, accessed December 2021.]

Ulrich, T., B. S. Kamber, P. J. Jugo, and D. K. Tinkham.
2009. Imaging element-distribution patterns in minerals by laser ablation-inductively coupled plasma-mass spectrometry (LA-ICP-MS). Can. Mineral. 47:1001–1012.

Victor, B. C., and E. B. Brothers.
1982. Age and growth of the fallfish *Semotilus corporalis* with daily otolith increments as a method of annulus verification. Can. J. Zool. 60:2543–2550.

Vigliola, L., and M. G. Meekan.
2009. The back-calculation of fish growth from otoliths. *In* Tropical fish otoliths: information for assessment, management and ecology. Reviews: methods and technologies in fish biology and fisheries, vol. 11 (B. S. Green, B. D. Mapstone, G. Carlos, and G. A. Begg), p.174–211. Springer, Dordrecht, Netherlands.

von Bertalanffy, L.
1938. A quantitative theory of organic growth (inquiries on growth laws. II). Hum. Biol. 10:181–243.

Walters, J. B., A. M. Cruz-Uribe, W. J. Song, C. Gerbi, and K Biela.
2022. Strengths and limitations of in situ U–Pb titanite petrochronology in polymetamorphic rocks: an example from western Maine, USA. J. Metamorph. Geol. 40:1043–1066.

Watson, J. E.
1967. Age and growth of fishes. Am. Biol. Teach. 29:435–438.

Wickham, H.
2016. ggplot2: elegant graphics for data analysis, 2nd ed., 260 p. Springer, Cham, Switzerland.

Woodhead, J. D., J. Hellstrom, J. M. Hergt, A. Greig, and R. Maas.
2007. Isotopic and elemental imaging of geological materials by laser ablation inductively coupled plasma-mass spectrometry. Geostand Geoanal. Res. 31:331–341.

Wright, P. J.
1991. The influence of metabolic rate on otolith increment width in Atlantic salmon parr, *Salmo salar* L. J. Fish Biol. 38:929–933.

Wright, P. J., P. Fallon-Cousins, and J. D. Armstrong.
2001. The relationship between otolith accretion and resting metabolic rate in juvenile Atlantic salmon during a change in temperature. J. Fish Biol. 59:657–666.

Wright, P. J., J. Panfili, B. Morales-Nin, and A. J. Geffen.
2002a. Types of calcified structures: otoliths. *In* Manual of fish sclerochronology (J. Panfili, H. de Pontual, H. Troadec, and P. J. Wright, eds.), p. 31–57. Ifremer-IRD, Brest, France.

Wright, P. J., D. A. Woodroffe, F. M. Gibb, and J. D. M. Gordon.
2002b. Verification of first annulus formation in the illicia and otoliths of white anglerfish, *Lophius piscatorius* using otolith microstructure. ICES J. Mar. Sci. 59:587–593.

Yamamoto, S., H. Shinomi, and A. Goto.
1997. The effect of birth date on growth of juvenile white-spotted charr *Salvelinus leucomaenis*. Fish. Sci. 63:931–933.

Fishery Bulletin

Guidelines for authors

Contributions published in *Fishery Bulletin* describe original research in marine fishery science, fishery engineering and economics, and marine environmental and ecological sciences (including modeling). Preference will be given to manuscripts that examine processes and underlying patterns. Descriptive reports, surveys, and observational papers may occasionally be published but should appeal to an audience outside the locale in which the study was conducted.

Although all contributions are subject to peer review, responsibility for the contents of papers rests upon the authors and not on the editor or publisher. *Submission of an article implies that the article is original and is not being considered for publication elsewhere.*

All submissions are subject to a double-blind review to remove the identity of author and reviewer during the review process.

Plagiarism and double publication are considered serious breaches of publication ethics. To verify the originality of the research in papers and to identify possible previous publication, manuscripts may be screened with plagiarism-detection software.

Manuscripts must be written in English; authors whose native language is not English are strongly advised to have their manuscripts checked by English-speaking colleagues before submission.

Artificial intelligence (AI), machine learning, or similar algorithmic tools should not be used to write or generate scientific content, including text, tables, and figures, for manuscripts submitted to *Fishery Bulletin*. Although some authors may use such tools to improve the readability or syntax of their manuscript, it must be done with extreme caution, and authors must review and edit the result. If such a tool is used, authors must declare the name of the tool, where it was used, and the purpose for which it was used in an "Artificial intelligence declaration" section after the "Acknowledgments" section. Authors remain accountable for all elements of their manuscript and should state that they take full responsibility for the content of their manuscript in the AI declaration.

Once a paper has been accepted for publication, online publication takes approximately 2 weeks.

There is no cost for publication in *Fishery Bulletin*.

Types of manuscripts accepted by the journal

Articles generally range from 20 to 30 double-spaced typed pages (12-point font) and describe an original contribution to fisheries science, engineering, or economics. Tables and figures are not included in this page count, but the number of figures should not exceed 1 figure for every 4 pages of text. Articles contain the following divisions: abstract, introduction, methods, results, discussion, and conclusions.

Notes are generally less than 10 double-spaced typed pages (12-point font), including the Literature cited section. Like articles, notes describe an original contribution to fisheries science. They follow a format similar to that for articles: abstract, introduction, methods, results, and discussion, but the results and discussion sections may be combined and a conclusions section should not be included. They should include no more than 2 figures or tables (2 of each would be too many). They are distinguished from full articles in that they report a noteworthy new observation or discovery—such as the first report of a new species, a unique finding, condition, or event that expands our knowledge of fisheries science, engineering, or economics—and do not require a lengthy discussion. Manuscripts on range extensions will not be considered.

Companion articles should be submitted together and are published together as a scientific contribution. Both articles should address a closely related topic and may be articles that result from a workshop or conference.

Review articles of exceptional quality may be considered occasionally for publication on a case-by-case basis. They address a timely topic that is relevant to aspects of fisheries science. They should include an abstract, but the format of the article, per se, will be up to the author. Please contact the scientific editor to discuss your ideas regarding a potential review article before embarking on such a project.

Perspective essays generally are less than 5 double-spaced typed pages (12-point font) and provide clarification of misused terms or misunderstood topics in fisheries science. Essays are accepted at the discretion of the scientific editor. Opinion pieces on policy will not be considered. They should include an abstract and a list of the literature cited, but no other sections should divide the article. Please contact the scientific editor to discuss your idea before making a submission.

Preparation of manuscript

Title page should include authors' full names, affiliations, mailing addresses, and the senior author's email address.

Abstract should be limited to 200 words (one-half typed page), state the main scope of the research, and emphasize the authors' conclusions and relevant findings. Do not review the methods of the study or list the contents of the paper. Because abstracts are circulated by abstracting agencies, it is important that they represent the research clearly and concisely.

General text must be typed in 12-point Times New Roman font throughout. A brief introduction should convey the broad significance of the paper; the remainder of the paper should be divided into the following sections: Materials and methods, Results, Discussion, Conclusions, and Acknowledgments. Headings within each section must be short, reflect a logical sequence, and follow the rules of subdivision (i.e., there can be no subdivision without at least 2 subheadings). The entire text should be intelligible to interdisciplinary readers; therefore, all acronyms, abbreviations, and technical terms should be written out in full and defined the first time they are mentioned. Abbreviations should be used sparingly because they are not carried over to indexing databases and slow readability for those readers outside a discipline. They should never be used for the main subject (e.g., species or method) of a paper.

For general style, follow the U.S. Government Publishing Office *Style Manual* (2016, available at website) and *Scientific Style and Format: the CSE Manual for Authors, Editors, and Publishers* (2014, 8th ed.) published by the Council of Science Editors. For scientific nomenclature, use the current edition of the American Fisheries Society's (AFS) *Common and Scientific Names of Fishes from the United States, Canada, and Mexico* and its companion volumes (*Crustaceans, Mollusks, Cnidaria and Ctenophora*, and *World Fishes Important to North Americans*). For species not found in the previously mentioned AFS publications and for more recent changes in nomenclature, use the Integrated Taxonomic Information System (ITIS, available at website), or, secondarily, the California Academy of Sciences *Catalog of Fishes* (available at website) for species names not included in ITIS. Common (vernacular) names of species should be lowercase. Citations must be given for the identification of specimens. For example, "Fish species were identified according to Collette and Klein-MacPhee (2002); sponges were identified according to Stone et al. (2011)."

Dates should be written as follows: 11 November 2018. Measurements should be expressed in metric units, for example, "58 metric tons (t);" if other units of measurement are used, please make this fact explicit to the reader. Use numerals, not words, to express whole and decimal numbers in the general text, tables, and figure captions (except at the beginning of a sentence). For example, "We considered 3 hypotheses. We collected 7 samples in this location." Use American spelling. Refrain from using the shorthand slash (/), an ambiguous symbol, in the general text.

Cite all software, special equipment, and chemical solutions used in the study within parentheses in the general text, including the version number, company name, and the city and state (or nation) of the company headquarters, for example, "SAS, vers. 9.4 (SAS Institute Inc., Cary, NC)."

Word usage and grammar that may be useful are the following:

- *Aging*
  For our journal, the word *aging* is used to mean both age determination and the aging process (senescence). Authors should make clear which meaning is intended where ambiguity may arise.

- *Fish and fishes*
  The plural of the word fish (a collective noun that implies individuals without regard to species) is *fish*.
  Example: The *fish* were collected by trawl net.
  Example: The numbers of *fish* collected that season were less than the numbers from previous years.

  The plural for *fish species* is *fishes* (a contrived plural used by taxonomists to mean several or more *fish species*) or one can use *fish species* (which is preferred in this journal for clarity across disciplines).
  Example: The *fishes* of Puget Sound [biodiversity is implied] or
  Example: The *fish species* of Puget Sound [preferred plural for clarity across disciplines].

- *Crab and crabs, squid and squids, etc.*
  The plural of the word *crab* (i.e., many individuals without regard to species) is *crab*.
  Example: The crab were sorted by weight.
  Example: Many red king *crab* were dying [Many individuals of one species of crab.]

  The plural of *crab species* is *crabs* (a word used by taxonomists) or *crab species* (the latter is preferred in this journal for clarity).
  Example: These *crabs* were selected for treatment. [Different crab species are implied.]
  Example: These *crab species* were selected for treatment. [Preferred word choice for clarity.]
  Example: Snow *crabs* are found throughout the North Pacific Ocean and Bering Sea. [There are 2 species of snow crab; therefore the word *crabs* can be used here.]
  Example: *Two species* of snow *crab* are found throughout the North Pacific Ocean and Bering Sea. [Preferred usage for clarity.]
  Example: Three crabs were selected for treatment. [3 species of crab are implied.]
  Example: Three crab species were selected for treatment. [Preferred word choice for clarity.]

- We use *fisherman* and *fishermen*, not *fisher* and *fishers*, in this journal. One can always use crew member, vessel operator, and angler (the latter for recreational fishing).

- *The definite article with common names of species*
  When the singular common name of a species represents the entire class or group to which it belongs, use the definite article.
  Example: Only one species of the genus *Salmo* is found in the Atlantic Ocean—*the* Atlantic salmon (*Salmo salar*).
  Example: The sonic emissions of *the* bottlenose dolphin are complex.

  For plural common names, this rule does not apply.
  Example: Chinook salmon are found throughout the Pacific Ocean.
  Example: Bottlenose dolphins are found in temperate and tropical waters.

- *Sex*
  For the meaning of male and female, use the word *sex*, not *gender*. Do not write, "fish were sexed." Write, "sex was determined."
- *Participles*
  As adjectives, participles must modify a specific noun or pronoun.
  Example: Using mark-recapture methods, these scientists determined the size of the population. [Correct. The participle *using* modifies the word *scientists*.]
  Example: These scientists, based on the collected data, concluded that the mortality rate of these fish had increased. [Incorrect. The scientists were not based on the collected data.]
  Example: These scientists concluded, on the basis of collected data, that the mortality rate of these fish had increased. [Correct. The offending participle has been eliminated and an adverbial phrase modifies the verb *concluded*.]

Equations and mathematical symbols should be set from a standard mathematical program (MathType or Equation Editor). Equations formatted in LaTex are not acceptable. For mathematical symbols in the general text (α, χ^2, π, ±, etc.), use the symbols provided by the MS Word program and italicize all variables, except those variables represented by Greek letters and the superscript and subscript parts of variables and expressions. Do not use photo mode when creating these symbols in the general text, and do not cut and paste equations, letters, or symbols from a different software program.

Number equations (if there are more than one) for future reference by scientists; place the number within parentheses at the end of the first line of the equation.

Literature cited section comprises published works and those accepted for publication (in press) in peer-reviewed journals. Follow the name and year system for citation format in this section (i.e., citations should be listed alphabetically by the authors' last names, and then by year if there is more than one citation by the same author. A list of abbreviations for citing journal titles can be found on our website.

Authors are responsible for the accuracy and completeness of all citations. Avoid the use of multiple citations when a single citation sufficiently supports a statement; cite the work that first reported the information that supports a statement, not all of the subsequent works. Literature citation format: Authors (last name, followed by initials for first name and, if given, middle name of first author; then list names of additional authors with initials before last names). Year. Title of article. Abbreviated title of the journal in which it was published. Always include either the range of page numbers (for a journal article) or a total number of pages (for a book or other type of publication). List a sequence of citations in the general text chronologically, for example, "(Smith, 1932; Green, 1998; Smith and Jones, 2015)."

Acknowledgments should be no more than 6 lines of text. Only those who have contributed in an outstanding way should be acknowledged by name. For recognition of other persons or groups, use a general term, such as *crew*, *observers*, or *research coordinators*, and do not include names with these terms.

Digital object identifier (doi) code ensures that a publication has a permanent location online. A doi link (which may include a doi code) should be included at the end of citations of published literature. Authors are responsible for submitting accurate doi links. Faulty links will be deleted at the page-proof stage.

Footnotes are used for all documents that have not been formally peer reviewed and for observations and personal communications, but these types of references should be cited sparingly in manuscripts submitted to the journal.

All reference documents, administrative reports, internal reports, progress reports, project reports, contract reports, personal observations, personal communications, unpublished data, manuscripts in review, and council meeting notes are footnoted in 10-point font and placed at the bottom of the page on which they are first cited. Footnote format is the same as that for formal literature citations. A link to the online source (e.g., [Available from http://www..., accessed July 2017.]), or the mailing address of the agency or department holding the document, should be provided so that readers may obtain a copy of the document.

Tables are often overused in scientific papers; it is seldom necessary to present all the data associated with a study. Tables should not be excessive in size and must be cited in numerical order in the text. Headings should be short but ample enough to allow the table to be intelligible on its own.

All abbreviations and unusual symbols must be explained in the table legend. Other incidental comments may be footnoted with numeral footnote markers. Use asterisks only to indicate significance in statistical data. Do not put a table legend on a page separate from the table; place the legend above the table. *Do not submit tables in photo mode.*

- Note probability with a capital, italic *P*.
- Provide a zero before all decimal points for values less than one (e.g., 0.07).
- Round all values to 2 decimal points.
- Use a comma in numbers of 5 digits or more (e.g., 13,000 but 3000).

Figures must be cited in numerical order in the text. Graphics should aid in the comprehension of the text, but they should be limited to presenting patterns rather than raw data. The number of figures should not exceed 1 figure for every 4 pages of text.

Figure legends should explain all symbols and abbreviations seen in the figure and should be double spaced on a separate page at the end of the manuscript.

Line art and halftone figures should be saved at resolutions >600 dots per inch (dpi) and >300 dpi, respectively. Color is allowed in figures to show morphological differences among species (for species identification), to show stain reactions, to show gradations (such as those of temperature and salinity within maps), and to distinguish between numerous lines and symbols in graphs. Figures approved for color should be saved in CMYK format.

All figures must be submitted as PDF, TIFF, or EPS files.

- Capitalize only the first letter of the first word and proper nouns in all labels within figures.
- Do not use overly large font sizes for labels in maps and for axis labels in graphs.
- Use the same point size for all labels, except for panel labels (e.g., **A**), which should be slightly larger than other labels (e.g., 11 point versus 8 point).
- Use a sans serif font for all labels. Panel labels (e.g., **A**), however, should be in Times New Roman font.
- Do not use bold fonts or bold lines in figures. Do not use italic fonts. Exceptions include use of italic fonts for labels of bodies of water in maps and a bold font for panel labels (e.g., **A**).
- Do not place outline rules around graphs.
- Do not include vertical and horizontal lines in the background of graphs. Ticks for values on the x-axis and y-axis will suffice.
- Place a north arrow and label degrees latitude and longitude (e.g., 170°E) in all maps. If scale of map requires more than degrees, use degrees minutes, not decimal degrees.
- Place panel labels (e.g., **A**, **B**, **C**) within the upper-left area of each graph or photo in a multi-panel figure, from left to right, then top to bottom. If the letter is not visible against a dark background, put a white box behind it. Do not use white labels.
- Avoid placing labels vertically or diagonally. Y-axis labels can be vertical. Words in horizontal labels can be stacked vertically to fit.
- Use symbols, shading, or patterns (not clip art) in maps and graphs.
- For scale bars in maps, use kilometers. Use the label *km* or *kilometers* (lowercased).

Supplementary materials that are considered essential, but are too large or impractical for inclusion in a paper (e.g., metadata, figures, tables, videos, and websites), may be provided at the end of an article. These materials are subject to the editorial standards of the journal. A URL to the supplementary material and a brief explanation for including such material should be sent at the time of initial submission of the paper to the journal.

- **Metadata, figures, and tables** should be submitted in standard digital format (MS Word or PDF file) and should be cited in the general text, for example, as "... was determined (Suppl. Table 3, Suppl. Fig. 1)."
- **Websites** should be cited with a URL in the general text.
- **Videos** must not be larger than 30 MB to allow a swift technical response for viewing the video. Authors should consider whether a short video uniquely captures what text alone cannot capture for the understanding of a process or behavior under examination in the article. Supply an online link to the location of the video.

Copyright law does not apply to *Fishery Bulletin*, which falls within the public domain. However, if an author reproduces any part of an article from *Fishery Bulletin*, reference to source is considered correct form (e.g., Source: Fish. Bull. 117:105).

**Failure to follow these guidelines
and failure to correspond with editors
in a timely manner will delay
publication of a manuscript.**

Submission of manuscript

Submit a manuscript online at the ScholarOne Manuscripts website for *Fishery Bulletin*. Commerce Department authors must provide proof of internal clearance of their manuscripts with either a completed and signed NOAA Form 25-700 or a copy of the clearance email from the Research Publication Tracking System. For further details on electronic submission, please contact the associate editor, Cara Mayo, at

cara.mayo@noaa.gov.

When requested, the text and tables should be submitted in MS Word format. Each figure should be sent as a separate PDF, TIFF, or EPS file. Send a copy of a figure in the original software if conversion to any of these formats yields a degraded version of the figure.

Questions? If you have questions regarding these guidelines, please contact the managing editor, Kathryn Dennis, at

kathryn.dennis@noaa.gov.

Questions regarding manuscripts under review should be addressed to Associate Editor Cara Mayo.

Fishery Bulletin

Subscription form

Superintendent of Documents **Publications** Order Form

*5178

☐ YES, please send me the following publications:

____ Subscriptions to *Fishery Bulletin*
for $32.00 per year ($44.80 foreign)

The total cost of my order is $ ________ . Prices include regular domestic postage and handling and are subject to change.

Charge your order. IT'S EASY!

VISA

MasterCard

____
(Company or Personal Name) (Please type or print)

____
(Additional address/attention line)

____
(Street address)

____
(City, State, ZIP Code)

____
(Daytime phone including area code)

____
(Purchase Order No.)

Please Choose Method of Payment:

☐ Check payable to the Superintendent of Documents
☐ GPO Deposit Account ☐☐☐☐☐☐☐–☐
☐ VISA or MasterCard Account
☐☐☐☐☐☐☐☐☐☐☐☐☐☐☐☐☐☐☐☐
☐☐☐☐ (Credit card expiration date)

To fax your orders (202) 512-2104

____
(Authorizing Signature)

Mail to: Superintendent of Documents
P.O. Box 979050, St. Louis, Missouri 63197
Tel. no. (U.S. callers): 866-512-1800
Tel. no. (International callers): 1-202-512-1800

Thank you for your order!

Also available online at
https://bookstore.gpo.gov/products/fishery-bulletin
email: ContactCenter@gpo.gov

SMITHSONIAN LIBRARIES
3 9088 02050 8925